Investigations of Fungal Highly Reducing Polyketide Synthases: The Biosyntheses of Lovastatin and Hypothemycin

by

Amy K. Norquay

A thesis submitted in partial fulfillment of the requirements for the degree of

Doctor of Philosophy

Department of Chemistry
University of Alberta

ABSTRACT

Fungal highly reducing polyketide synthases (HR-PKSs) are large, multi-domain enzymes central to the biosynthesis of fungal polyketides. They assemble complex secondary metabolites, called polyketides, through the condensation of two-carbon acetate units and tailoring of the functional groups at each round of chain extension. Two such fungal polyketides are lovastatin, a cholesterol-lowering therapeutic, and hypothemycin, an anti-cancer kinase inhibitor. Studies into the biosynthesis of these two natural products were undertaken to expand our understanding of the complex processes performed by HR-PKS enzymes.

Firstly, the hypothesized reaction sequence of HR-PKS enzymes for these metabolites, proposed based on their similarity to fatty acid synthases, had never been fully proven experimentally. In our study of hypothemycin biosynthesis, we synthesized the proposed enzyme bound intermediates as *N*-acetylcysteamine thioesters with ^{13}C labels to use in incorporation assays with purified enzymes. We observed conversion of the partially assembled intermediates into intact PKS products, confirming their intermediacy and validating our understanding of HR-PKS reaction sequences. In order to extrapolate these findings to other systems, the proposed intermediates of lovastatin were also synthesized, and enzymatic assays are forthcoming.

Secondly, it has been proposed that an enzyme-catalyzed Diels-Alder cyclization is a key step in the assembly of the lovastatin intermediate dihydromonacolin L by the HR-PKS LovB. In order to study this LovB-catalyzed cyclization, two potential substrates were synthesized and various fragments of LovB were expressed heterologously. NMR techniques were developed to determine the products of the cyclization assays. By monitoring the conversion of the hexaketide triene to the enzymatic decalin product, it was determined that the Diels-Alder activity was

preserved in the LovB fragment where the condensation (CON) domain was deleted (LovBΔCON). Therefore our hypothesis that the CON domain is the Diels-Alderase is incorrect. It was also found that LovB did not catalyze the cyclization of a proposed heptaketide tetraene intermediate, and therefore the substrate scope of this conversion is still being investigated in order to better understand how this reaction occurs in nature.

Finally, the acyl carrier protein domains of both LovB, and the hypothemycin polyketide synthase, Hpm8, were expressed as stand-alone proteins. Our goal was to obtain a solution structure using NMR spectroscopy but the inherent properties of the protein made that impossible. Herein I explore the properties of these domains and discuss other possible ways we can use the expressed proteins to better understand the HR-PKS class of enzymes.

ACKNOWLEDGEMENTS

Graduate school is a humbling experience during which one truly learns the extent to which their accomplishments are not their own, but the product of a wider community.

I would like to begin by acknowledging those whose expertise had a direct impact on the content of this thesis. Thank you to all of the Scientific Services staff in the Department of Chemistry for the dedication to excellence in your work that allowed me to perform the high quality experiments of this thesis. In particular I would like to thank Gareth Lambkin (Biological Services), Mark Miskolzie (NMR Laboratory), Béla Reiz (Mass Spectrometry) and Wayne Moffat (Analytical and Instrumentation Laboratory).

Teamwork is as much an essential component of science as it is of sport, and so I would like to thank the amazing chemists in the Vederas Group. Firstly, thank you to my fellow polyketide team members, Zhizeng Gao, Randy Sanichar and Rachel Cochrane for being excellent teachers and supportive colleagues. A special thanks as well to Kaitlyn Towle, Shaun McKinnie and Chris Lohans for being wonderful friends both in and out of the lab, and finally to Christian Foerster for proofreading this thesis.

Quality friendships uplift us, and there is no question I would not have been successful without my incredible community in Edmonton. In addition to the friends mentioned above, I would like to thank fellow chemistry graduate students Thomas Scully and Samantha Kwok for their support and friendship. I am also indebted to my teammates and coaches from the University of Alberta Synchronized Swimming Team for 5 years of camaraderie. I would be amiss if I did not thank my classmates of the U of A Medicine Class of 2019, who have made the last two years some of the best of my life, despite being the most challenging. Lastly, to my old

friends back home in Winnipeg, I am truly blessed to have had you to cheer me on all these years.

I am a product of those who raised me, and so this thesis is as much theirs as it is mine. Thank you to my father, Donald Norquay, for instilling in me a love of learning and a passion for making the world a better place. Thank you to my mother, Dr. Glenda Buchik, for teaching me about care, self-sacrifice, and a dedication to quality. Thank you to my grandmother (my "Nona"), Rose Buchik, for financing my education, but mostly for loving me unconditionally and teaching me the importance of family and self-care.

Finally, thank you to my supervisor, Professor John Vederas, for making all of this possible. Thank you for taking me on as a graduate student, providing me to the opportunity to be a steward of your amazing legacy. Thank you for your mentorship all these years, for looking out for me when I did not think I was capable and supporting my career goals.

LIST OF ABBREVIATIONS

[α]	Specific rotation
A	Adenylation (domain)
Å	Ångström
ACP	Acyl carrier protein
ARO	Aromatase
AT	Acyl transferase (domain)
ATP	Adenosine triphosphate
bsgHMBC	Band-selective gradient heteronuclear multiple bond coherence
c	Concentration
CD	Circular dichroism
CON	Condensation (domain)
CHS	Chalcone synthase
CoA	Coenzyme A
CSSF-TOCSY	Chemical shift selective filtered totally correlation spectroscopy
CYC	Cyclase
δ	Chemical shift in parts per million
d	Doublet
DCC	Dicyclohexylcarbodiimide
DCM	Dichloromethane
DEBS	6-Deoxyethronolide B synthase

DH	Dehydratase (domain)
DHZ	Dehydrozearalenol
DIBAL-H	Diisobutylalumninum hydride
DIPEA	*N,N*-diisopropylethylamine
DHML	Dihydromonacolin L
DHZ	Dehydrozearalenol
DMAP	4-(Dimethylamino)pyridine
DMP	Dess-Martin periodinane
DTT	Dithiothreitol
EDTA	Ethylenediaminetetraacetic acid
eq	Equivalents
ER	Enoyl reductase (domain)
ER^0	Inactive enoyl reductase (domain)
ESI	Electrospray ionisation
FAD	Flavin adenine dinucleotide
FAS	Fatty acid synthase
HMG-CoA	3-Hydroxy-3-methylglutaryl-coenzyme A
HPLC	High performance liquid chromatography
HRMS	High resolution mass spectroscopy
HR-PKS	Highly reducing polyketide synthase
HWE	Horner-Wadsworth-Emmons
HSQC	Heteronuclear single quantum coherence

IPTG	Isopropyl thio-β-D-galactoside
IR	Infrared
J	J coupling, in Hertz
kDa	kilodalton
KR	Ketoreductase (domain)
KS	Ketosynthase (domain)
LHMDS	Lithium hexamethyldisilazide (also known as lithium bis(trimethylsilyl)amide)
LB	Lysogeny broth
LC-MS	Liquid chromatography/mass spectrometry
Ni-NTA	Nickel nitrilotriacetic acid
NRPS	Non-ribosomal peptide synthetase
m	Multiplet
m/z	Mass to charge ratio
MALDI	Matrix assisted LASER desorption/ionisation
MAT	Malonyl-CoA:acyltransferase (domain)
MEK-ERK	Mitogen-activated protein kinase kinase-extracellular signal-regulated kinase (pathway)
mFAS	Mammalian fatty acid synthase
MSAS	6-Methylsalicylic acid synthase
MT	Methyltransferase (domain)
NADPH	Nicotinamide adenine dinucleotide phosphate
NMR	Nuclear magnetic resonance

NR-PKS	Non-reducing polyketide synthase
PCP	Peptidyl carrier protein
ppm	Parts per million
PR-PKS	Partially reducing polyketide synthase
PT	Product template (domain)
pTsOH	*p*-Toluenesulfonic acid
q	Quartet
RAL	Resorcylic acid lactone
SAM	*S*-Adenosylmethionine
SAT	Starter unit acyltransferase (domain)
SDS-PAGE	Sodium dodecylsulfate polyacrylamide gel electrophoresis
SNAC	*N*-acetylcysteamine
t	Triplet
TBS	*Tert*-butyldimethylsilyl
TE	Thioesterase (domain)
THF	Tetrahydrofuran
THID	Thioesterase/interdomain
TOCSY	Total correlation spectroscopy
TRIS	Tris(hydroxymethyl)aminomethane

TABLE OF CONTENTS

LIST OF FIGURES

LIST OF TABLES

CHAPTER 1: INTRODUCTION

The polyketide natural products form a highly diverse class of secondary metabolites, grouped together based on their common biosynthetic origin. The diversity of their structures, important biological activities and elegant biosyntheses have long fascinated researchers. Figure 1 shows a selection of clinically relevant polyketides, highlighting the complexity of their varied structures and diverse uses as pharmaceuticals.[1]

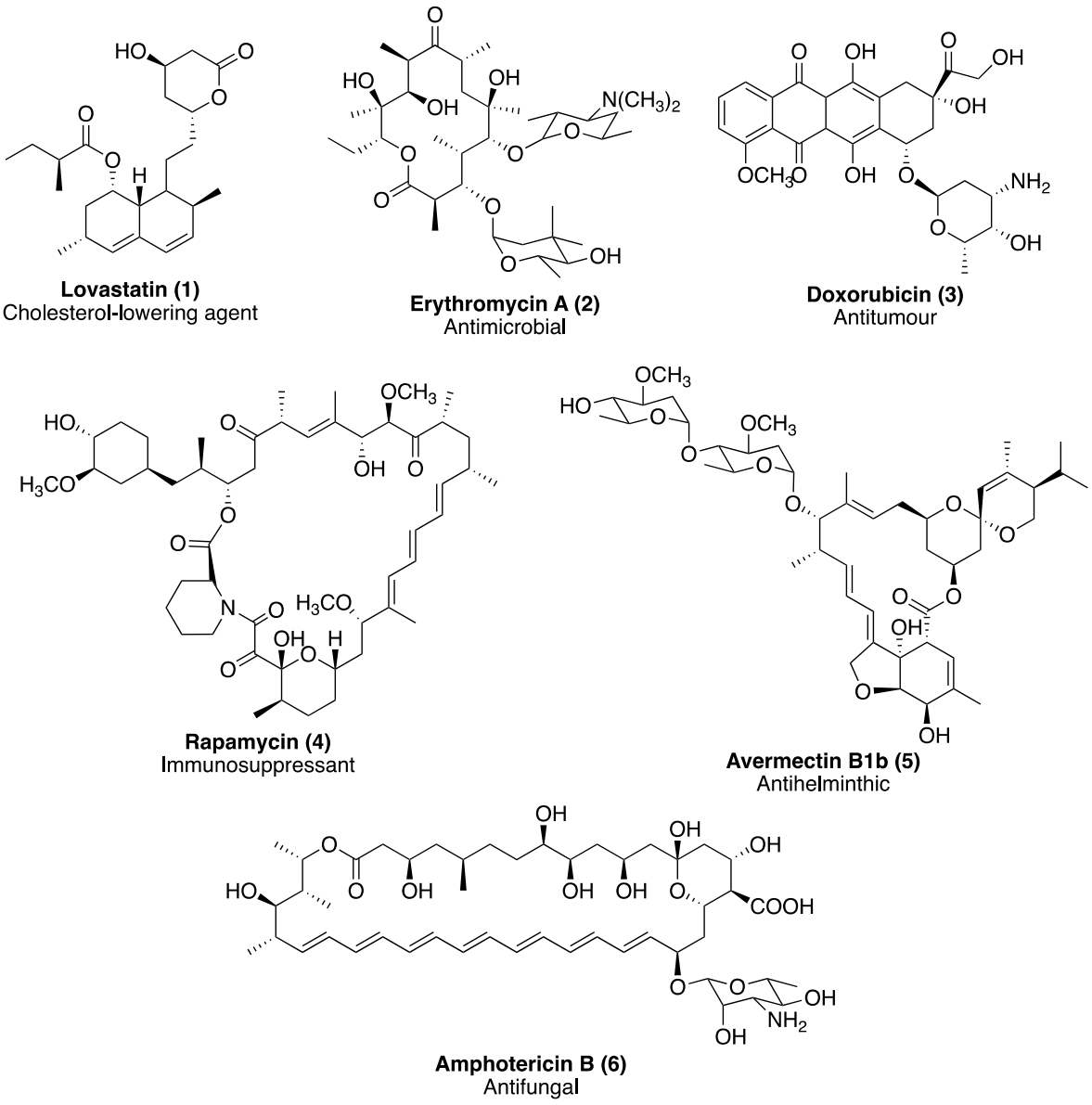

Figure 1: Examples of polyketides and their clinical uses.

Polyketide Biosynthesis

Fundamentals

Our knowledge of polyketide biosynthesis has expanded dramatically since the 1950s, when Arthur Birch *et al.* first demonstrated that polyketides are generated from the repeated condensation of acetate units by feeding isotopically labelled acetate to a polyketide-producing organism.[2] The developments of the last century were summarized thoroughly in a review by Staunton and Weissman.[3] The fundamentals of polyketide biosynthesis are best understood through comparison to fatty acid biosynthesis.[4] These two classes of natural products have the same precursor, acetic acid, and therefore their common biosynthetic pathway has been described as the acetate pathway (Figure 2).[5] The acetate units are first activated by thioesterification to acetyl-CoA (starter unit) and malonyl-CoA (extender unit). The acyl transferase (AT) domain transfers the acyl group of acetyl-CoA to the acyl carrier protein (ACP), covalently linked to the protein through the sulfur atom of its phosphopantetheine prosthetic group. The ACP then delivers the starter unit to the ketosynthase (KS) domain, and is available to receive the extender unit, malonyl-CoA, catalyzed by the AT as well. At this point the key carbon-carbon bond forming reaction occurs, in which the KS catalyzes a decarboxylative Claisen condensation to produce a β-ketothioester. In order to achieve the fully reduced structure of a fatty acid, a series of tailoring reactions must occur. First, using NADPH as a hydride source, the ketoreductase (KR) reduces the β-ketone to a β-hydroxyl group, which can be eliminated through the action of the dehydratase (DH) domain to produce an α,β-unsaturated intermediate. Finally, the enoyl reductase (ER) reduces the double bond to create the fully saturated chain which is still enzyme bound. This reaction series is considered to be one round of chain elongation, after which the synthesis of a four-carbon chain is complete. The ACP-bound

intermediate could then be delivered back to the KS for another round of chain elongation. Alternatively, if the final chain length is achieved, the thioesterase (TE) domain can release the fatty acid from the enzyme through hydrolysis of the labile thioester group.

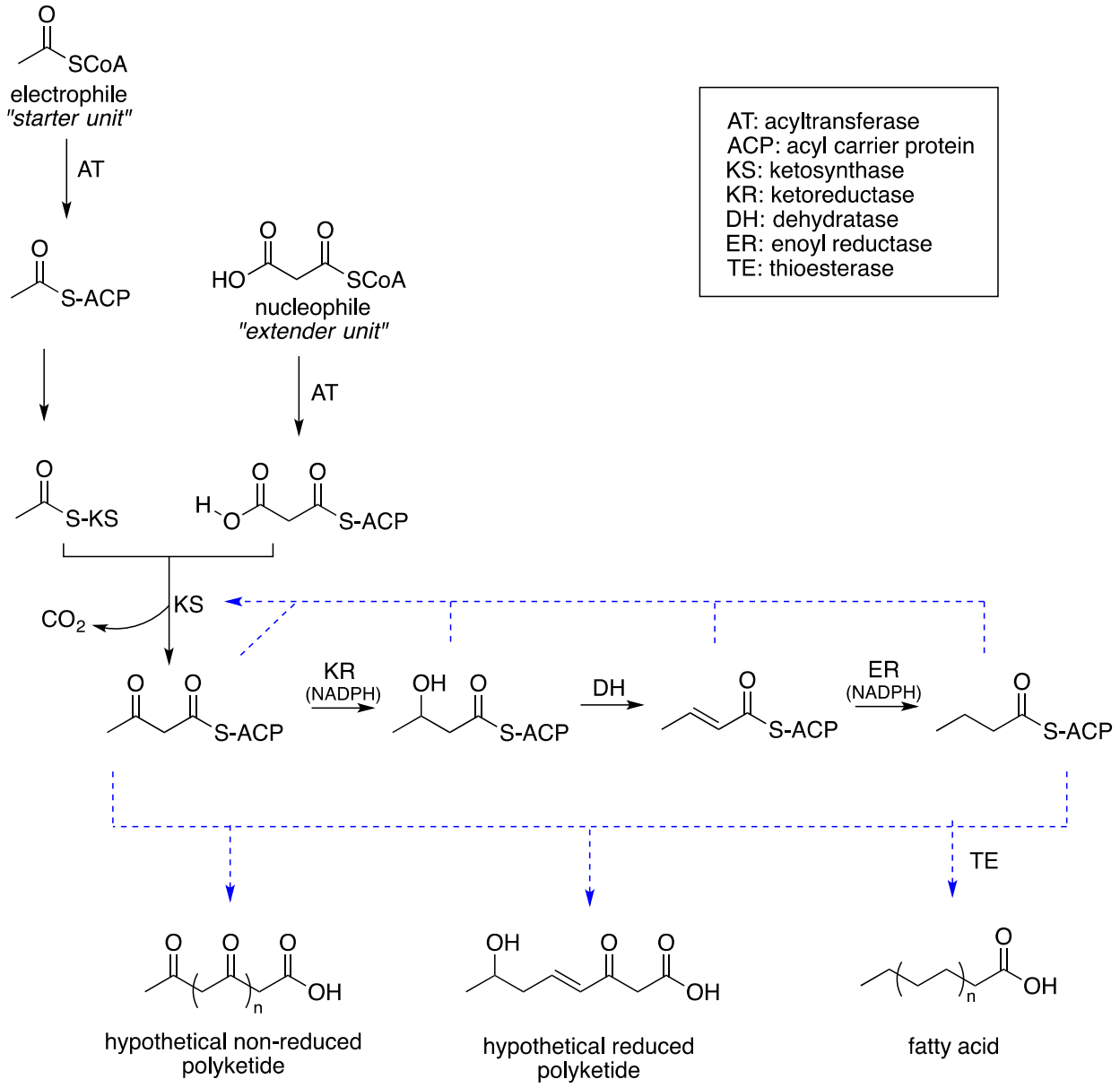

Figure 2: Fundamental reactions of FA and PKS biosynthesis

Polyketide biosynthesis differs from fatty acid biosynthesis by the following key concept: for each round of chain elongation, not all the tailoring reactions are necessarily used prior to the next condensation reaction or chain termination. Any of the four functionalities of the β-carbon shown in Figure 2 can be achieved by returning the intermediate to the KS instead of delivering it to the next tailoring domain. It is this principle that provides some of the dramatic structural diversity within polyketides. This diversity is supplemented by possible additional reactions, such as methylation during the chain elongation, as well as modifications by other enzymes, such as oxidation following the release of the polyketide chain. Examples of these additional reactions and modifications will be discussed herein where relevant. Additionally, other starter and extender units can be employed. Therefore, while the fundamental reactions of the biosynthesis of fatty acids and polyketides are identical, the differences in the products formed are striking. Fatty acid biosynthesis has evolved to faithfully produce saturated chains for primary metabolism across all domains of life, while polyketide biosynthesis is highly adaptable, allowing the construction of natural products diverse in structure and activity.[6]

PKS Structure Classification

Polyketide biosynthesis is performed by entities known as polyketide synthases (PKSs), which are categorized into 3 distinct types (Figure 3).[7] Each type will be briefly introduced in turn in the following sections.

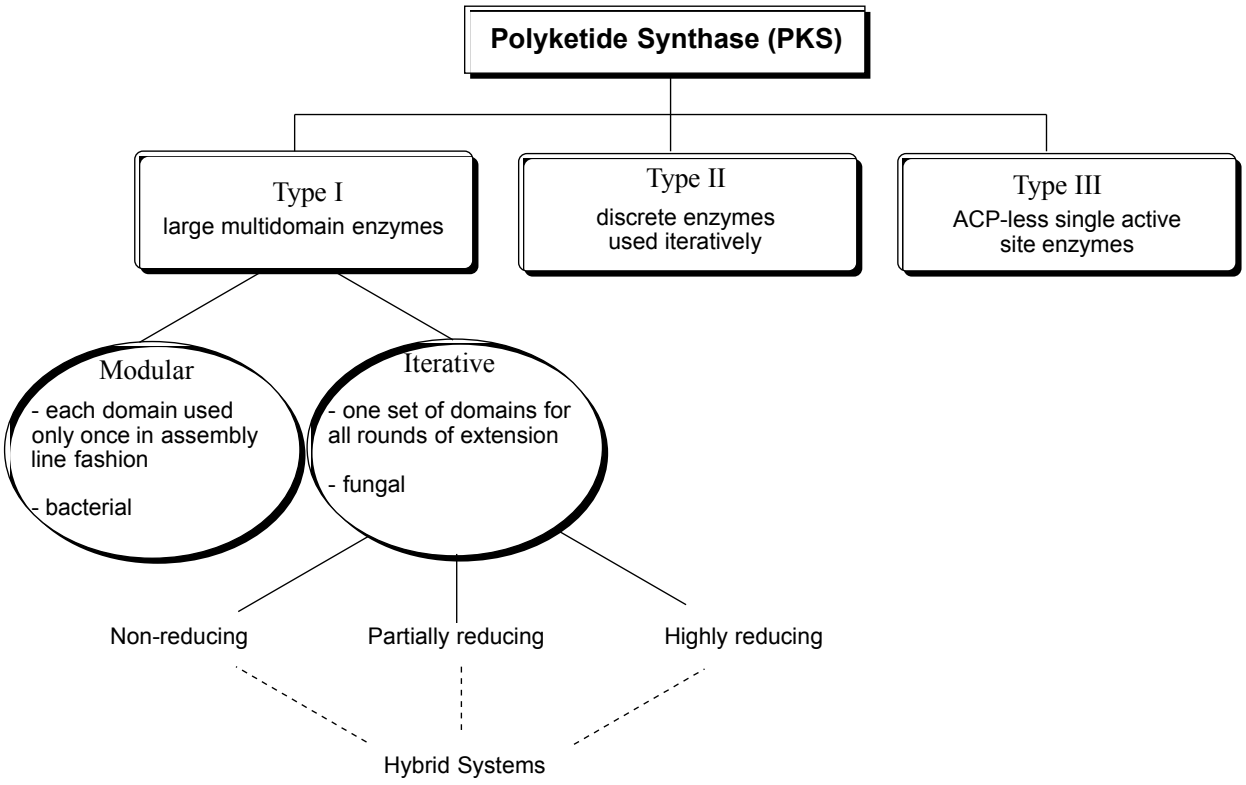

Figure 3: Classification of PKS Systems

Type I Polyketide Synthases

Type I systems are large multi-domain enzymes where numerous catalytic sites are found on a single polypeptide chain. This type is subdivided into modular and iterative PKSs, which are found in bacteria and fungi, respectively. They are so named based on how they function; modular PKS have their domains arranged in modules that operate one by one sequentially, whereas an iterative PKS has one set of domains that is used repeatedly in each iteration. Fungal type I iterative polyketide synthases are the subject of this thesis and will be discussed thoroughly in the forthcoming sections, while their modular counterparts will be discussed first.

Type I Modular PKSs

Bacterial type I modular polyketide synthases have been extensively studied since the discovery of the erythromycin biosynthetic gene cluster in the early 1990s by the groups of Leadlay[8] and Katz.[9] The biosynthesis of erythromycin (**2**) is depicted in Figure 4, highlighting the key intermediate 6-deoxyerythronolide B (**7**) produced by the modular PKS deoxyerythronolide B synthase (DEBS). The discovery and sequencing of DEBS revealed the molecular program referred to as "the DEBS paradigm" for bacterial polyketide synthases.[10] The DEBS paradigm states that a polyketide synthase is overtly programmed in a fashion where each round of chain extension has its own module, and each module contains the required set of domains for the functionality of the corresponding unit in the final product. Each domain is used only once, and the growing chain is transported along the megasynthase in the forward direction (although there have been examples since that do not fit the paradigm exactly).[11] As shown in Figure 4, after the loading domain loads a propionate unit, Module 1 has the necessary domains for Claisen condensation with a second preloaded propionate (KS), and ketoreduction (KR), to produce the diketide shown. This diketide can be acted on by the domains in Module 2 to furnish the triketide shown. We can contrast this to Module 4, which contains all the domains of a HR-PKS to produce a fully saturated methylene in the β-position of the pentaketide. As well, varying the active site motif of the KR domain sets the stereochemistry of both the hydroxyl and methyl groups of the priopionate unit, through directed delivery of hydride and epimerisation capability.[12] This overt programming, where the protein sequence has a direct and clear relationship to the polyketide structure, has allowed the exploration of combinatorial biosynthesis and the production of "unnatural natural products" using rationally designed PKSs.[13] This is in stark contrast to the covert programming of the iterative fungal PKSs

introduced in the next section, though recent years have seen progress in understanding and manipulating these enzymes.[14-16]

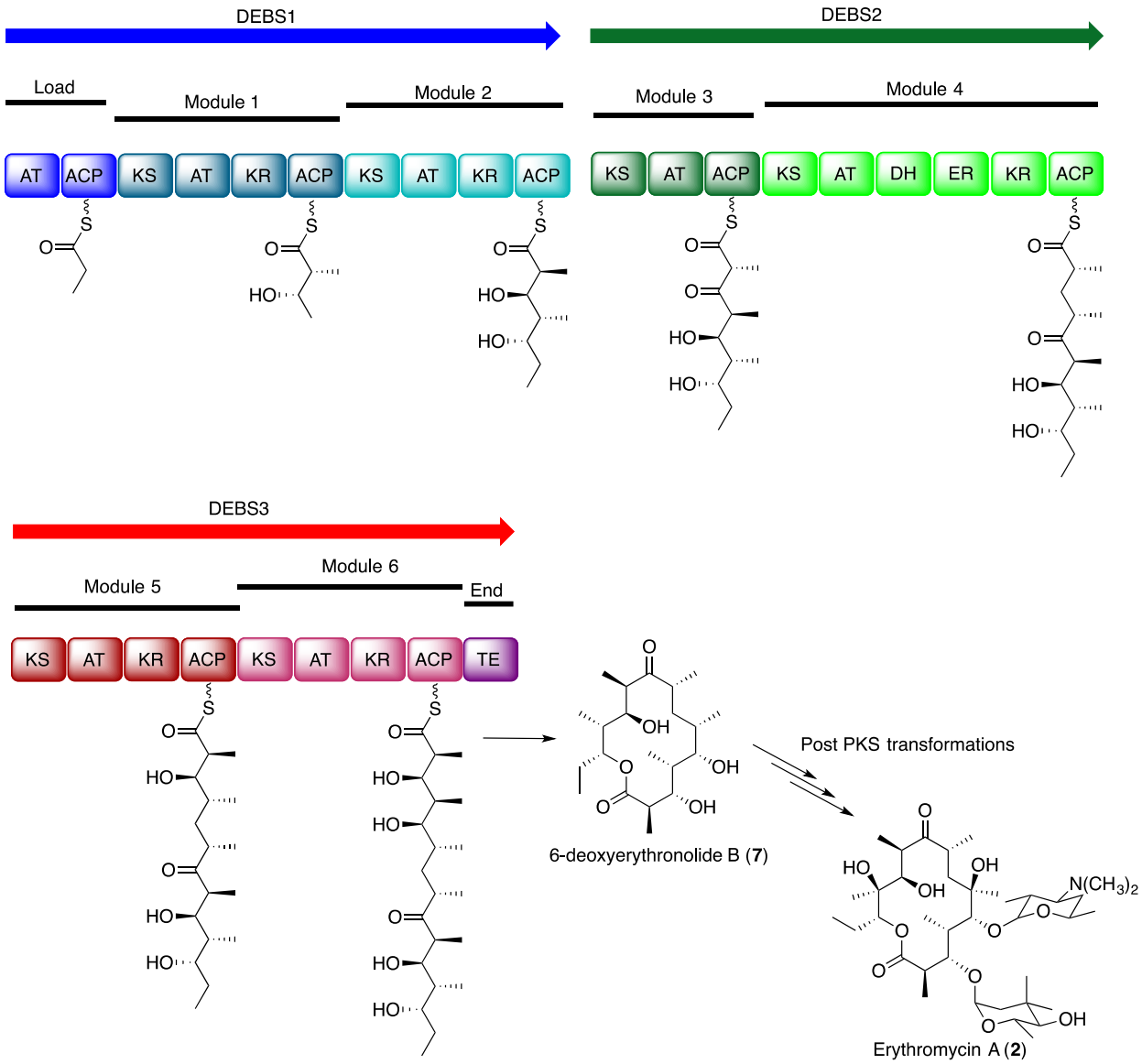

Figure 4: Erythromycin biosynthesis

Type I Iterative PKSs

In type I iterative polyketide synthesis, found in fungi, the polyketide assembly takes place on a multidomain megasynthase similar to a single module of a type I modular PKS. This

single polypeptide chain contains one set of all the required domains, akin to a mammalian fatty acid synthase.[4] Each domain is reused during the chain extension, in contrast to the bacterial type I modular system where the growing chain is only passed downstream.

Iterative PKSs are subdivided based on the presence or absence of the fundamental β-position tailoring domains in the sequence: Non-reducing PKSs contain no reductive tailoring domains, partially reducing PKSs contain a KR, but no ER, whereas highly reducing PKSs contain both. Each has its own unique characteristics and will be discussed in turn using representative examples for each class.

Aflatoxin B_1 (**8**) biosynthesis in *Aspergillus* spp. is representative of non-reducing type I polyketide biosynthesis (Figure 5).[17] The polyketide synthase (PksA) contains the minimal requisite domains, KS, AT and ACP, as well as others common to the class. At the N-terminus is the starter-unit acyl transferase (SAT). While the AT selects malonyl-CoA as an extender unit, the SAT selects hexanoyl-CoA as a starter unit. Variation in SAT domain selectivity is an important source of diversity in polyketides.[18] N-terminal to the ACP domain is a product template domain (PT). Product templates domains are an integral part of aromatic polyketide biosynthesis, as they orient the poly-β-keto chain and catalyze the aldol cyclizations yielding the aromatized product.[19] Finally, the TE/CYC domain catalyzes the final Claisen/Dieckmann condensation to release the PKS product noranthrone (**9**) en route to aflatoxin B1 (**8**).

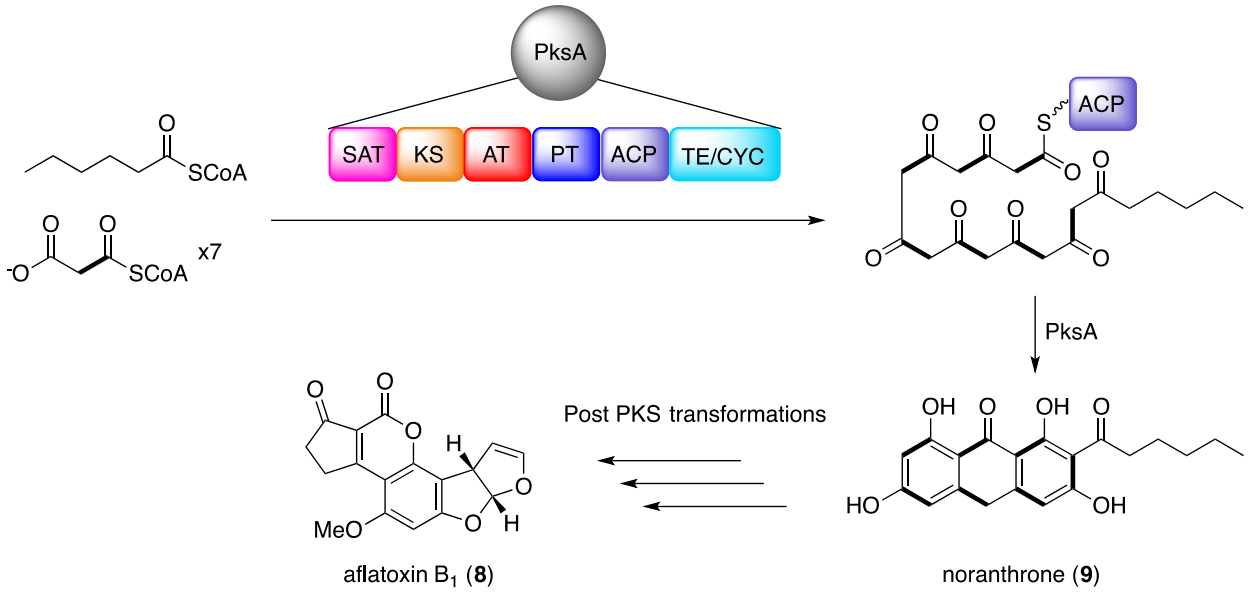

Figure 5: Biosynthesis of aflatoxin B_1 (8), representing NR-PKSs. To follow the incorporation of malonate, two carbon units are represented by a bold bond.

Partially reducing polyketide synthases, though they were the PKSs first isolated,[20,21] have the fewest examples in the literature.[4] The classic example is 6-methylsalicylic acid synthase (6-MSAS), whose domain architecture is shown in Figure 6. One ketoreduction and one dehydration are required to produce the aromatic product 6-methylsalicylic acid (**10**). 6-MSAS does not have an ER domain, but does have a non-catalytic "core" domain akin to mFAS. Recent literature has casted doubt on whether the dehydration is enzyme catalyzed, and suggests that the DH and core domain may be better described as a single domain, the thioesterase/interdomain (THID), involved in product templating and release.[22]

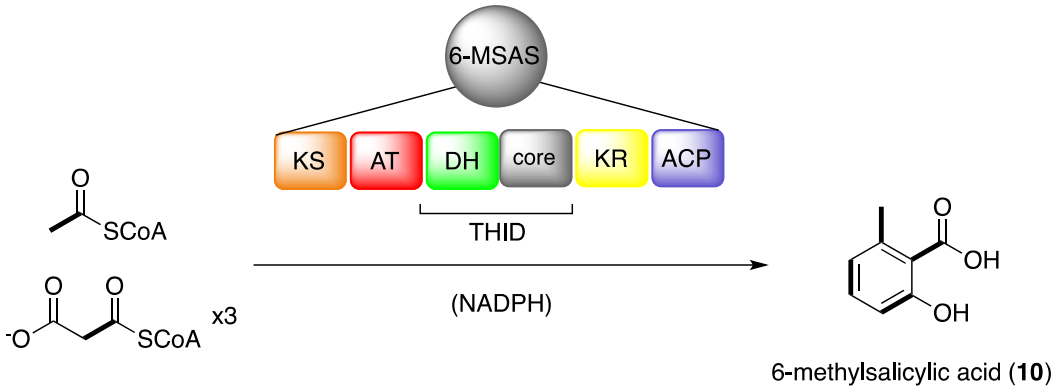

Figure 6: Biosynthesis of 6-methylsalicylic acid (10), representing PR-PKSs

Highly reducing polyketide synthases (HR-PKSs) contain both KR and ER domains, and also supplementary tailoring domains such as methyltransferases (MTs). Each chain length is tailored to a specific degree, creating a diversity of functional groups in a single polyketide chain. This is a similar concept to the type I modular PKSs, however the mechanism and enzyme structure are entirely different. In HR-PKSs, there is only one set of domains that is used iteratively, and it remains elusive how each HR-PKS can be "programmed" to use the tailoring domains only at specific chain lengths to make such diverse natural products. Lovastatin (**1**) is a representative example of a natural product assembled in this manner.[23,24] The biosynthesis will be discussed in detail in the upcoming sections, and a summary is shown in Figure 7 as an introduction to HR-PKSs.[25] Using the fundamental reactions discussed previously, LovB, the lovastatin PKS, assembles the polyketide product dihydromonacolin L (DHML, **11**), the precursor to the bioactive compound **1**. LovB has all of the domains found in a mammalian fatty acid synthase, with a few key differences. First, C-terminal to the DH domain is a MT domain, which installs the methyl group residing at the 6 position of the decalin at the tetraketide stage using the co-factor *S*-adenosylmethionine (SAM).[15] Second, the constituent enoyl reductase in

LovB is inactive and instead this role is performed by a *trans*-acting enoyl reductase known as LovC.[24] Finally, the C-terminus of LovB is particularly notable. The protein ends with a part of a non-ribosomal peptide synthetase module (NRPS), truncated after the condensation (CON) domain.[26] (This appears to be remnant of a PKS-NRPS hybrid, an example of the "hybrid" class alluded to in Figure 3 and discussed in the upcoming sections.) The CON domain is known to be required for DHML (**11**) production, but to date it has no known function.[25] This truncation also results in the absence of a domain to release the polyketide product, and the transacting TE (LovG) performs this role.[27]

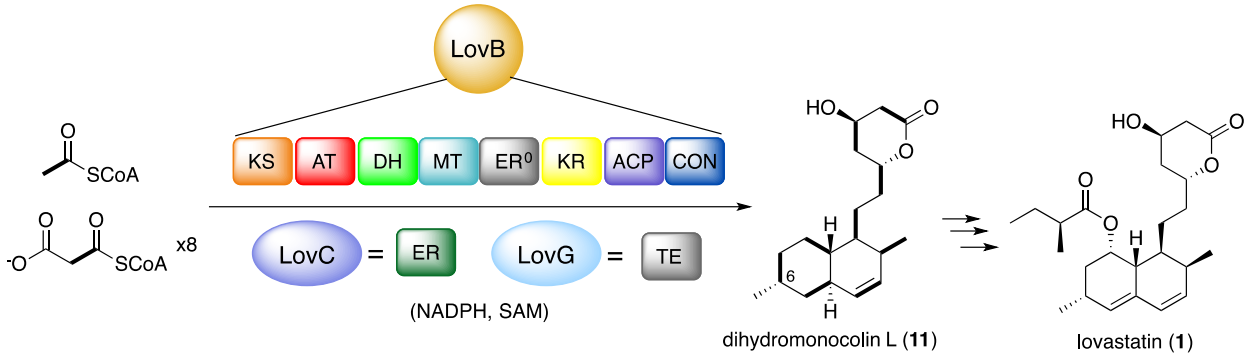

Figure 7: Biosynthesis of lovastatin (1), representing HR-PKSs

Fungal polyketides often do not conform to the simple model of NR-, PR- and HR-PKSs. Many are biosynthesized by systems that are hybrids of these types, or of other natural product classes. Examples include HR/NR-PKS partners, PKS/NRPS hybrids and meroterpenoids (Figure 8). HR/NR-PKS hybrids synthesize natural products such as hypothemycin (**12**),[28] whose biosynthesis is studied in this thesis and will therefore be elaborated in its own section. PKS/NRPS hybrids are akin to LovB, however the NRPS modules that follow their HR-PKS portions are not truncated and are capable of installing an amino acid at the end of the polyketide chain prior to offloading. The bioactive natural products made by this class of megasynthases are

highly diverse, as illustrated by the structures of fusarin C (**13**), equisetin (**14**) and cytochalasin E (**15**) in Figure 8.[29] Meroterpenoids are natural product hybrids containing polyketide and terpenoid moieties.[4]

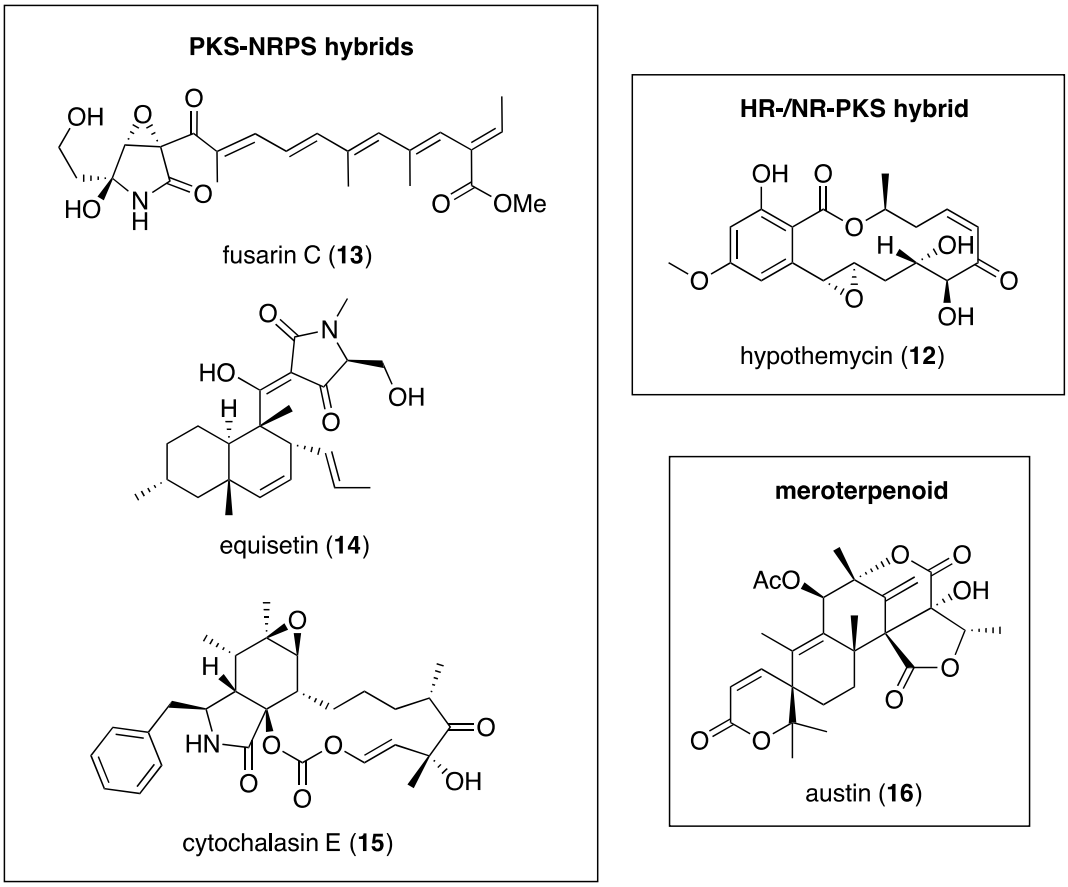

Figure 8: Hybrid fungal polyketides

Type II and Type III PKSs

Type II and type III PKSs are not the subject of this thesis, and will be discussed briefly for completeness.

Type II PKSs are multienzyme complexes where each reaction takes place on a discrete enzyme that is used iteratively. The products are phenolic/aromatic in nature, akin to products of

fungal NR- and PR-PKSs, but the enzymatic machinery differs in that the domains are not found in a megasynthase. The classic example is actinorhodin (**17**) biosynthesis in *Streptomyces coelicolor* (Figure 9).[30] The minimal PKS domains (KSα, KSβ and ACP) assemble the polyketide chain, and through the action of the tailoring enzymes KR, CYC and aromatase (ARO), synthesize enzyme-bound intermediate **18** en route to actinorhodin (**17**).

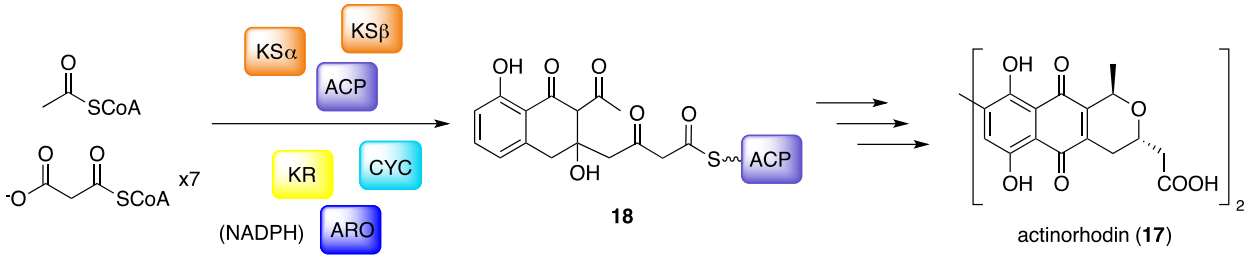

Figure 9: Actinorhodin biosynthesis

Type III PKSs catalyze the condensation of coenzyme-A bound intermediates without the involvement of ACPs or tailoring domains.[31] They are simple homodimers of KS domains, found primarily in plants and also in bacteria. The classic example is chalcone synthase (CHS), which assembles the product chalcone (**19**) from sequential condensation of 4-coumaryl-CoA (**20**) with malonyl-CoA (Figure 10).

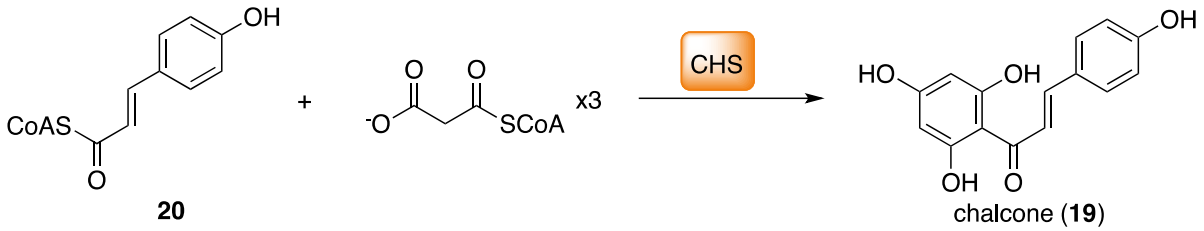

Figure 10: Chalcone biosynthesis

Polyketides Studied in this Thesis

Among the vast diversity of polyketides in Nature, of which a broad picture was painted in the previous section, are found the two natural products explored in this thesis. Each will be introduced in turn.

*Hypothemycin (**12**)*

Hypothemycin (**12**) is a resorcylic acid lactone (RAL) isolated from *Hypomyces subiculosus* and related fungi.[32-34] RALs are typically cytotoxic compounds, but the pattern and modes of action of their cytotoxicity make them attractive anti-cancer drug leads.[35] For example, hypothemycin (**12**) has been shown to inhibit the mitogen-activated protein kinase kinase-extracellular signal-regulated kinase (MEK-ERK) pathway in cells, a promising chemotherapy target.[36] This is distinct from the closely related RAL radicicol, whose mechanism of cytotoxity is the inhibition of protein chaperone HSP90.[37]

The biosynthesis of hypothemycin (**12**) begins with the cooperation of two PKSs, one HR-PKS and one NR-PKS, as introduced in the previous section and summarized in Figure 11.[33] First the HR-PKS Hpm8 is loaded with acetate and completes five rounds of chain extension with the appropriate tailoring to produce the enzyme bound hexaketide chain depicted. Next, the SAT domain of Hpm3 catalyzes the chain transfer from Hpm8-ACP to Hpm3-ACP, so that Hpm3 can complete 3 more rounds of chain extension. The PT domain then transforms the β-polyketothioester intermediate to a resorcylate moiety via an aldol-type cyclization. Macrolactonization releases the PKS product dehydrozearalenol (DHZ, **21**). Post-PKS modifications, namely methylation, oxidation and olefin rearrangement, produce the bioactive final product **12**.

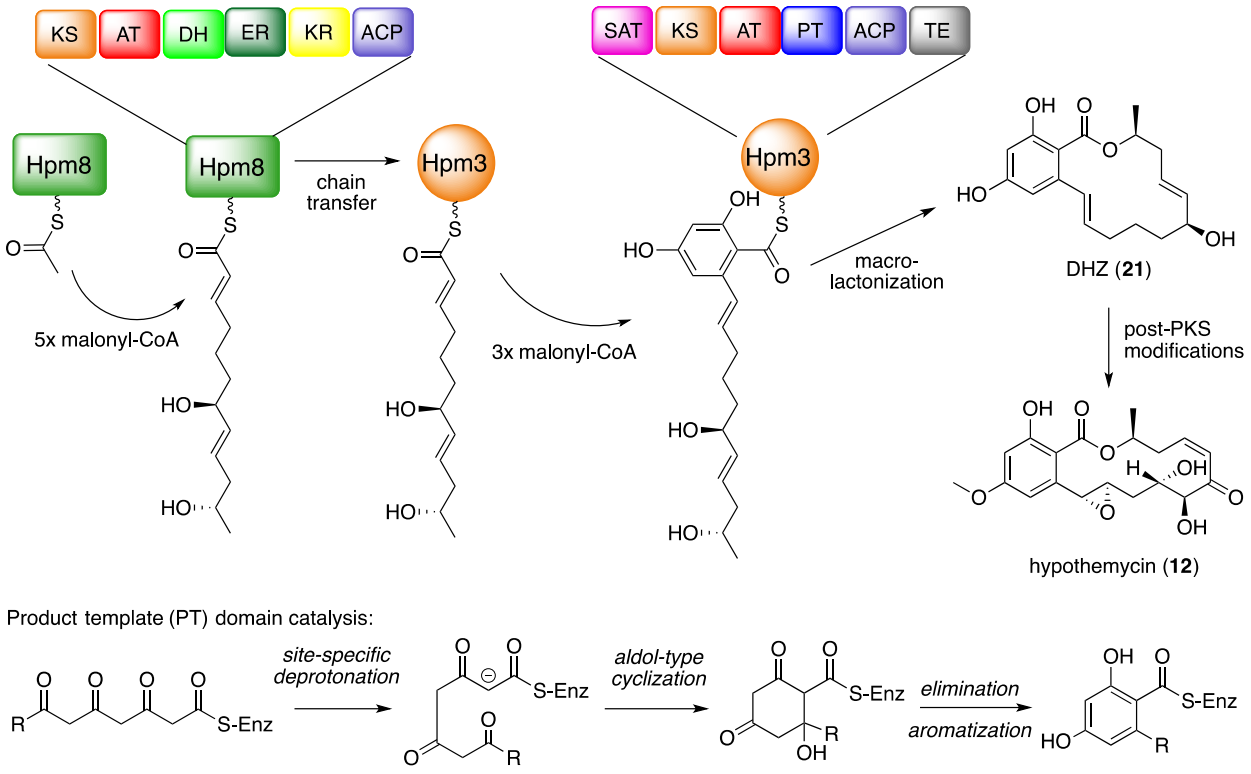

Figure 11: Hypothemycin (12) biosynthesis

In the years following this biosynthesis proposal based on gene sequence,[33] our knowledge regarding the details of the dehydrozearalenol (**21**) assembly process has expanded. The pathway was reconstituted *in vitro* in 2010 with enzymes expressed in *Saccharomyces cerevisiae* BJ5464-NpgA.[28] In these experiments, we learned that Hpm8 cannot function without its non-reducing partner. When Hpm3 was absent, only shunt products were observed. Also, no RAL products could be formed when Hpm8 was paired with the equivalent NR-PKS partner from a similar biosynthetic pathway, meaning the pairs cannot be mixed and matched. The SAT domain was found to be an important mediator in the protein-protein cross talk. However, a small molecule analogue representing the hexaketide intermediate could be incorporated into DHZ (**21**) through the solo action of Hpm3 with or without its SAT domain. Finally, the *in vitro*

reconstitution also produced adequate amounts of DHZ (**21**) to assign the stereochemistry of the 6' hydroxyl as (*S*). As is evident by the linear representation of the hexaketide intermediate in Figure 11, this suggested that the Hpm8 KR domain can reduce from both faces of the growing chain. It was determined in 2012 that the KR is programmed to select a face based on the length of the growing chain.[14]

At the commencement of this body of work, the product of the Hpm8-Hpm3 partnership was known, as was the hexaketide intermediate transferred from Hpm8 to Hpm3. However, it had never been shown that the proposed intermediates of HR-PKSs were true intermediates. One goal of my study of hypothemycin (**12**) was to demonstrate the intermediacy of the proposed Hpm8-bound triketide, which will be discussed in Chapter 2, and was published as part of an article appearing in the Journal of the American Chemical Society.[38] A second goal of my study of hypothemycin (**12**) was to characterize the ACP domain of a HR-PKS, and a discussion of this will take place in Chapter 4.

*Lovastatin (**1**)*

Lovastatin (**1**) is a polyketide isolated from *Aspergillus terreus*, famed for its use in the treatment of hypercholesteremia under the trade name Mevacor (Merck).[39] It was discovered in 1980,[40] a few years after the discovery of the less successful analogue compactin (**22**) using activity guided fractionation of fungal extracts.[41] The commercialization of lovastatin and development of its synthetic and semi-synthetic analogues, the statins (Figure 12),[42] revolutionized the treatment of high cholesterol,[43] in addition to earning pharmaceutical companies billions of dollars each year.[39] High cholesterol levels in blood lead to the development of atherosclerotic cardiovascular disease ("hardening of the arteries") and are a

major risk factor for potentially fatal and debilitating events such as heart attack or stroke.[44] Cardiovascular disease, encompassing diseases of the heart and cerebral vasculature, was the second leading cause of death in Canada in 2012, accounting for 25% of all deaths.[45] According to Statistics Canada, between 2007 and 2011, 11.6% of adults aged 20-79 living in Canadian provinces were being treated with a statin, and if the guidelines for treatment were followed for all at risk patients, that number would be 27.1% or 6,518,200 people.[46] Statistics Canada estimates that complete treatment of the Canadian at-risk population with statins would prevent 386,200 cardiovascular events over 10 years. Therefore, the significance of this small polyketide and its analogues cannot be overstated.

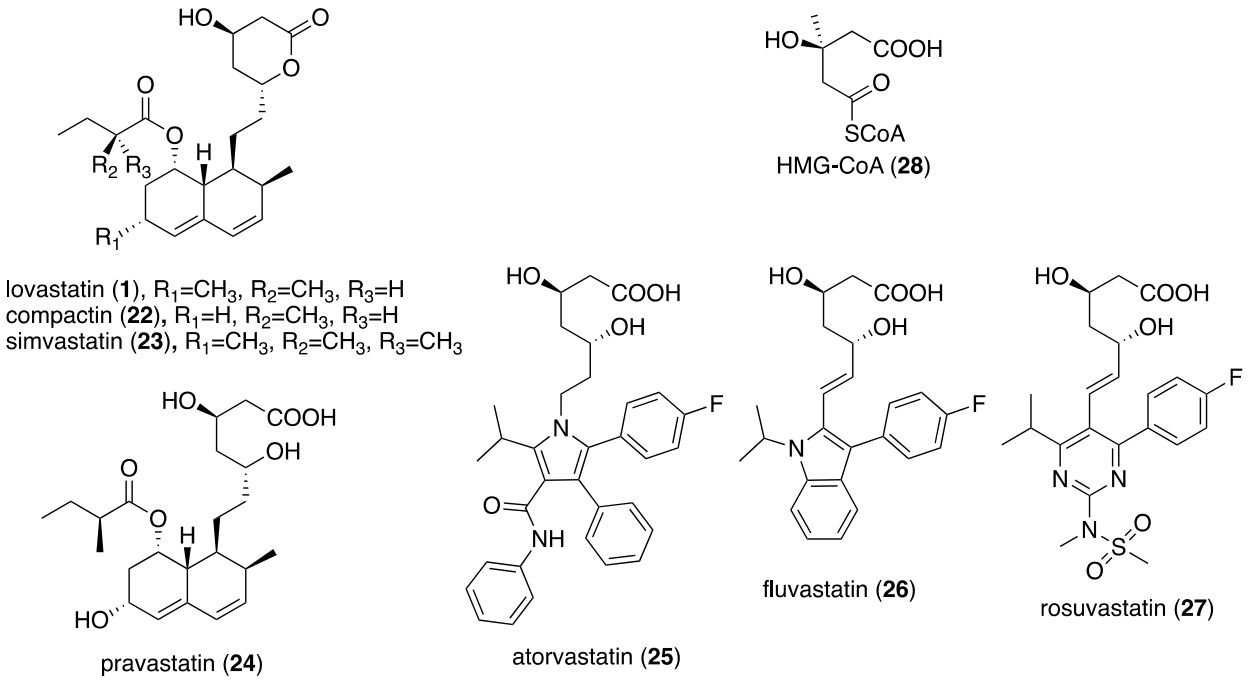

Figure 12: Statins available to prescribe in Canada, compared to HMG-CoA (28)

Statins work through the inhibition of HMG-CoA reductase, the rate-limiting step in cholesterol biosynthesis in the liver.[43] This inhibition causes the liver cells to increase their

concentrations of low-density lipoprotein receptors to clear cholesterol from the blood stream. The "war-head" shared by all these molecules resembles the substrate of the reductase, hydroxymethylglutaryl-CoA (HMG-CoA, **28**), and binds reversibly and competitively in the active site.

In addition to the impact of lovastatin (**1**) in healthcare, investigations of its biosynthesis have had a large impact in the field of polyketide chemistry since its assembly from acetate was first demonstrated in the early 1980s.[47,48] A summary of our understanding of lovastatin biosynthesis prior to this work is summarized in Figure 13. As previously introduced, LovB, with the help of LovC and the necessary cofactors, assembles the nonaketide chain.[25] It is known that LovB also catalyzes an intramolecular Diels-Alder reaction to form the decalin ring, which is proposed to take place at the hexaketide chain as shown.[49,50] The nonaketide is released by LovG to provide the key intermediate dihydromonacolin L (**11**).[27] LovA then performs two oxidations in succession to produce monacolin J.[51] LovF, another HR-PKS, assembles the methylated dipeptide shown, which LovD then transfers to the newly installed hydroxyl group to furnish lovastatin (**1**).

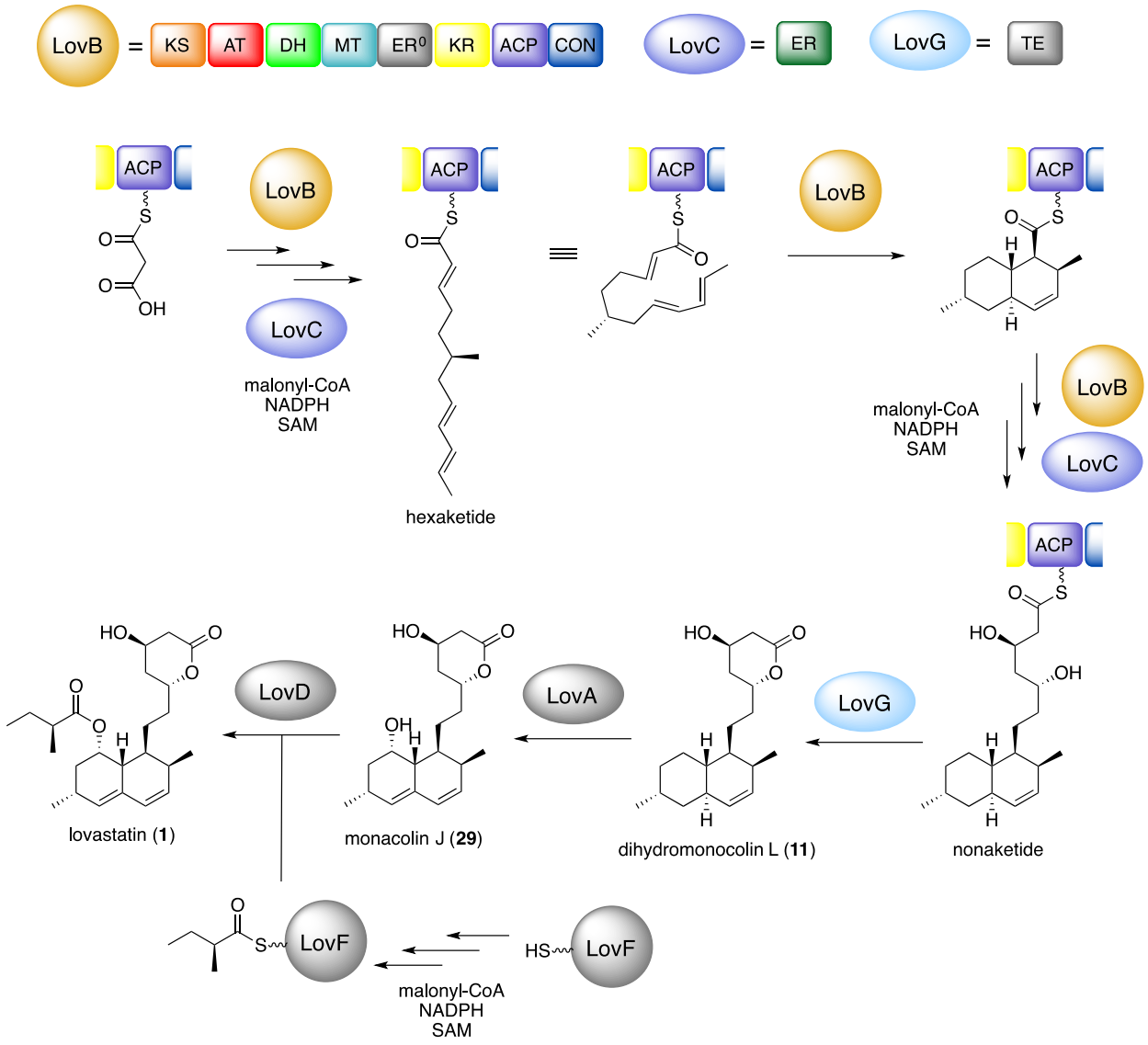

Figure 13: Lovastatin biosynthesis overview

The heterologous expression of the biosynthetic enzymes has allowed some interesting details to come to light, and has permitted the investigations in this thesis. For example, we have learned that the CON domain, which has no known function, is required for correct functioning of the enzyme.[25] It has been proposed to be involved in the Diels-Alder cyclization, which will be the main focus of Chapter 3, where I describe my work characterizing the LovB Diels-

Alderase activity. As with DHZ (**21**), the expression of purified enzymes has allowed the investigations into the enzyme-bound intermediates in dihydromonacolin L (**11**) assembly. The synthesis of the intermediates for this assay is discussed in Chapter 2 alongside the equivalent DHZ experiments. Finally, the LovB-ACP was expressed as a stand-alone enzyme, as discussed in Chapter 4 with Hpm8-ACP.

CHAPTER 2: INCORPORATION OF PARTIALLY ASSEMBLED INTERMEDIATES INTO POLYKETIDE SYNTHASE PRODUCTS

Introduction

In order to prove a compound's intermediacy in a metabolic pathway, it is convention to synthesize this compound with certain positions bearing non-natural isotopes and follow their conversion by organisms or enzymes. This was first done with radioactive isotopes ^{14}C and ^{3}H, but the surge of NMR techniques since the 1970s allowed the use of stable isotopes such as ^{13}C, ^{2}H, ^{18}O and ^{15}N in these so-called "feeding" experiments.[52] However, when it comes to polyketides, one must remember that the true intermediates are enzyme bound. As alluded to in the introduction, the growing polyketide chains are linked to the ACP domain through a phosphopantetheine prosthetic group (Figure 14).[53] Often referred to as an "arm", this flexible moiety is responsible for shuttling the growing intermediate to the various active sites of the synthase. Therefore, in order to elucidate the structures of the enzyme bound intermediates, chemists needed to develop methodology that would allow the PKS to recognize partially assembled polyketides as substrates, even though in Nature these intermediates are not present in solution. Abbreviating the phosphopantetheine group to an *N*-acetylcysteamine moiety (abbreviated as SNAC) appeared to be adequate for enzyme recognition, and the first partially assembled polyketide intermediates were successfully incorporated into macrolide polyketide products in 1987.[54,55]

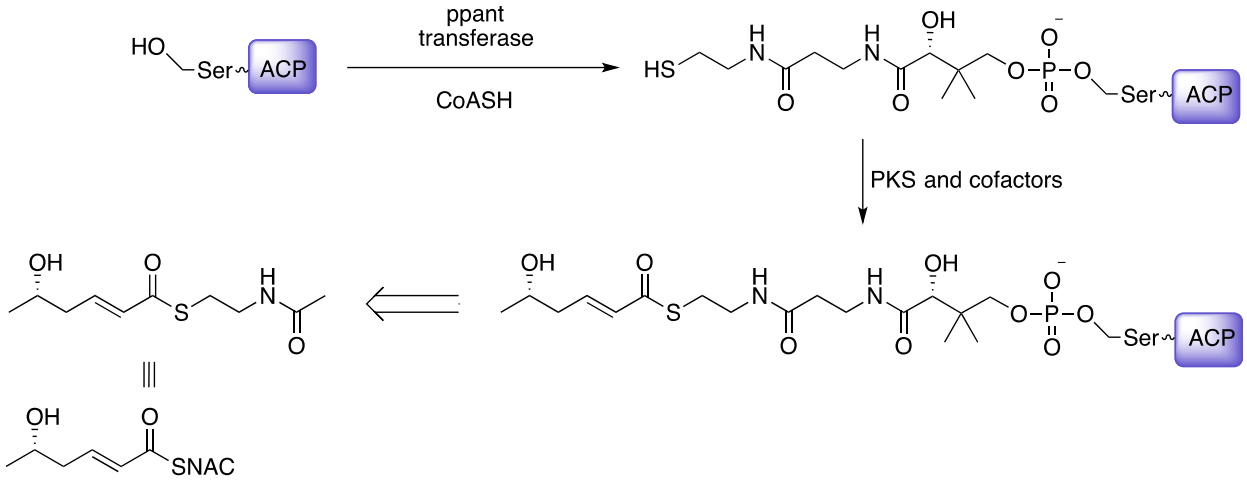

Figure 14: The phosphopantetheine prosthetic group carries the growing polyketide chain. N-acetylcysteamine (SNAC) thioesters can approximate this group

These pioneering experiments, collegially accomplished by the groups of Hutchinson and Cane, were the first to confirm the processive nature of polyketide biosynthesis. In these experiments, the researchers fed ^{13}C-labeled SNAC intermediates directly to live cultures of the producing bacteria, and these intermediates were elaborated by enzymes that would later be characterized as modular type I PKSs that use proprionate building blocks. It was anticipated that this methodology could be applied to acetate-derived polyketides in fungi, however there was limited success due to the β-oxidation of labeled precursors.[56] The work described in this thesis, and published in the Journal of the American Chemical Society in 2013,[38] was the first example of incorporating partially assembled intermediates into polyketide products by a PKS using purified enzymes, instead of intact cells or cell-free extracts. This avoids the degradation of the substrates by cellular machinery and makes a definitive link with the enzymes. In the discussion that follows, I will describe the methodology behind this work involving the hypothemycin (**12**) system, clearly indicating the portion of the publication attributable to me, and discuss the

contributions of these experiments to the field. I will then discuss on-going work to apply similar methodology to the lovastatin (**1**) system.

At the onset of this work, our group had previously demonstrated the intermediacy of the hexaketide shown in Figure 11 (Chapter 1), by its successful elaboration by Hpm3 to produce DHZ (**21**).[28] What remained to be demonstrated was that the series of reactions shown in Figure 15 is in fact how Hpm8 assembles the highly reduced portion of DHZ (**21**). Based on our knowledge of fatty acid biosynthesis and modular type I polyketide biosynthesis, this reaction series was for a long time assumed to be correct for iterative polyketide biosynthesis, but our work was the first to confirm this hypothesis using purified enzymes.

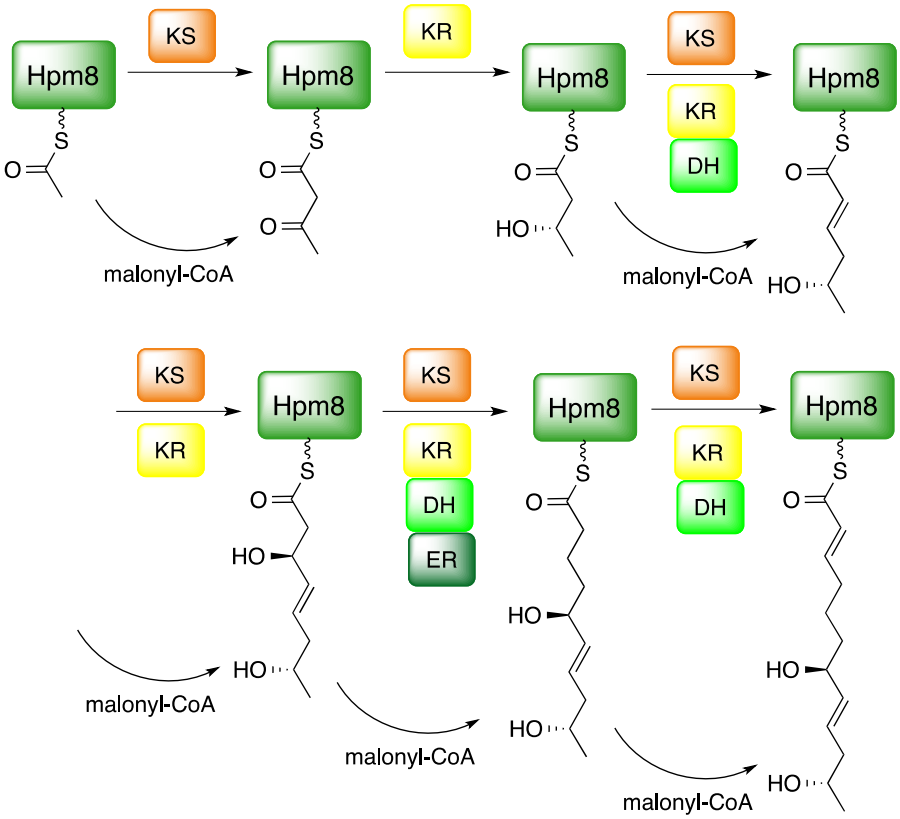

Figure 15: 14 discrete enzymatic steps catalyzed by Hpm8, highlighting the structure of each intermediate before the subsequent condensation reaction

.

Results and Discussion

*Incorporation of ^{13}C-SNAC Triketide (**30**) into DHZ (**21**) by Hpm8/Hpm3*

The first Hpm8 intermediate to be tested was the triketide **30**. The synthetic route to intermediate **30** is shown in Figure 16. The ^{13}C label was commercially available as triethylphosphonoacetate (**31**), labeled at the carbonyl carbon as indicated by the asterisk. Through saponification and DCC/DMAP coupling to *N*-acetylcysteamine, phosphonate **31** becomes phosphonate **32**. A Masamune variation of the Horner-Wadsworth-Emmons reaction, which uses mild base, condenses reagent **32** with aldehyde **33**, assembling protected triketide **35**.[57] The stereogenic centre of aldehyde **33** is purchased as ester **34**, which is converted by a known procedure.[58] Facile deprotection of the *tert*-butyldimethylsilyl ether **35** furnishes ^{13}C-SNAC-triketide **30**.

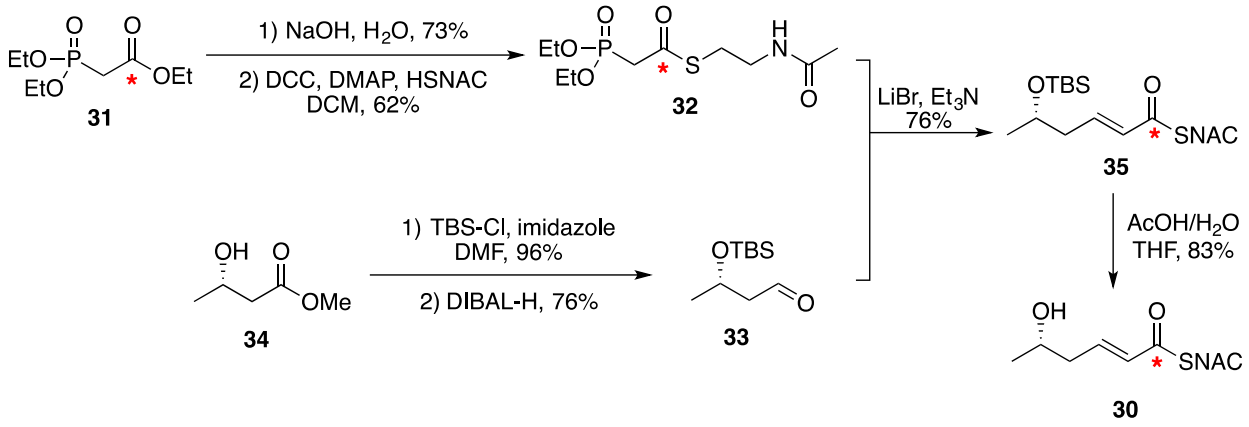

Figure 16: Synthesis of ^{13}C labelled triketide 30 (* = ^{13}C)

With triketide **30** in hand, our focus turned to the enzymatic assay with Hpm8 and Hpm3. Heterologous expression of the enzymes in *S. cerevisiae* strain BJ5464-NpgA was performed by our collaborators Yi Tang and coworkers at the University of California (Los Angeles). They performed the assay depicted in Figure 17. The challenge of such an assay is to create conditions

where the loading of triketide **30** is favoured over a background reaction where Hpm8/Hpm3 build DHZ (**21**) entirely out of malonyl-CoA. Our collaborators achieved this by premixing the enzymes with the synthetic precursor. The resulting "feed and chase" method involved 10 rounds of first feeding the substrate, waiting 15 minutes, then chasing with malonyl-CoA. The reactions were incubated for 10 hours total with the addition of malonyl-CoA every hour and substrate every 2 hours. Liquid chromatography mass spectrometry (electrospray ionization) confirmed the incorporation of the triketide into DHZ (**21**), and the reaction was scaled up to obtain an adequate quantity to confirm the product and location of the label by NMR.

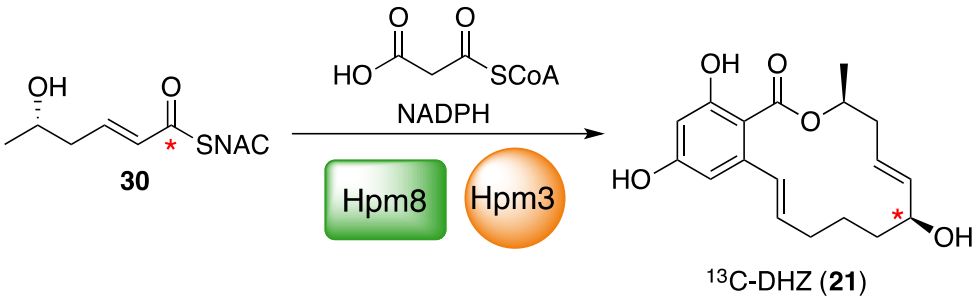

Figure 17: Incorporation of ^{13}C-triketide 30 into DHZ (21) by Hpm8 and Hpm3

This result confirmed the intermediacy of the proposed triketide and validated the "feed and chase" assay method. At this point, the project was completed by fellow PhD student, Zhizeng Gao, who synthesized seven other proposed intermediates, and four unnatural analogues. Ultimately, we found all eight intermediates we tested (and three of four analogues) to be incorporated into DHZ (**21**), confirming the reaction series proposed in Figure 15.

Synthesis of Proposed LovB Intermediates

Encouraged by our success with hypothemycin, our goal was to replicate these experiments with the lovastatin system. We reasoned this was a worthy endeavour because (1) it would demonstrate that the conclusions drawn from the hypothemycin study apply to other PKS systems (such as the LovB, which is similar to a PKS-NRPS hybrid), and (2) we might learn more about the nature of the LovB-bound intermediates and enzymatic steps en route to DHML (**11**).

The synthetic targets required for this assay are shown in Figure 18. We sought to synthesize the proposed ketide of each chain length as the corresponding SNAC thioester with either a ^{13}C or ^{2}H label. When I joined this project, fellow graduate student Rachel Cochrane had synthesized diketide **36**, triketide **37** and tetraketide **38**, all labeled with ^{13}C at their thioester carbonyl carbons. Our collaborators had recreated the assays described in the section above with LovB, LovC and a thioesterase. They found that, while the diketide **36** did not incorporate into DHML (**11**), both the triketide **37** and tetraketide **38** were successfully elongated.

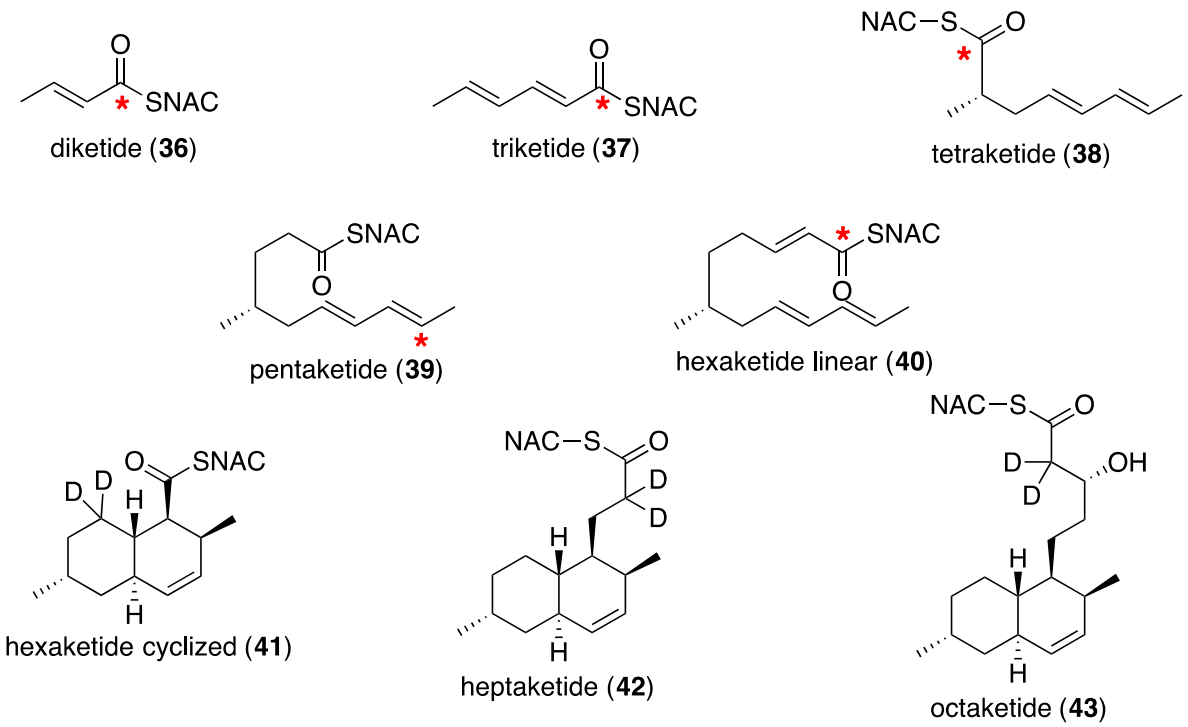

Figure 18: Proposed LovB ketides, as their isotope labelled SNAC thioesters (* = ^{13}C)

With these encouraging early results, I began the synthesis of pentaketide **39** and linear hexaketide **40**. Both are assembled in the same manner, based on a modified version of the procedure Dave Witter developed for the hexaketide in 1996 (Figure 19).[49] The synthesis begins with commercially available (*R*)-citronellol (**44**), which possesses the key methyl group as the stereogenic centre. Protection as the acetate **45** precedes an ozonolysis with *in situ* protection to furnish acetal **46**.[59] Subsequent deprotection and oxidation with Dess-Martin periodinane[60] affords the aldehyde **47** that will be the first substrate for a series of Wittig-type reactions to elaborate the chain. First, a Horner-Wadsworth-Emmons[61] reaction produces the ester **48**. Functional group manipulation leads to a second aldehyde **49**, the substrate for a Schlosser modification of the Wittig,[62] which selectively produces the *trans* dienal **50**. It is at this step the synthesis diverges; for the pentaketide, the reaction installs a ^{13}C from ethyltriphosphonium

iodide, while a natural abundance phosphonium salt is used for the hexaketide synthesis. Deprotection of acetal **50** with saturated oxalic acid reveals a third aldehyde **51**. En route to the pentaketide, this aldehyde is oxidized using the Pinnick procedure[63] to acid **52**. DCC/DMAP coupling to *N*-acetylcysteamine produces the labeled pentaketide **39**. The natural abundance aldehyde **51** meanwhile is elaborated by a Masamune variant of the Horner-Wadsworth-Emmons reaction,[57] using the ^{13}C-SNAC phosphonate **32,** previously described.

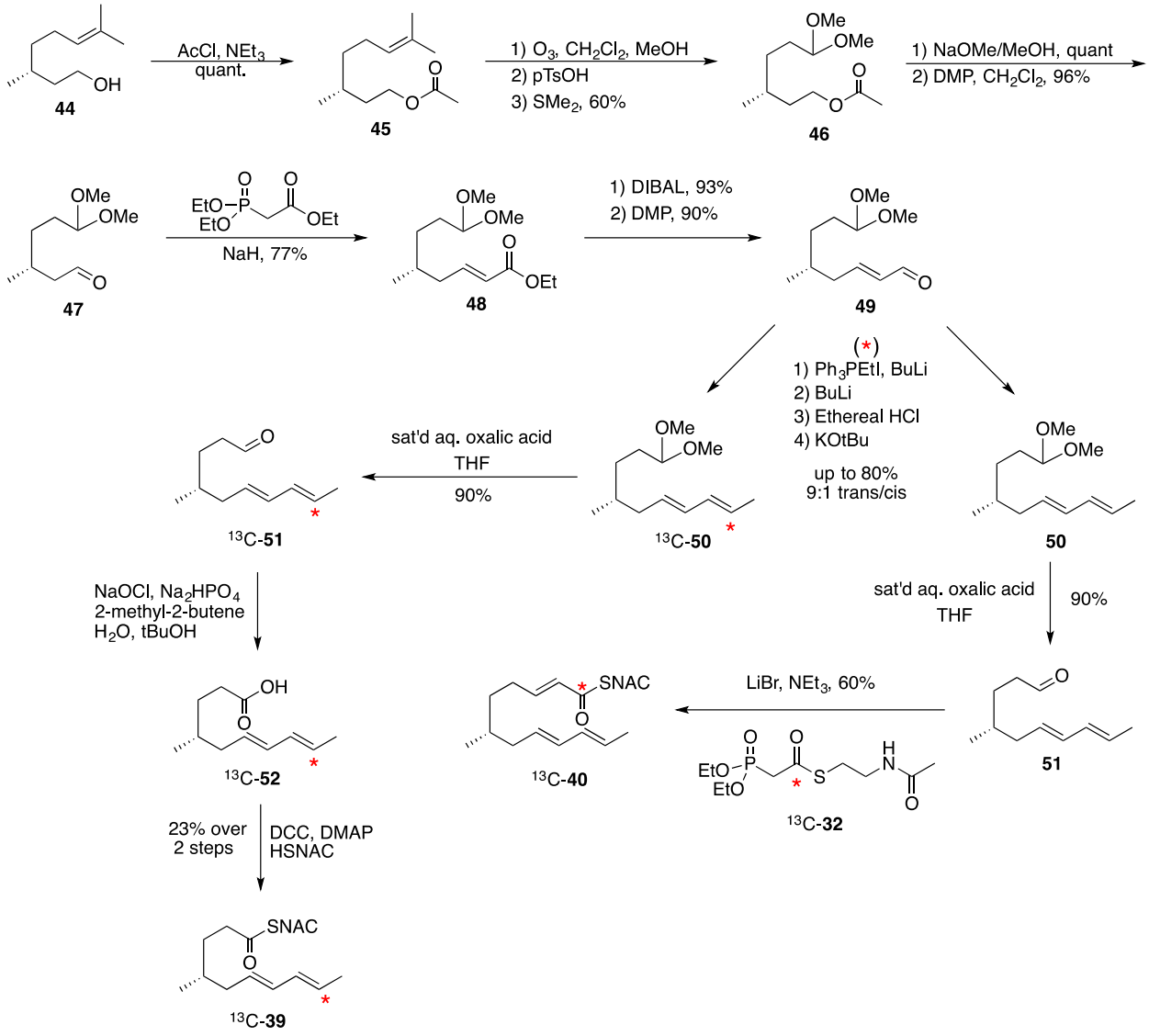

Figure 19: Synthetic Route to ^{13}C pentaketide 39 and hexaketide 40 (* = ^{13}C)

The next task was the synthesis of the deuterium labeled heptaketide **42** and octaketide **43**. Instead of building up from commercially available starting material, these syntheses were accomplished through the degradation of DHML (**11**), using a procedure developed by John Sorensen in his PhD thesis (Figure 20).[64] Fermentation of an *Aspergillus nidulans* strain complemented with both the LovB and LovC genes produces the DHML (**11**) used as a starting material.[24] The reaction series relies on ozonolytic cleavage of alkenes to shorten the chain two carbons at a time, and therefore the double bond within the decalin of DHML (**11**) must be protected as the dibromide **53**. Mesylation/elimination of the lactone alcohol provides the α,β-unsaturated compound **54**. Ozonolysis of the olefin is performed in the presence of sodium methoxide and methanol, leading to ester **55**.[65] Having achieved the octaketide skeleton, the reaction series now diverges. To complete the synthesis of the octaketide, first the bromides are removed using zinc in acetic acid to recreate the double bond and produce octaketide methyl ester **56**. For the installation of the deuterium atoms α to the ester, it was determined that equilibrium conditions were optimal, where in the presence of base (potassium tert-butoxide) and an excess of deuterated methanol, the compound is fully deuterated after two days at room temperature. In the same pot, the subsequent addition of a small amount of deuterium oxide produces octaketide acid **57** without requiring the isolation of the deuterated ester. DCC/DMAP coupling to *N*-acetylcysteamine converts the free acid **57** to the SNAC thioester **43**.

For the heptaketide synthesis, another round of mesylation/elimination and ozonolysis is required to shorten the chain by two more carbons. First, brominated ester **55** is treated with methylsulfonium chloride and triethylamine to produce α,β-unsaturated ester **58**, then repeating the same ozonolysis conditions affords ester **59**. Deprotection regenerates the olefin and produces heptaketide ester **60**. An identical deuteration/saponification procedure leads to the

deuterated heptaketide acid **61**, and DCC/DMAP coupling leads to the final product, SNAC-heptaketide **42**.

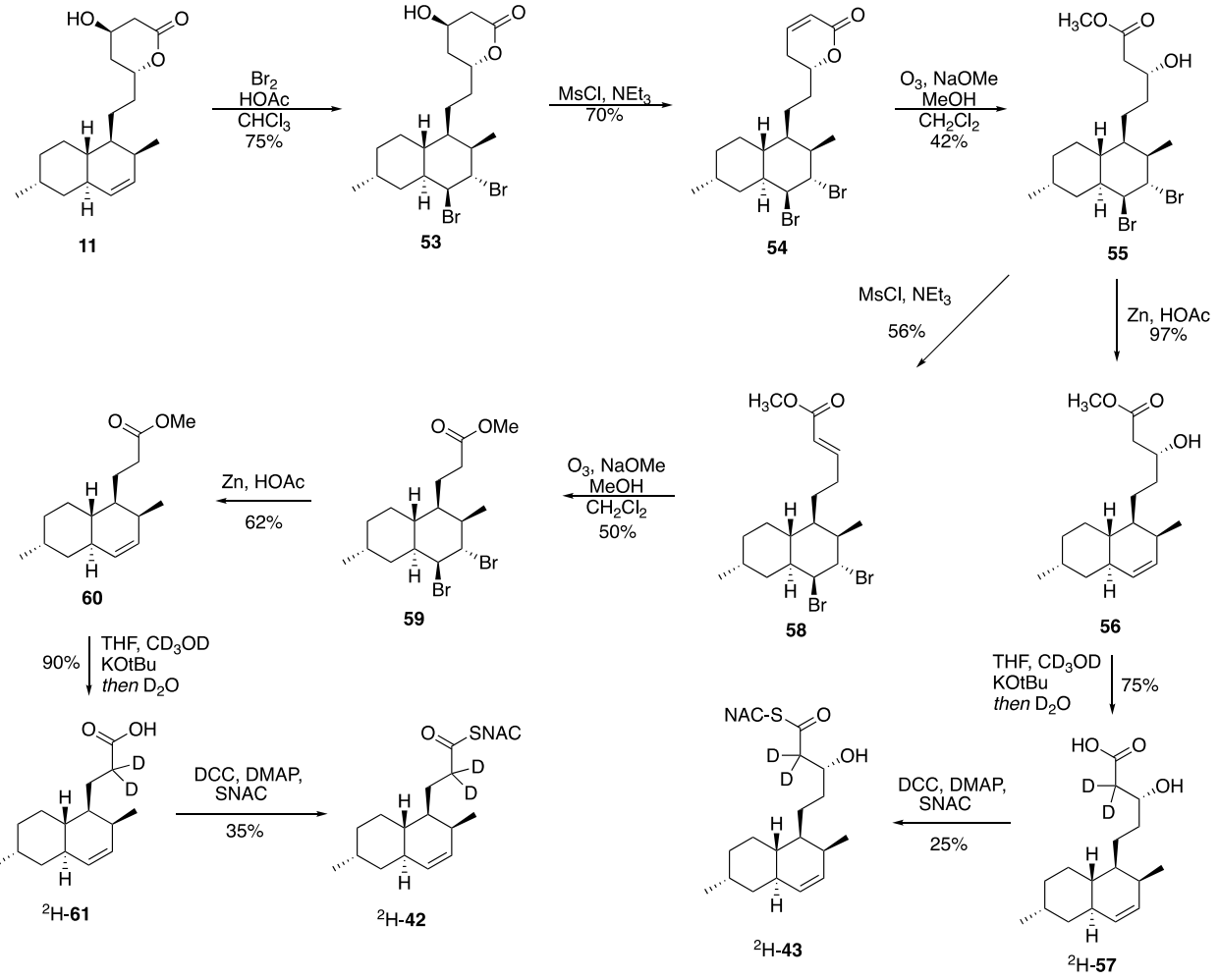

Figure 20: DHML (11) degradation to synthesize ^{2}H-labelled heptaketide 42 and octaketide 43

With the completion of the DHML (**11**) degradation to make heptaketide **42** and octaketide **43**, the only proposed ketide left to synthesize was the cyclized hexaketide **41**. This task was attempted by fellow PhD student Eva Rodriguez-Lopez, who obtained an interesting result in the final steps of the work. Having constructed the hexaketide skeleton as the ethyl ester **62**, the plan was then to saponify and couple to *N*-acetylcysteamine, as shown in Figure 21.

However, saponification was not successful, even with heating and prolonged reaction times. We concluded that the hydrophobicity of the molecule and steric bulk of the reacting centre prevented hydroxide from attacking the ester to form the tetrahedral intermediate. If this is the case, it has interesting implications for our proposed biosynthetic pathway. A review of Figure 2 shows that at every chain length, the growing polyketide must be transferred from the ACP back to the KS for the next round of extension. If the steric bulk of compound **62** was too crowded for saponification, one could imagine that transthioesterification of the enzyme bound hexaketide from the ACP phosphopantetheine to the KS cysteine would also be very slow. The sheds doubt on the intermediacy of this structure. An alternative biosynthetic scheme is presented in the upcoming chapter.

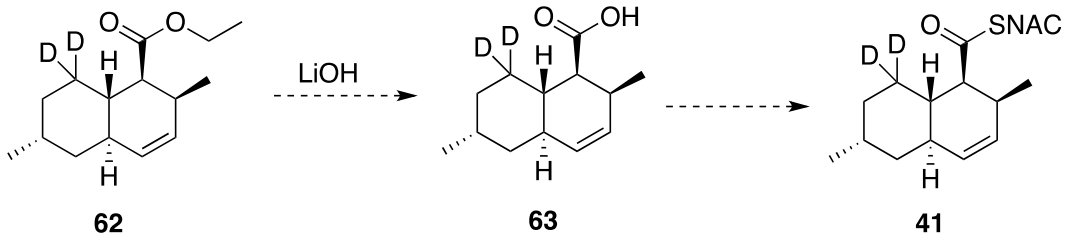

62 **63** **41**

Figure 21: Due to the failed saponification, hexaketide 41 could not be synthesized

With one isotope-labeled ketide per chain length synthesized, the next step is the enzymatic assays to be performed by our collaborators to see if these proposed intermediates can be elongated into DHML (**11)**.

CHAPTER 3: INVESTIGATIONS INTO THE DIELS-ALDERASE ACTIVITY OF LOVB

Background

The Diels-Alder Reaction

The Diels-Alder reaction, named for the chemists who first characterized it in 1928, is the concerted [4+2] cycloaddition of a 1,3 diene and an electron poor alkene, referred to as the dienophile (Figure 22).[66] Over the past century, the reaction has proven to be of great synthetic utility thanks to the large amount of complexity that can be installed in one reaction under mild conditions and with atom economy. Two carbon-carbon bonds and four contiguous stereocenters are formed in one stereocontrolled step. However, compared to the plethora of enzyme-catalyzed reactions involving charged or radical intermediates, there are few known examples of pericyclic reactions catalyzed by enzymes.

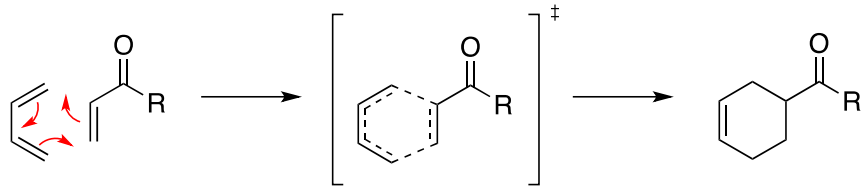

Figure 22: A typical Diels-Alder reaction, showing the concerted transition state.

Diels-Alderase Activity of LovB

One such "Diels-Alderase" is LovB, as introduced previously, which has been extensively studied by our group. The possibility of a Diels-Alder reaction in the biosynthesis of lovastatin was first proposed in 1985 following labeling studies with ^{13}C, ^{2}H and ^{18}O precursors.[48] The isotope pattern observed was consistent with this proposition, and subsequently its feasibility could be explored by studying the equivalent non-enzymatic process. In 1996,

Witter and Vederas first synthesized hexaketide triene **40** and found that it does indeed undergo a Diels-Alder reaction spontaneously.[49] The results of these key experiments are summarized in Figure 23. Triene **40** has 4 theoretical cyclization geometries, based on the combinations of the endo versus exo relationship of the diene and thioester, and the pseudo-axial versus pseudo-equatorial conformation of the methyl group. The transition state geometry leading to the natural product would, for example, have the methyl group in a pseudo-axial position, and an endo relationship between the reacting partners, leading to compound **41**. When heated in organic solvent, it was found that the reaction progressed through transition states with pseudo-equatorial methyl groups only, leading to non-natural stereoisomers **65** and **66**. In Lewis-acid catalyzed conditions, only isomer **66** was isolated. In aqueous conditions, the reaction progressed with a half-life of two and a half days, and once again the natural stereochemistry was not observed. From these three experiments, the following conclusions are drawn: First, it is feasible that a biological Diels-Alder reaction takes place during lovastatin biosynthesis. Second, if this reaction did occur, it would require an enzyme because the correct stereochemistry is not observed. Even though a slow background cyclization takes place, the reaction rate leading to the correct product is zero without an enzyme.

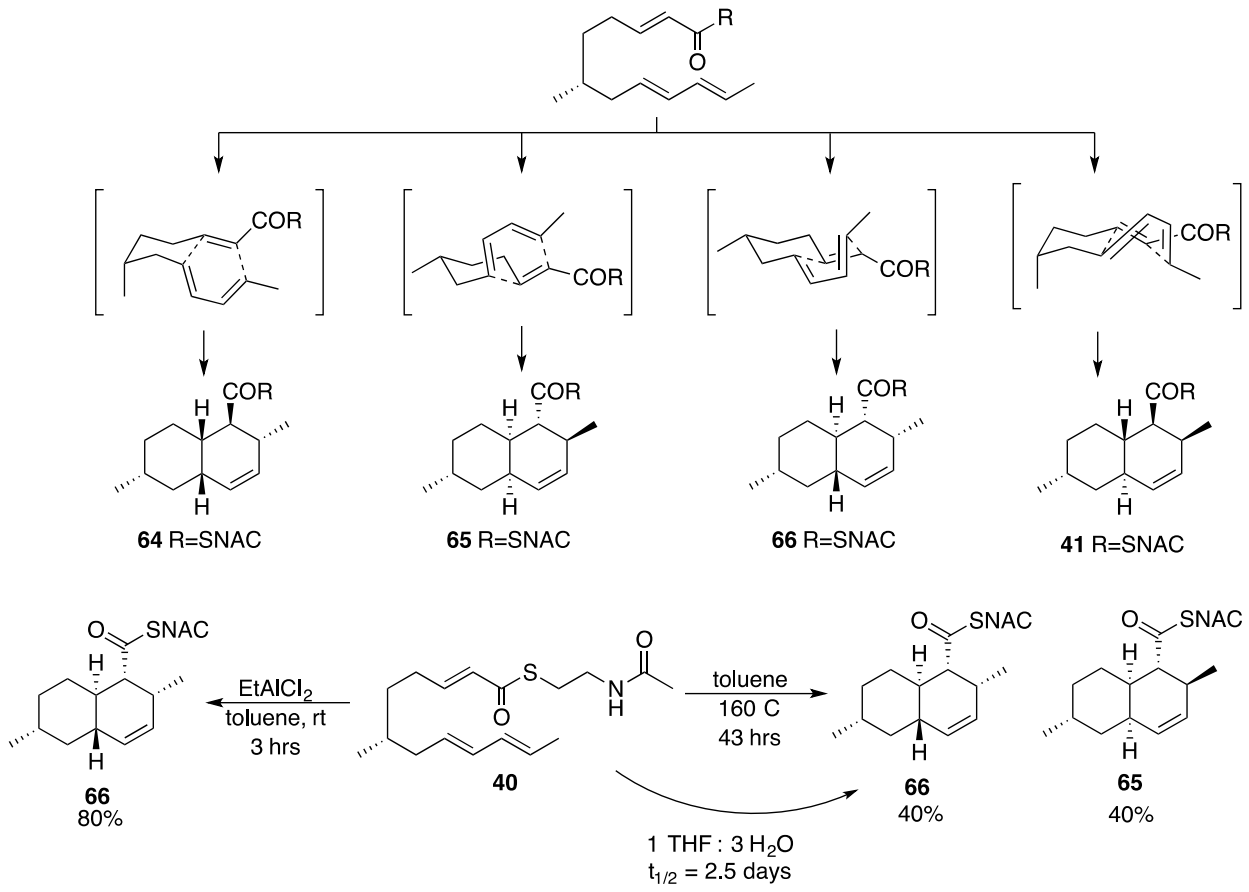

Figure 23: Cyclization modes of triene 40, and results of enzyme-free reactions.

The identification of the LovB gene and its heterologous expression in *A. nidulans*[24] allowed the study of this hypothesis with purified enzymes. Auclair *et al* exposed hexaketide triene **40** to LovB and obtained the results described in Figure 24.[50] After three days of reaction, a mixture of inseparable thioesters was isolated. Reacting the mixture with sodium ethoxide in ethanol converted the product to their ethyl esters, which were separated and characterized as compounds **67**, **68**, and **62**, in a 15:15:1 ratio. The stereochemistry of the natural product (equivalent to the stereochemistry of thioester **41** and ethyl ester **62**) was not present in the

products of control reactions, where the enzyme was either absent or heat inactivated. Therefore, it was concluded that LovB does catalyze the conversion of triene **40** to decalin **41**.

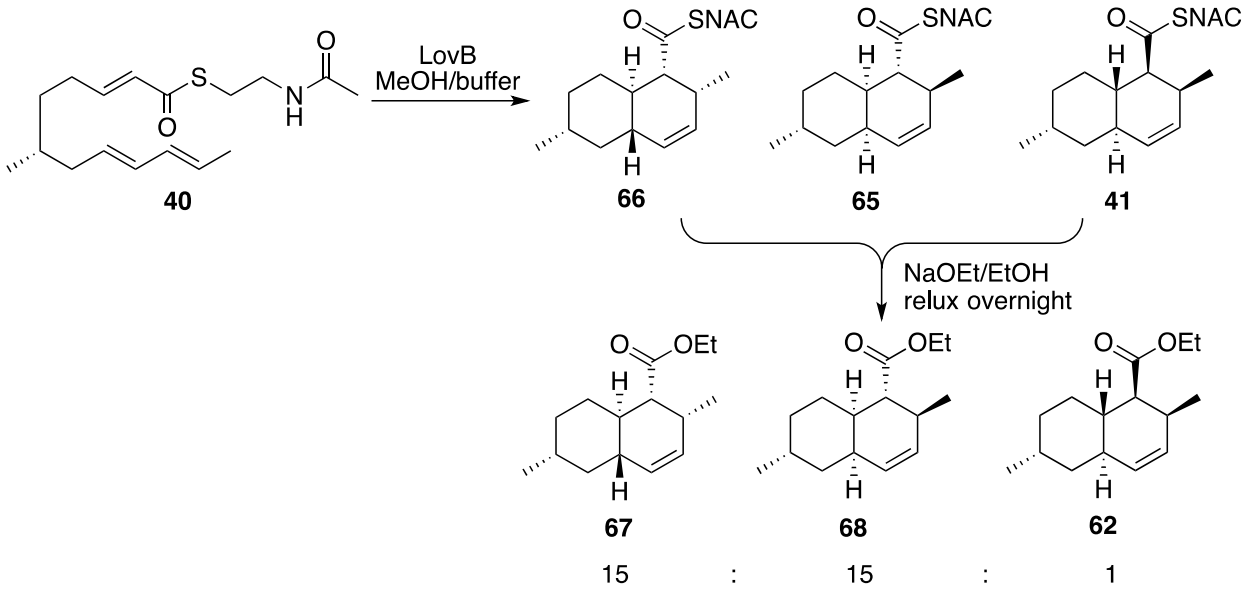

Figure 24: Assay studying the LovB catalyzed cyclization of triene 40

However, there are many questions left to be answered, some of which will be explored in this thesis. First, the extent to which a [4+2] cyclization is concerted is a matter requiring investigation. In order to be a Diels-Alderase, LovB would need to catalyze this reaction in one concerted step, rather than the equivalent step-wise nucleophilic process. However, in order to study the mechanistic details of this reaction, one would need to isolate the Diels-Alderase activity. LovB is a large multi-domain enzyme, and one of our goals is to pinpoint which domain actually catalyzes the cyclization. Lastly, these experiments do not prove the intermediacy of hexaketide triene **40**. It is possible that the Diels-Alderase domain is somewhat promiscuous and the conversion of triene **40** to decalin **41** is not a representation of its native activity. In fact, because the triene is SNAC bound, as opposed to ACP bound, we are already working with a

substrate analogue, which may explain the slow reaction rate. So while there is no doubt that LovB catalyzes the conversion of **40** to **41**, there are still many questions to answer regarding this aspect of lovastatin biosynthesis.

Overview of Known Diels-Alderase Enzymes

Relatively few naturally-occuring enzymes are known to catalyze a [4+2] cycloaddition, and the topic has been covered in numerous reviews.[67-74] Herein I will give a brief introduction to the enzymes that, in addition to LovB, catalyze [4+2] cyclizations, possibly by a Diels-Alder mechanism, en route to natural products. While there is currently no evidence to support or refute a pericyclic, concerted [4+2] cycloaddition for each enzyme, it is convention to refer to these enzymes as "Diels-Alderases", recognizing this term is currently defined as an enzyme that catalyzes the formation of a cyclohexene ring from a conjugated diene and an alkene stereoselectively.[72]

With the diversity amongst the Diels-Alderases, it is difficult to categorize them. At present, two common themes can be used to group the enzymes into four categories (Table 1).[72,74] Firstly, a few of the Diels-Alderase enzymes catalyze the formation of decalin systems. Secondly, they can be mono- or multi-functional. Table 1 contains, to the best of my knowledge, all enzymes proposed to be Diels-Alderases, grouped by homology, though the level of evidence supporting the proposals varies. Enzymes in bold have been purified to homogeneity and the catalysis has been replicated *in vitro*, and therefore the evidence for classifying these nine enzymes as Diel-Alderases is strongest. Non-bolded enzymes have some evidence, such as homology with known Diels-Alderases or through gene-deletion experiments, though *in vitro* reconstitution of the proposed reaction has yet to be accomplished.

Table 1: Proposed Diels-Alderases

	Monofunctional	Multifunctional
Decalin-forming	**PyrE3**, VstK, KijA, ChlE3, TcaE1	**Sol5**
	MycB, Fsa2, CghA, Eqx3, gNR600, CcsF	**LovB**
		Bet1
Non-decalin product	**SpnF** **TclM**, **TbtD** **PyrI4**, **AbyU**, VstJ, KijU, ChlL, TcaU4	**Macrophomate Synthase** **Riboflavin Synthase**

*see text for references

Multifunctional Decalin-Forming Diels-Alderases

LovB, the subject of this chapter, shares the category of multifunctional decalin-forming Diels-Alderases with two enzymes, Sol5 and Bet1. Sol5, or solanopyrone synthase, was the first example of a purified/reconstituted Diels-Alderase, published in 1998.[75,76] In the last step of the biosynthesis of solanopyrone A (**69**), Sol5 employs molecular oxygen to oxidize the primary alcohol to an aldehyde, activating the dienophile for [4+2] cycloaddition shown in Figure 25.

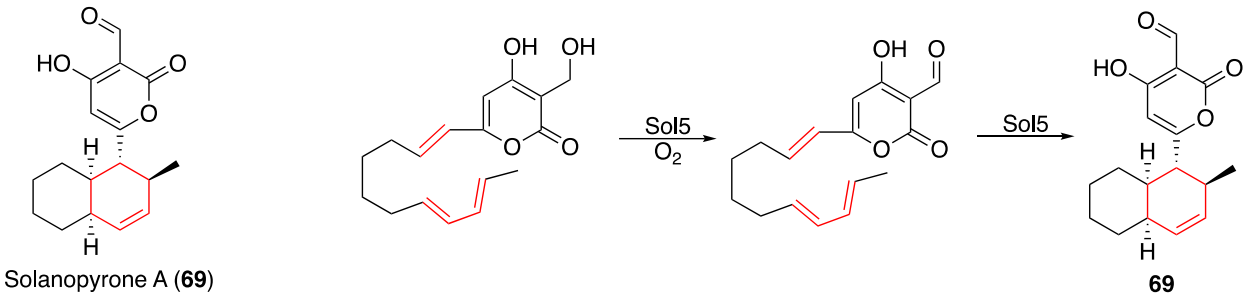

Figure 25: Reaction catalyzed by Sol5

Bet1, in contrast, was only recently characterized.[77] Like LovB it is a HR-PKS, and in cooperation with *trans*-acting enoyl reductase Bet3, it catalyzes the formation of polyketide product dehydroprobetaenone I (**70**). *A. oryzae* complemented with the *bet1* and *bet3* genes produced the PKS product **70** in fermentation, however, the activity of this protein pair has not

yet been reconstituted *in vitro*, and the potential of Bet1 as a Diels-Alderase has not been investigated further. Three possible pathways were proposed based on the order of the Diels-Alder reaction, chain extension and reductive offloading with the reductase domain (Figure 26). The authors did however note an interesting result likely ruling out the pathway following Diels-Alder A. When compound **70** was treated with $NaBH_4$, only the terminal aldehyde was reduced, while the ketone was spared. Further molecular modelling showed this carbonyl to be in a highly sterically congested environment. The authors postulate that if steric crowding prevents nucleophilic attack of $NaBH_4$, then it would likely also prevent attack by the enolate of malonate during assembly, thus making any chain extension post-Diels-Alder reaction very unlikely. This finding is relevant to the discussion of our findings concerning LovB.

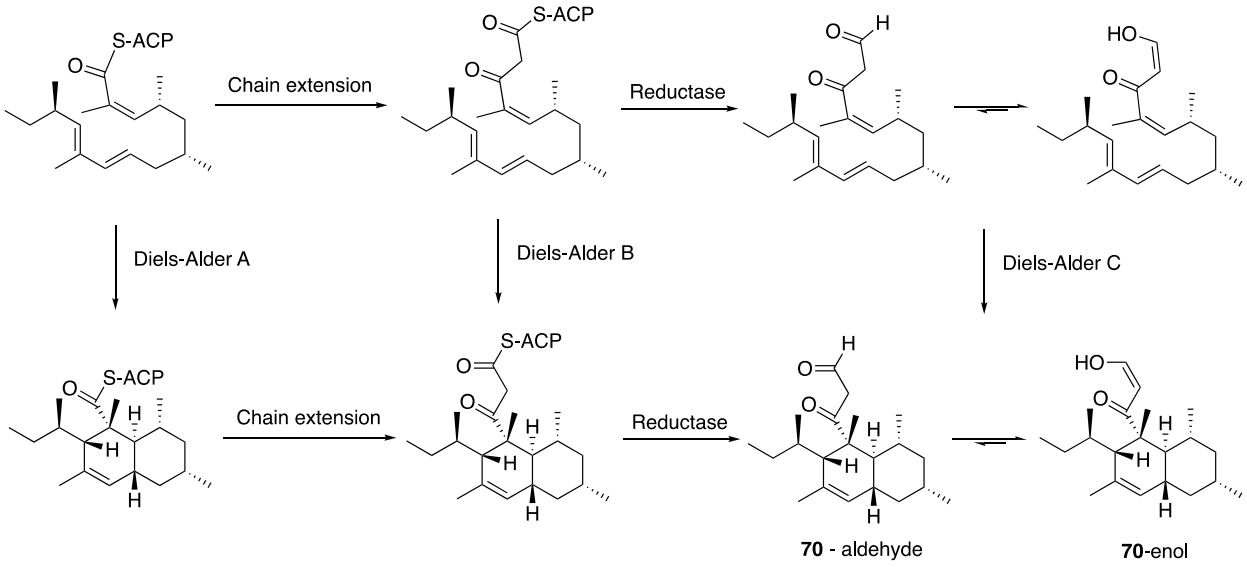

Figure 26: Proposed biosynthesis of dehydroprobetaenone I (70)

Monofunctional Decalin-Forming Diels-Alderases

PyrE3 is the first putative monofunctional Diels-Alderase for which catalysis leading to a decalin structure has been shown *in vitro*.[78] En route to the natural product pyrroindomycin,

PyrE3 was shown to perform the first of two [4+2] cyclization reactions, from intermediate **71** to decalin **72** (Figure 27). PyrI4, another monofunctional Diels-Alderase, then forms the spirocyclic cyclohexene found in intermediate **73**. Interestingly, PyrE3 contains a FAD binding motif, and will not catalyze the decalin formation without FAD bound, though no oxidation takes place. A number of gene clusters for similar natural products contain homologues for PyrE3, and thus it is suggested that these are also decalin-forming Diels-Alderases (See Table 1).[72,79]

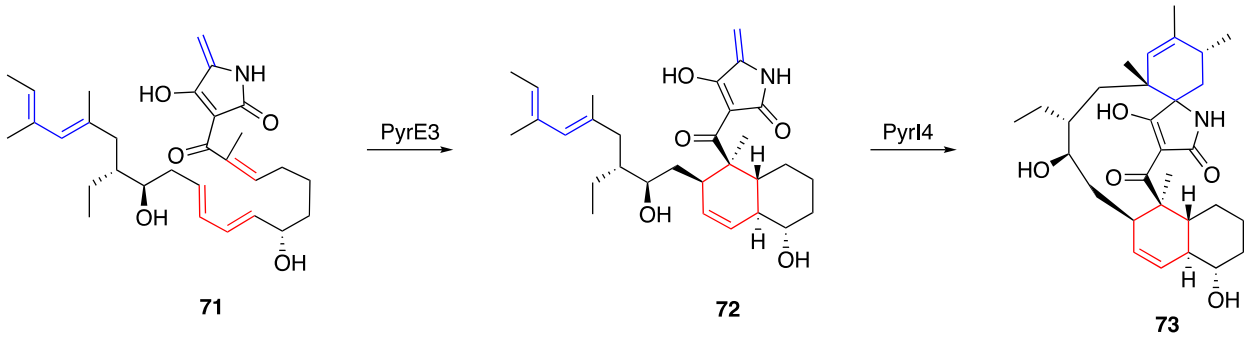

Figure 27: Diels-Alder sequence forming the pentacyclic core of pyrroindomycin

There is another group of monofunctional decalin-forming Diels-Alderases, whose Diels-Alderase was first proposed based on their homology to the enzyme FsaA. The gene *fsaA* was found in the gene cluster for fusarisetin A (**74**) in *Fusarium* sp. FN080326.[80] The authors suggest that the biosynthesis begins with the action of PKS-NRPS hybrid Fsa1, and its *trans*-acting ER Fsa3, to produce trichosetin (**75**), which is methylated to form equisetin (**76**), the final product in the related fungal species *Fusarium heterosporum* (Figure 28). The gene *fsa2* showed no known homologues, and thus to elucidate its function, the authors created a *Δfsa2* deletion mutant. From this culture, they were able to isolate the diastereomer of equisetin (**77**), which could be made by an exo Diels-Alder reaction.[80] Since only the endo diastereomer (equisetin, **76**) is found in the

wild type fungus, it was determined that Fsa2 plays a role in enhancing the stereoselectivity of the biosynthetic Diels-Alder reaction, and thus Fsa2 and its homologues may be Diels-Alderases.

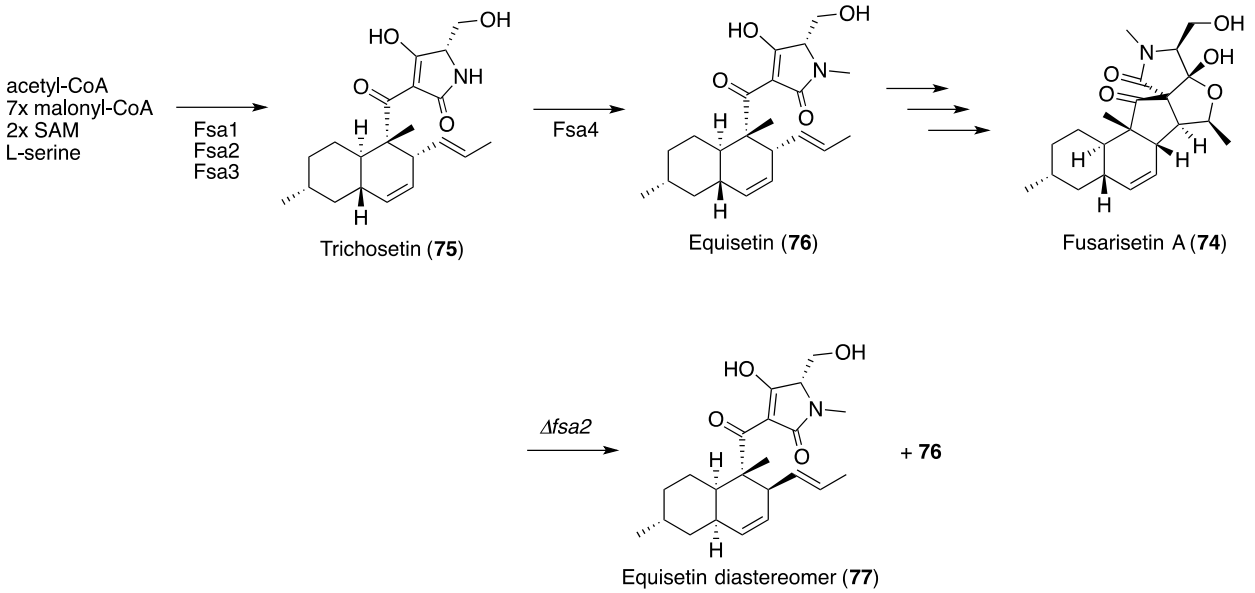

Figure 28: Biosynthesis of fusarisetin A (74)

A recent communication in the Journal of the American Chemical Society confirmed that one homologue of Fsa2, MycB is indeed a Diels-Alderase.[81] The authors searched the genome of the fungus that produces the natural product myceliothermophin E (**78**) (Figure 29). They found a gene cluster that contains a PKS-NRPS gene (*mycA*), an ER gene (*mycC*) and a third gene, *mycB* that has sequence homology to the proposed Diels-Alderase CghA, which through deletion experiments was confirmed to be involved in the production of the natural product **78**. When *mycB* alone was deleted, the production of all cyclized products was abolished, and the strain gave primarily linear compound **79** in its enol form and some air-oxidized compound **80**. MycB was heterologously expressed and found to convert compound **80** to final product **78**, while in the absence of enzyme compound **80** was degraded, confirming MycB is a Diels-Alderase.

However, MycB could not cyclize **79** in its enol form, suggesting the keto functionality is essential to the catalysis. The authors propose the biosynthetic pathway show in Figure 29. The product of the PKS-NRPS MycA/C is the keto form of compound **79**, which could be acted on immediately by MycB to produce cyclized product **81**, whose enolization/oxidation would lead to the final product **78**. Alternatively, **79** could enolize and be oxidized by air to produce **80**, which is a known substrate of MycB.

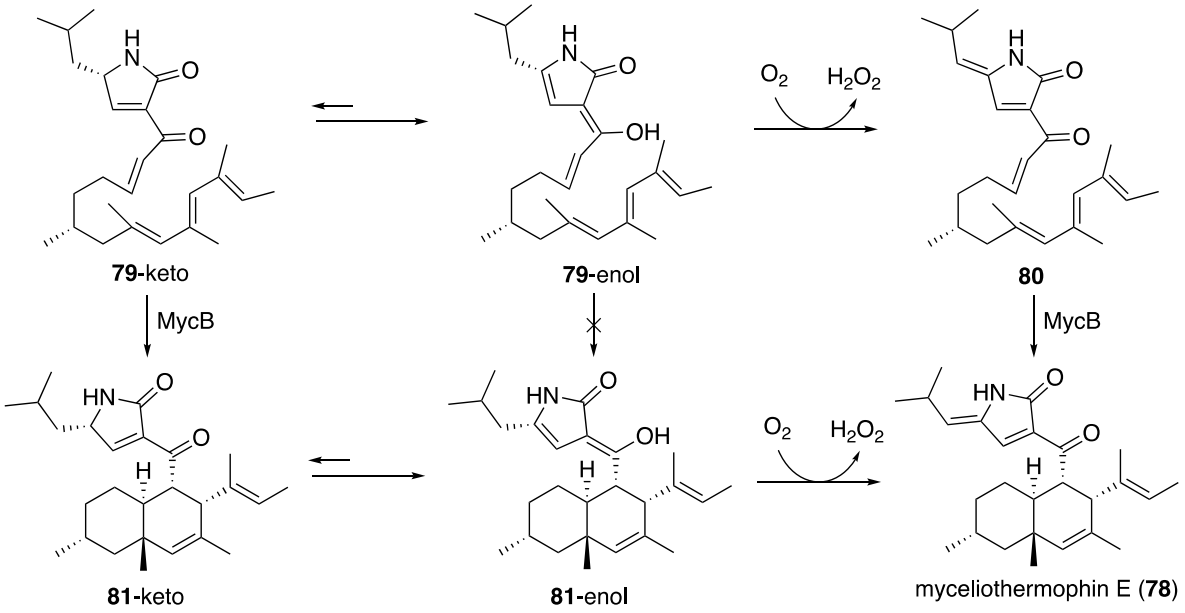

Figure 29: The MycB catalyzed Diels-Alder reaction enroute to myceliothermophin E (78)

Non-Decalin Forming Diels-Alderases

As shown in Table 1, six non-decalin forming Diels-Alderases have been purified and reconstituted *in vitro*. These enzymes are included for completeness but won't be discussed in detail. PyrI4 was introduced in the above section (see Figure 27) and the remaining five enzymatic conversions are shown in Figure 30. These are macrophomate synthase,[82] riboflavin synthase,[83] SpnF,[84,85] AbyU,[86] and TclM/TbtD.[87,88] TclM and TbtD perform the equivalent reaction towards two different thiopeptides, and therefore only one is shown for conciseness.

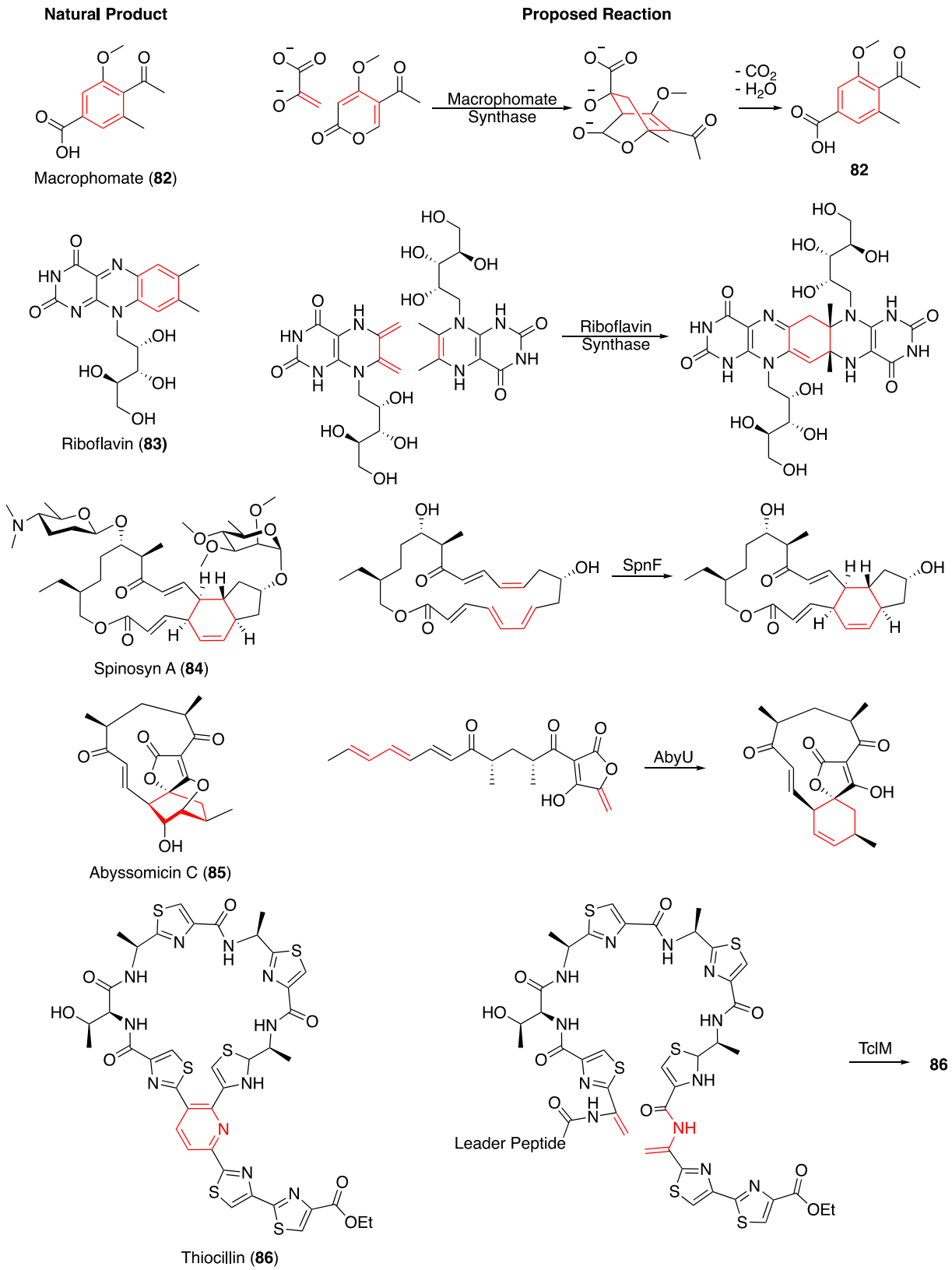

Figure 30: Non-decalin forming Diels-Alderases

Goals of this Chapter

This thesis seeks to further our understanding of how LovB catalyzes the [4+2] cycloaddition during the biosynthesis of DHML (**11**). The first goal was to isolate the Diels-Alderase activity to one of the many domains present on the HR-PKS. During our investigations, we found evidence to suggest the intermediate is not necessarily the hexaketide, and thus the substrate scope of the LovB Diels-Alderase activity became a second objective.

Isolating the Diels-Alderase Domain

As detailed in the introduction, LovB has many catalytic domains. In order from N- to C-terminus they are KS, AT, DH, MT, ER^0, KR, ACP and CON. The only domain with no known function is the CON domain, and this was a logical area of investigation. The CON domain, short for condensation, is the remnant of an NRPS module, for which the A (adenylation) and PCP (peptidyl carrier protein) domains have been lost over evolution. Not only is a CON incapable of condensing an amino acid onto the polyketide chain without the A and PCP domains, but LovB's CON domain also has a critical active site mutation. The HHXXXDG motif required for condensation activity has been mutated to HRLVGDG. When our group reconstituted the LovB/LovC assembly of DHML (**11**) *in vitro*, it was found that LovB could not be replaced with LovBΔCON, a construct of LovB with the C-terminus truncated to omit the CON domain; no DHML (**11**) was observed in reaction mixtures that contained all the necessary co-factors.[25] However, when the CON domain was supplemented in *trans* as a stand-alone domain, DHML (**11**) production resumed. Therefore, while the function of the CON domain is unknown, it is clearly integral to the activity of LovB.

Further evidence of the plausibility of the CON domain's involvement in the Diels-Alder reaction was published in 2014, when the group of Eric Schmidt (University of Utah) was studying the combinatorialization of PKS-NRPS hybrid systems.[89] The researchers exchanged the PKS and NPRS portions of different hybrid megasynthases and searched the extracts of the heterologous expression to find which products the various combinations produced. Constructs that contained the PKS portion of LovB, and the NRPS portion of EqxS, the equisetin megasynthase, provided compound **87** on fermentation (Figure 31). Presumably spontaneous decarboxylation of octaketide **88** leads to ketone **87**. When drawn in this way, one can recognize octaketide **88** as an intermediate that did not undergo Diels-Alder reaction, and whose elaboration to DHML was not completed. This further implicates the CON domain in the Diels-Alder reaction.

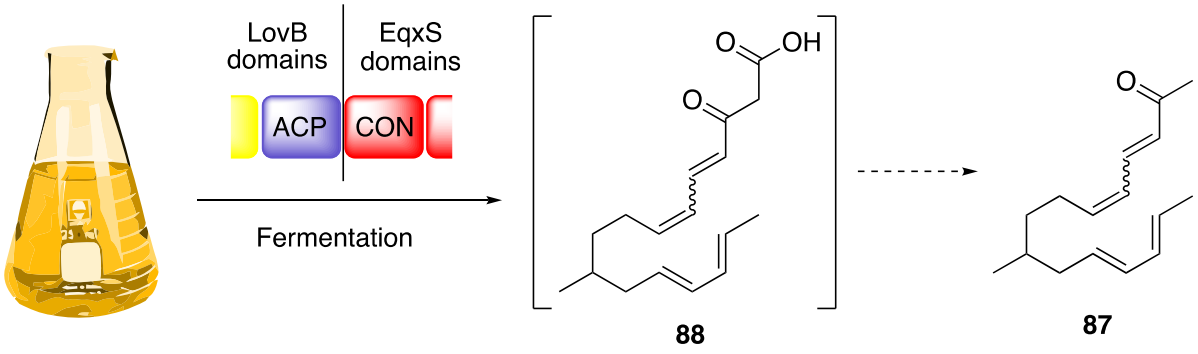

Figure 31: Literature evidence supporting the CON domain as the Diels-Alderase, isolation of compound 87 from the action of a LovB/EqxS hybrid

The other domain I chose to investigate as the potential Diels-Alderase is the dehydratase (DH). While there is no specific evidence for this related to LovB, dehydratase domains have literature precedence for their ability to activate the product α,β-unsaturated ketones to Michael addition, and thus it is known they can possess additional activites.[90] This Michael addition

would be analogous to the reverse hydration reaction catalyzed by hydratase enzymes, where water is the nucleophile. I therefore postulated it was possible that, following dehydration, the DH domain could act as a general acid catalyst to lower the LUMO of the dienophile and perform the cyclisation before the linear hexaketide triene leaves the active site (Figure 32).

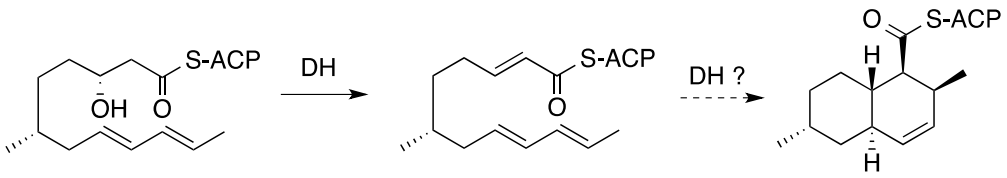

Figure 32: Biosynthetic proposal employing the LovB DH domain as the Diels-Alderase

Substrate Scope of LovB

It is not uncommon for enzymes to convert compounds other than their natural substrate. In fact, as discussed, our group studied the Diels-Alderase activity of LovB with SNAC-hexaketide triene **40**. Since a true intermediate would be enzyme bound, the work illustrated that LovB has enough promiscuity to recognize SNAC in place of the *holo*-ACP. Therefore, it is possible that the hexaketide is not the true substrate, but its cyclization is in fact a promiscuous activity, and that DHML (**11**) assembly can proceed through a different route than that proposed in Figure 13. Figure 33 is a web that outlines possible routes from the hexaketide triene to decalin heptaketides. The routes using Diels-Alder reaction A and B have been the focus of our investigations prior to this thesis. However, as discussed in the previous chapter (Figure 21), the carbonyl of the cyclized hexaketide may be too sterically hindered for downstream transthioesterification and attack by the malonate enolate, suggesting the chain may be further elongated prior to Diels-Alder reaction. For that reason, in addition to further investigating

pathway A/B, I also synthesized heptaketide tetraene **89** to study its cyclization via Diels-Alder reaction D. Based on the results, pathway C may be studied at a later date.

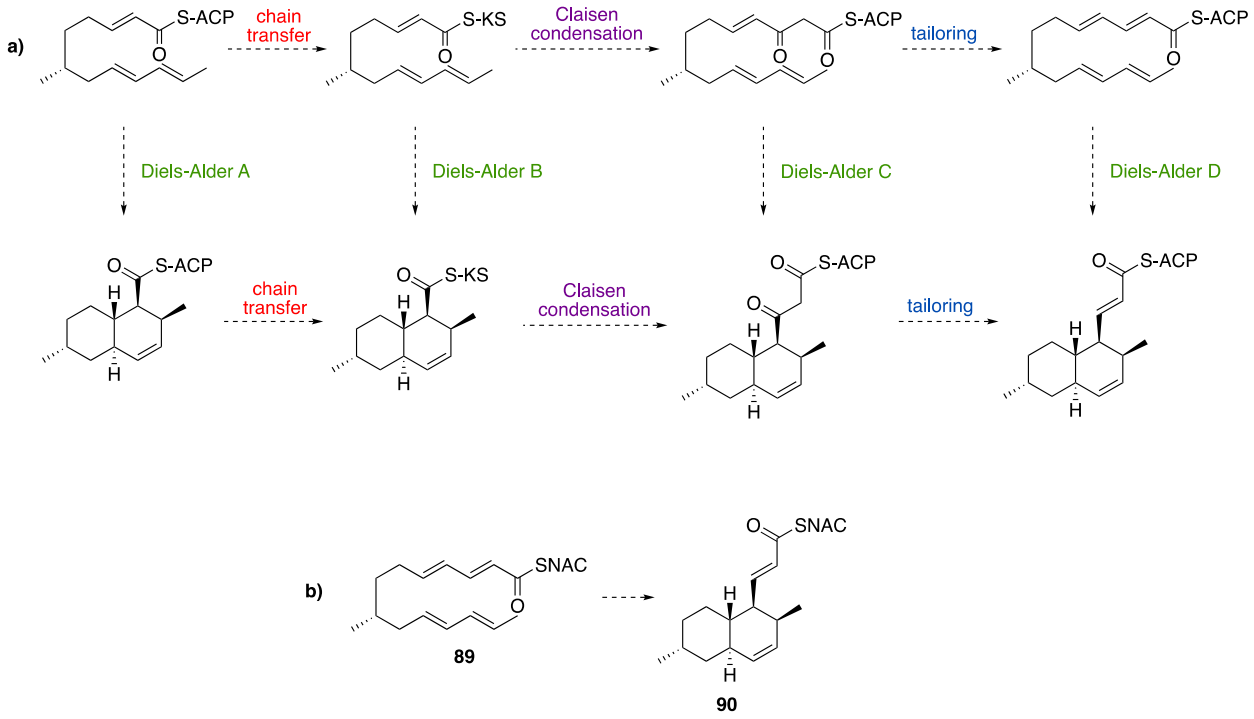

Figure 33: Possible cyclization routes during the LovB catalyzed biosynthesis of DHML (11)

Results and Discussion

Substrate Syntheses

The synthesis of hexaketide triene **40** was described in the previous chapter (see Figure 19). Heptaketide tetraene **89** can be assembled using the same methodology. Figure 34 describes two routes I employed in the synthesis of heptaketide tetraene **89**. First, using the hexaketide-SNAC **40** already in hand, I envisioned employing the same strategy of functional group modification and HWE reaction to elaborate the chain by two additional carbons. Unfortunately, the thioester was susceptible to 1,4 reduction, producing saturated alcohol **91** when treated with

both DIBAL and Superhydride. To circumvent this, ethanolysis was used to furnish ester **92**, which could be reduced to the desired allylic alcohol **93** using DIBAL. Oxidation with DMP provided aldehyde **94**, which is elongated by the familiar Horner Wadsworth Emmons (HWE) reaction to provide the heptaketide **89**. An alternative procedure can also be followed, which branches from the hexaketide synthesis at the key aldehyde **51**. Four carbons can be added simultaneously using the extended HWE reagent **95**.[91,92] This reaction requires a stronger base, LHMDS, and therefore is not compatible with the *N*-acetylcysteamine thioester and the ethyl ester is employed in its place, generating heptaketide **96**. Due to the lipophilicity of ester **96**, its hydrolysis to acid **97** was slow and required a large amount of THF as a co-solvent. Heating to near the boiling point of THF under a continuous stream of argon slowly concentrated the reaction as the hydrolysis progressed and complete conversion was achieved. Coupling to SNAC to produce the final product **89** was performed using DCC without the usual catalyst DMAP. When DMAP was present, neither starting material nor product could be recovered. Instead a mixture of non-identifiable materials were obtained, and presumably the DMAP adduct of the tetraene was too reactive to be coupled. Fortunately, the catalyst was not required, and repeating the reaction without DMAP furnished the product.

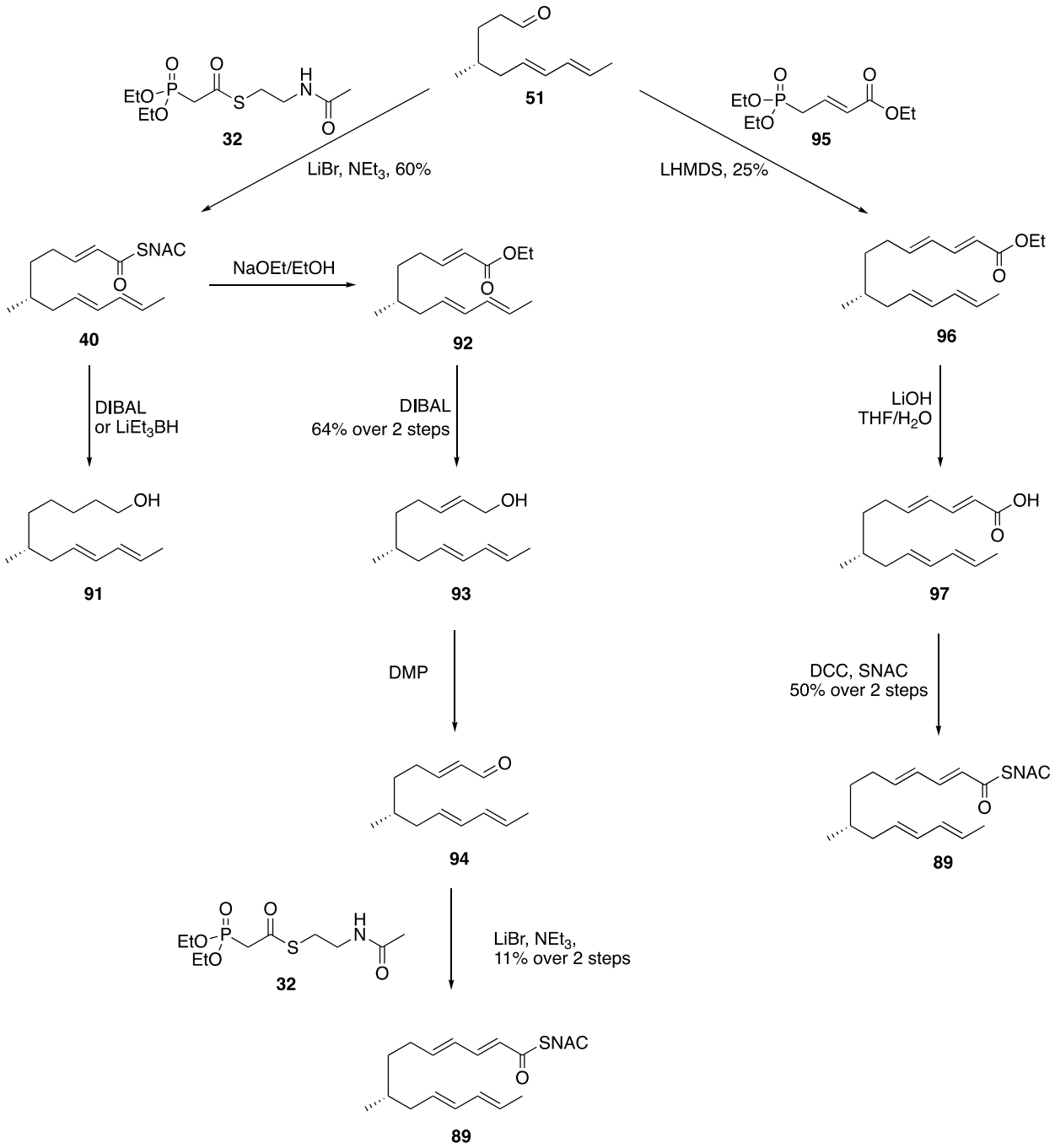

Figure 34: Synthesis of heptaketide tetraene 89

Expression of Enzymes

LovB and LovBΔCON Expression in *S. cerevisiae*

Our colleagues in the Yi Tang group at UCLA expressed LovB and LovBΔCON for the *in vitro* reconstitution of the pathway to DHML (**11**) in collaboration with our group.[25] They provided me with their *S. cerevisiae* cells, transformed separately with the expression plasmids to purify both megasynthases individually. LovB could then be used as a positive control, while LovBΔCON is a fragment to be tested for potential Diels-Alderase activity, and would not be active if the CON domain is the catalyst.

The expression system uses *S. cerevisiae* strain BJ5464-NpgA, which has been genetically modified to contain a phosphopantetheinyl transferase gene, *npga*, enabling the post-translational transfer of the essential phosphopantetheine group to the ACP domain.[93] The *lovB* and *lovBΔCON* genes are cloned behind an ADH2 promoter, such that expression is induced by depletion of glucose from the media.[94] The proteins were purified using N-terminal hexahistidine tags, and are shown on a gel in Figure 35.

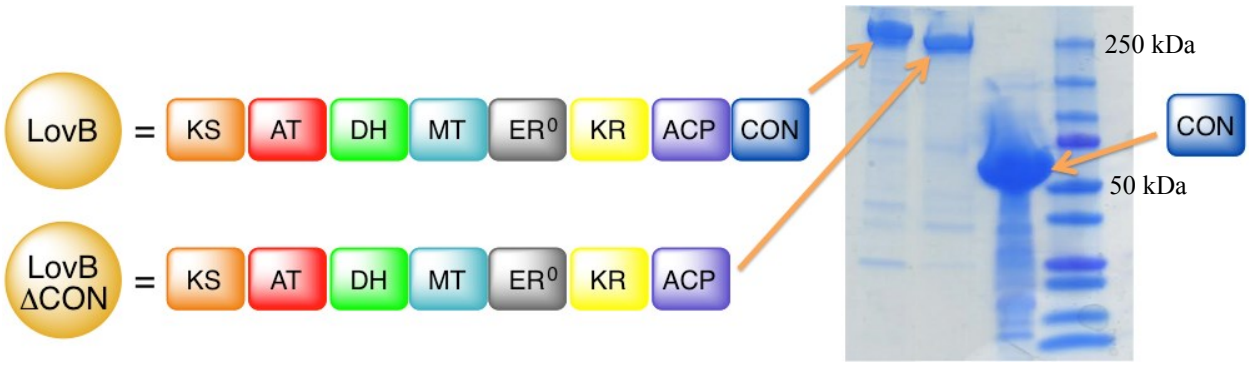

Figure 35: SDS-PAGE gel of proteins expressed for Diels-Alderase assay, labelled with their schematic representations

Expression of CON and DH in *E. coli*

In contrast to LovB and LovBΔCON, the individual domains expressed as stand alone proteins can be expressed in *E. coli* under the control of a *lac* promoter. For the CON domain I transformed BL21(DE3) cells with a plasmid obtained from the Yi Tang group for expression. The DH domain had not been expressed prior to this work, and I opted to have the gene synthesized and subcloned into pET-28a by Bio Basic Inc.

Cyclization Studies

Hexaketide Background Reaction – NMR-based Assay

NMR techniques have improved dramatically since our group first published the Diels-Alderase activity of LovB. For this reason, I chose to begin my investigation of this activity with the development of an assay that uses NMR for direct detection of products, in contrast to the derivatization and manual separation employed in 2000.[50] Our intention was to take advantage of small differences in chemical shifts between the 3 possible isomers of the cyclized hexaketide (Figure 36) and using 2 dimensional techniques to clearly distinguish which isomers are present or absent.

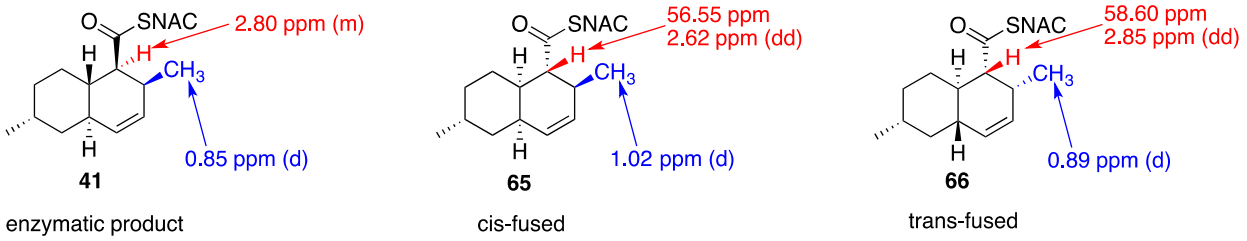

Figure 36: Key differences in chemical shifts of select nuclei in the three decalin isomers. No ^{13}C-NMR data has been previously published for enzymatic product 41

Hexaketide cyclizations in absence of enzyme were monitored by NMR in order to test the feasibility of this method. The first NMR technique employed was an HSQC (500 MHz) (Figure 37). The two isomers were clearly distinguishable using the 1 position of the decalin, with the exo isomer signal appearing around (2.85 ppm, 56 ppm) and the endo isomer signal around (2.62 ppm, 54 ppm). Furthermore, the expected ^{1}H chemical shift of H-1 of enzymatic product is 2.80 ppm, and is not expected to overlap with the non-enzymatic products' signals.

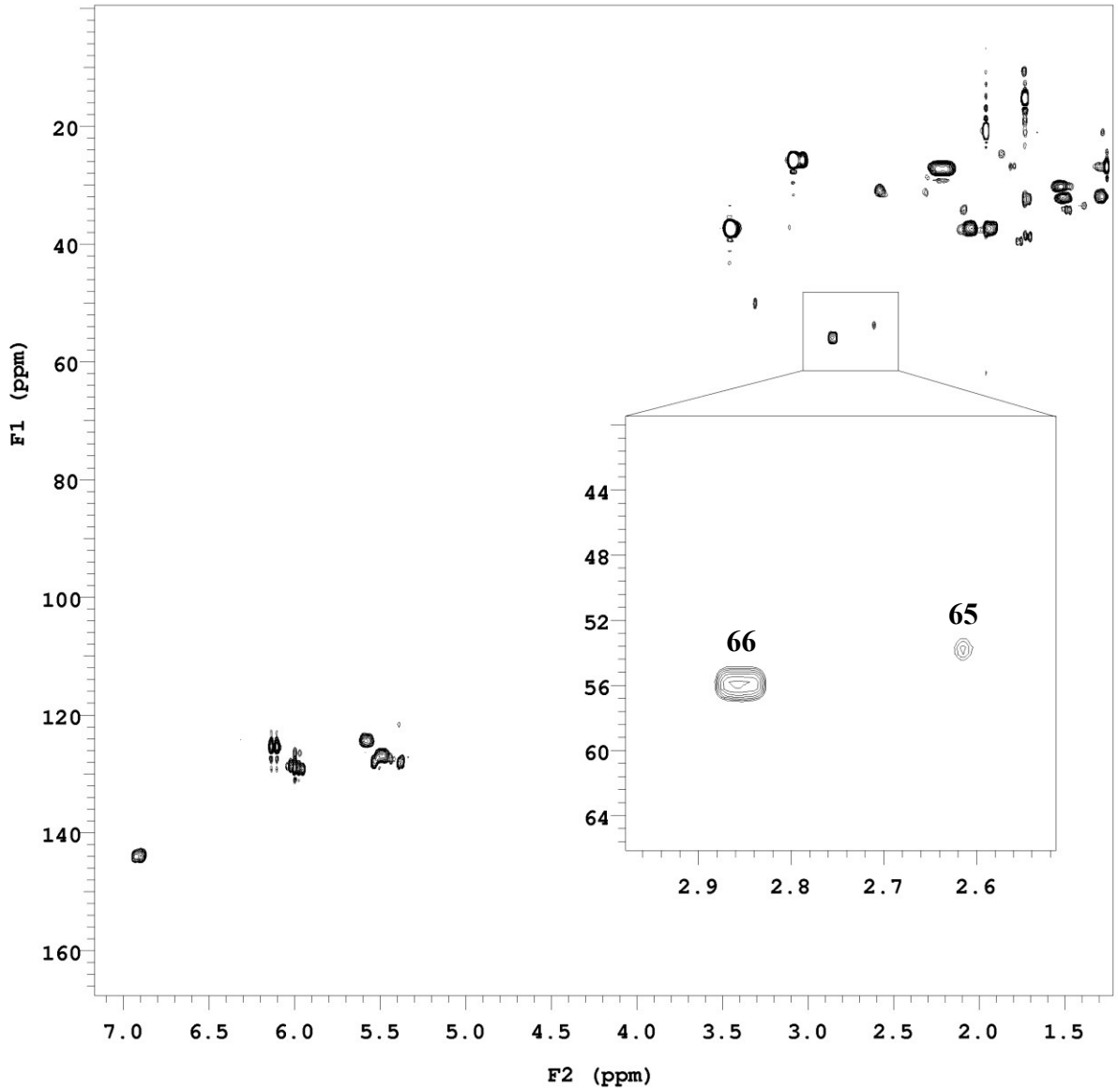

Figure 37: HSQC of control cyclization of triene 40 (500 MHz in $CDCl_3$), showing the differentiation of decalin products 65 and 66

While HSQC appeared to be a promising method, another possible analysis was the chemical shift selective filtered TOCSY (CSSF-TOCSY). With this experiment, the investigator selectively irradiates a specific proton chemical shift, and then detects all of the protons in its spin system. This technique has added benefits due to the excellent NMR properties of the ^{1}H

nucleus (abundance, gyromagnetic ratio), and the added information contained in proton spectra relative to carbon spectra. The results of the control reaction are shown in Figure 38. Selective excitation of H-1 of the *trans*-fused product **66** (2.86 ppm), followed by excitation of the C2-Me of the *cis*-fused product **65** (1.02 ppm) can pull out the individual ^{1}H-NMR spectra of the two decalin systems, effectively separating them from unreacted triene and confirming their identities through comparison with literature spectra.

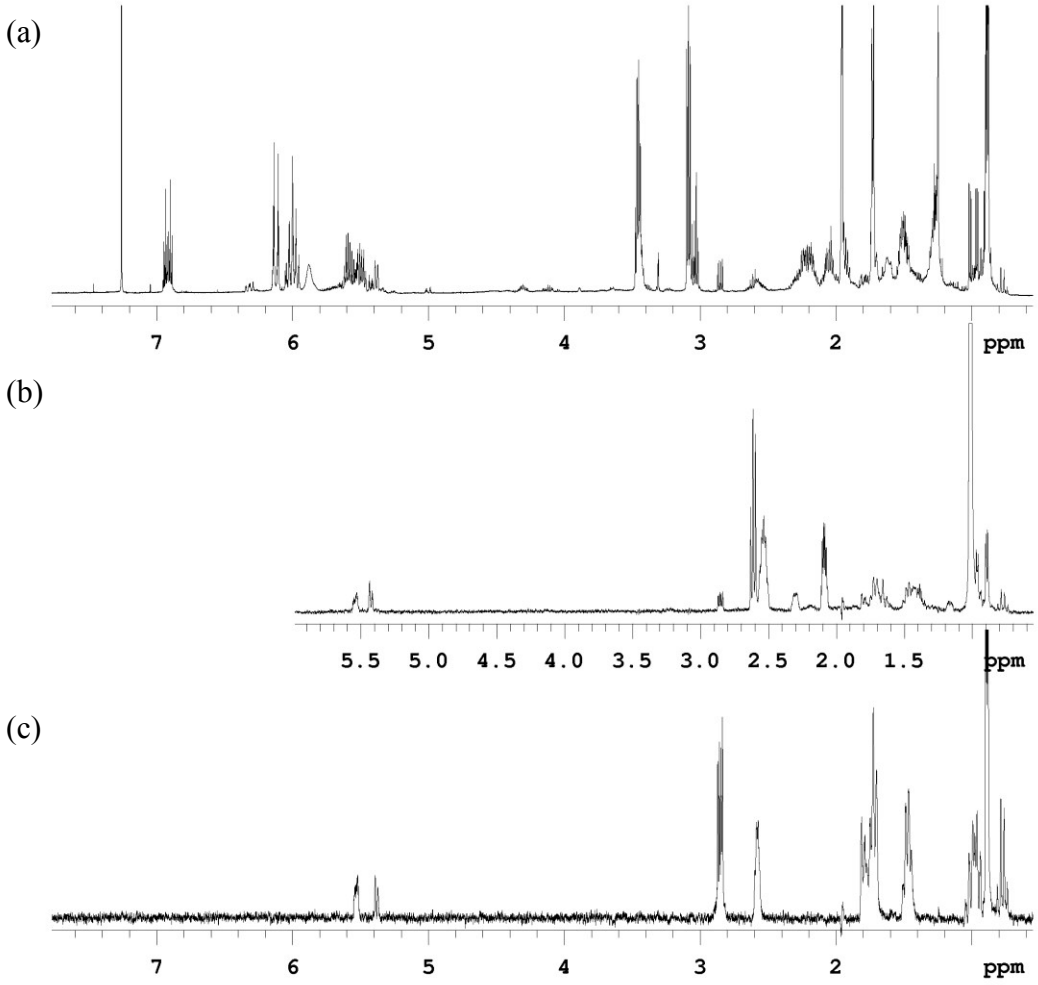

Figure 38: CSSF-TOCSY of the control cyclization of triene 40 (500 MHz in $CDCl_3$). (a) ^{1}H-NMR of the mixture. (b) Selective excitation of 1.02 ppm, isolating the spectrum of the *cis*-fused product 65. (c) Selective excitation of 2.86 ppm, isolating the spectrum of the *trans*-fused product 66

At this time, I performed the reaction with the CON domain. Unfortunately, no additional cross-peaks were observed in HSQC. Furthermore, the 1D ^{1}H-NMR did not show evidence of the product and there was therefore no peak to irradiate for a CSSF-TOCSY experiment. While it was possible to conclude that the CON domain did not catalyze the reaction, this assay had not been validated and therefore that conclusion should not be drawn at this time. In order to address this, LovB was expressed to use as a positive control and further experiments were paused until the synthesis of the product standard (**41**) could be completed so that the assay could be validated.

Heptaketide Cyclizations

As mentioned previously, the synthesis of the standard product, cyclized hexaketide **41** was not complete due to incomplete saponification of the ethyl ester (see Figure 21), and this result led us to question the intermediacy of the ACP-bound equivalent of **41**, and motivated us to investigate the cyclizations of heptaketide tetraene **89**.

First, the cyclizations were performed on small scale using 3 μg (9 nmol) of tetraene **89**. The negative control was performed in 30 μL of buffer, while the reaction contained 400 μg (1.2 nmol) of LovB. After overnight incubation at 37 °C, the reaction mixtures were extracted with dichloromethane, and the extracts were analyzed by LC-MS. However, despite many attempts for method optimization, only one peak was observed for both the control and LovB reactions, and this peak matched the starting material in both retention time and mass to charge ratio (Figure 39). This suggested there was no change overnight for either reaction.

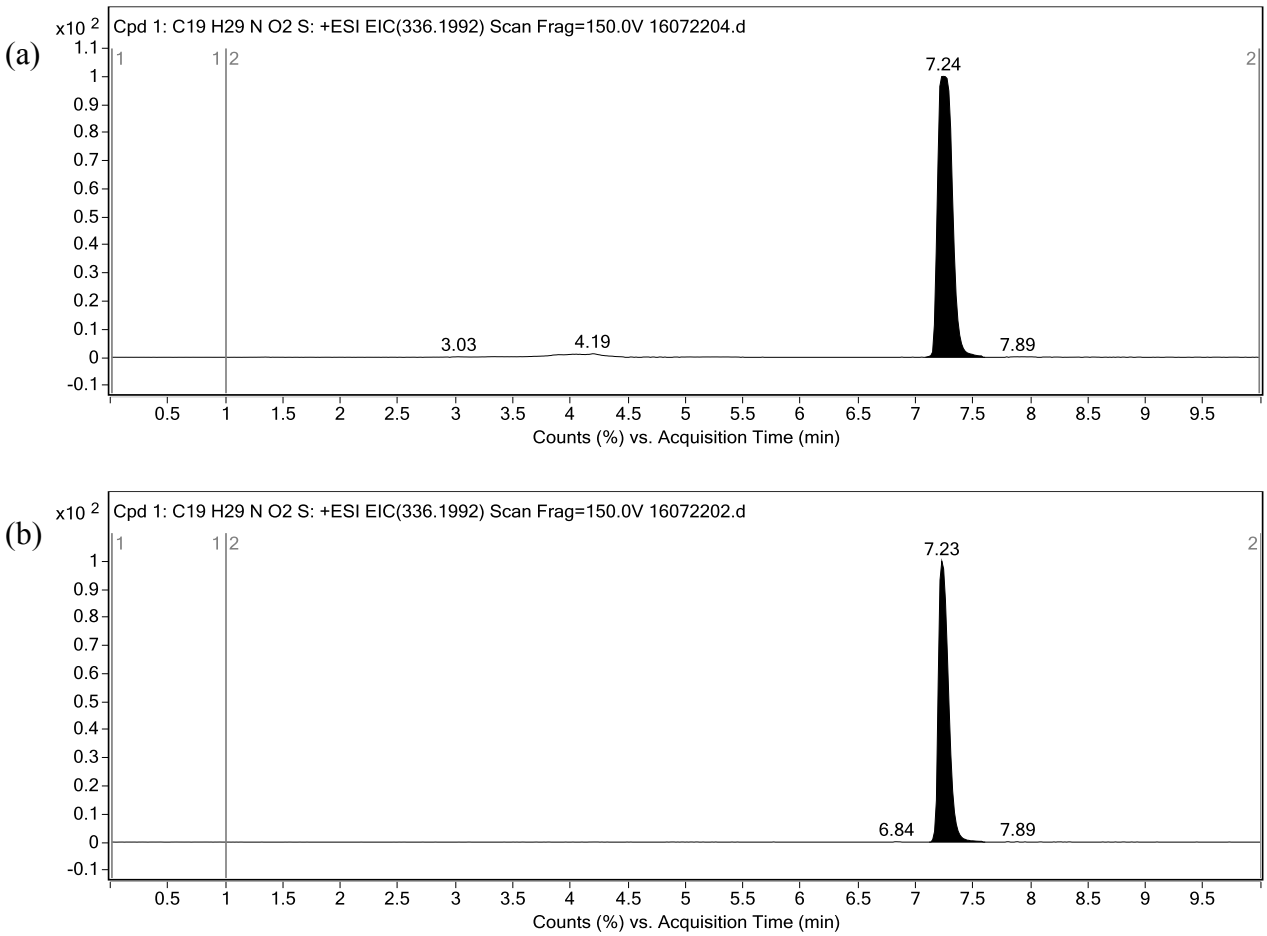

Figure 39: LC-MS extracted ion chromatogram for heptaketide 89 (a) and overnight reaction of 89 with LovB (b)

To confirm the mass specrometry results and rule out co-elution of isomers, a larger scale reaction was performed with NMR-monitoring of a solution of 2.6 mg of tetraene **89** in 0.7 mL of a THF-d8/D_2O mixture (Figure 40). The spectrum did not change overnight, and pure unreacted starting material could be re-isolated, in concordance with the LC-MS results. We can therefore conclude that LovB likely does not catalyze the cyclization of the heptaketide tetraene **(89**), effectively ruling it out as a substrate of the biological Diels-Alder reaction. A standard

product could confirm this, by eluting from LC-MS at a different retention time, however the synthesis was not undertaken because the unlikelihood that tetraene **89** is the substrate.

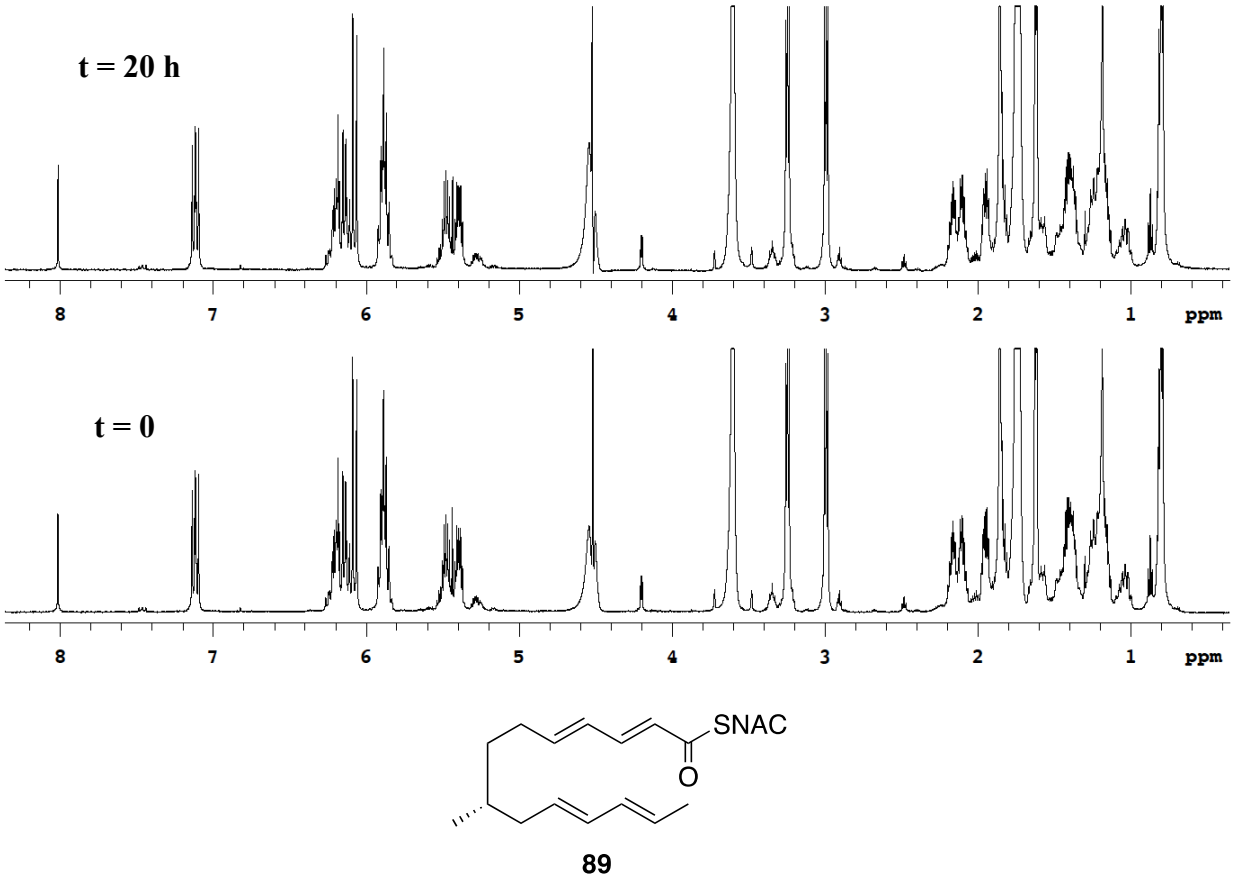

89

Figure 40: ^{1}H NMR of heptaketide 89 and 0 and 20 hours, showing no change overnight in THF-d_8/D_2O

Assay Employing ^{13}C Hexaketide

The failure of heptaketide **89** to cyclize redirected our efforts back towards the hexaketide. At this stage, the majority of the synthesized hexaketide triene **40** had been consumed towards the synthesis of heptaketide **89**, leaving less than 10 mg of each the natural abundance and ^{13}C-labelled compounds. Because the LovB cyclization reaction is low yielding (5 mg of starting material yielded 0.1 mg of enzymatic isomer **41** in the original work[50]), the

isotope label would improve detection of the products by NMR. Therefore, a portion of ^{13}C-labelled triene (^{13}C-**40**) synthesized for incorporation experiments was redirected for the purpose of studying the Diels-Alder reaction. Five reactions were set up in tandem, each containing 1 mg of ^{13}C-**40** in 5 mL of buffer, and one of either LovB (positive control), LovBΔCON, CON, DH or no enzyme (negative control). After reacting overnight, the mixtures were extracted with dichloromethane, and the extracts were analysed by NMR. First, 1D carbon NMR was used to distinguish the number of labelled isomers present, and their chemical shifts relative to those seen in the positive and negative controls (Figure 41). The presence of clear differences between the positive and negative controls implied a reaction did in fact take place in the presence of LovB that did not occur in its absence. Moreover, the DH and CON containing reactions resembled the negative control, with signals at 204.5 ppm and 201.5 ppm (the CON reaction also contained unreacted triene, observed at 190.6 ppm). In contrast, both the spectra of the LovB and LovBΔCON experiments contained two additional peaks at 198.4 ppm and 198.3 ppm. However, no ^{13}C-NMR spectrum had ever been recorded for the enzymatic product (**41**), so further analysis was required.

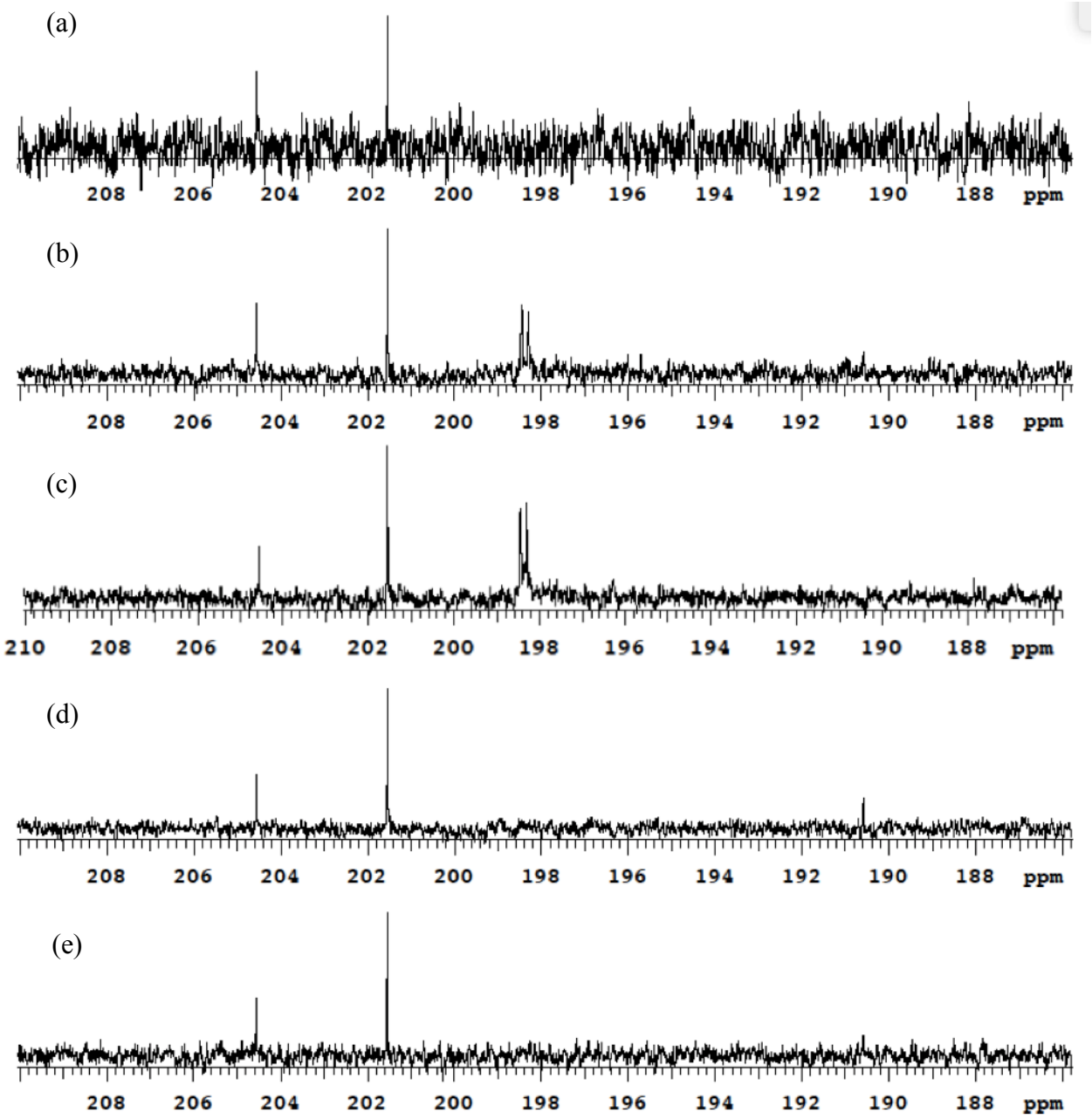

Figure 41: ^{13}C-NMR of the products of hexaketide (^{13}C-40) cyclization in the presence of (a) buffer only, (b) LovB, (c) LovBΔCON, (d) CON and (e) DH.

In order to detect the chemical environment around the ^{13}C-labelled centre, a gHMBC experiment would be ideal. However, the resolution was inadequate. To improve the resolution in the ^{13}C dimension of the gHMBC, we used a modification of the pulse sequence called a

"band-selective gHMBC" (bsgHMBC).[95] This variant uses a selective pulse to excite only the ^{13}C nuclei in the frequency range under investigation, allowing smaller increments to be sampled without unreasonable experiment duration. Both the typical gHMBC, and bsgHMBC are show in Figure 42 with matching window sizes for comparison.

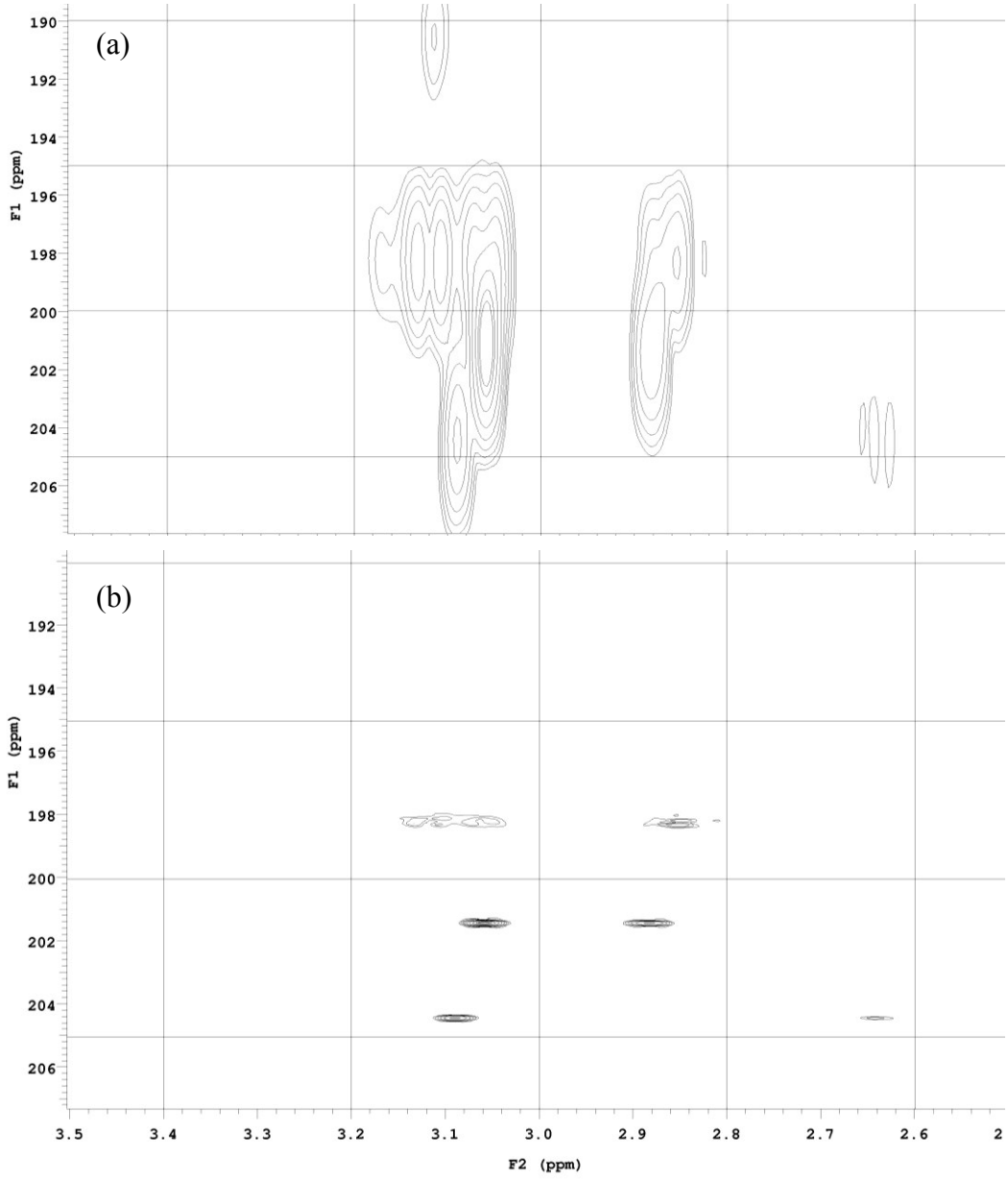

Figure 42: (a) gHMBC of LovB catalyzed cyclization of ^{13}C-hexaketide 40. (b) bsgHMBC of same sample.

The improved resolution allowed for further analysis of the spectrum and identification of the components. A zoomed-in view of the bsgHMBC (with F1 and F2 switched) is shown in Figure 43. Firstly, the isomer at 204.6 ppm in the ^{13}C dimension can be identified as *cis*-fused isomer **65**, based on comparison to ^{1}H chemical shifts reported by Witter, 2.62 ppm (H-1) and 3.06 ppm (H-3').[49] The spectrum was then referenced to these values in the ^{1}H dimension. I referenced the ^{13}C dimension to the chemical shifts of my own 1-D experiment, which had been referenced to $CDCl_3$ (77.16 ppm). The *trans*-fused isomer **66** appears next at 201.5 ppm. The ^{1}H cross-peaks agree with Witter's results as well, as he recorded 2.85 ppm (H-1) and 3.03 ppm (H-3').[49] Finally, the two ^{13}C signals not present in the control reaction (198.4 ppm and 198.3 ppm) give overlapping, irregularly shaped cross-peaks in the range of 2.80-2.85 ppm and 3.00-3.12 ppm. The proton chemical shifts recorded in Auclair's thesis for H-1 and H-3' are 2.80 ppm and 3.04, respectively.[96] Therefore, the values I observe are consistent with one of the signals at 198 ppm corresponding to the enzymatically cyclized product **41**. Unfortunately, the bsgHMBC did not provide any insight into why there are two discrete peaks at 198 ppm. My results are not inconsistent with the possibility that the enzymatic product **41** exists as two conformers whose interconversion is slow on the NMR time scale, however Auclair did not discuss any evidence for or against this in her thesis.[96] In order to answer this question conclusively, one would need to purify the reaction components and study their NMR spectra in isolation.

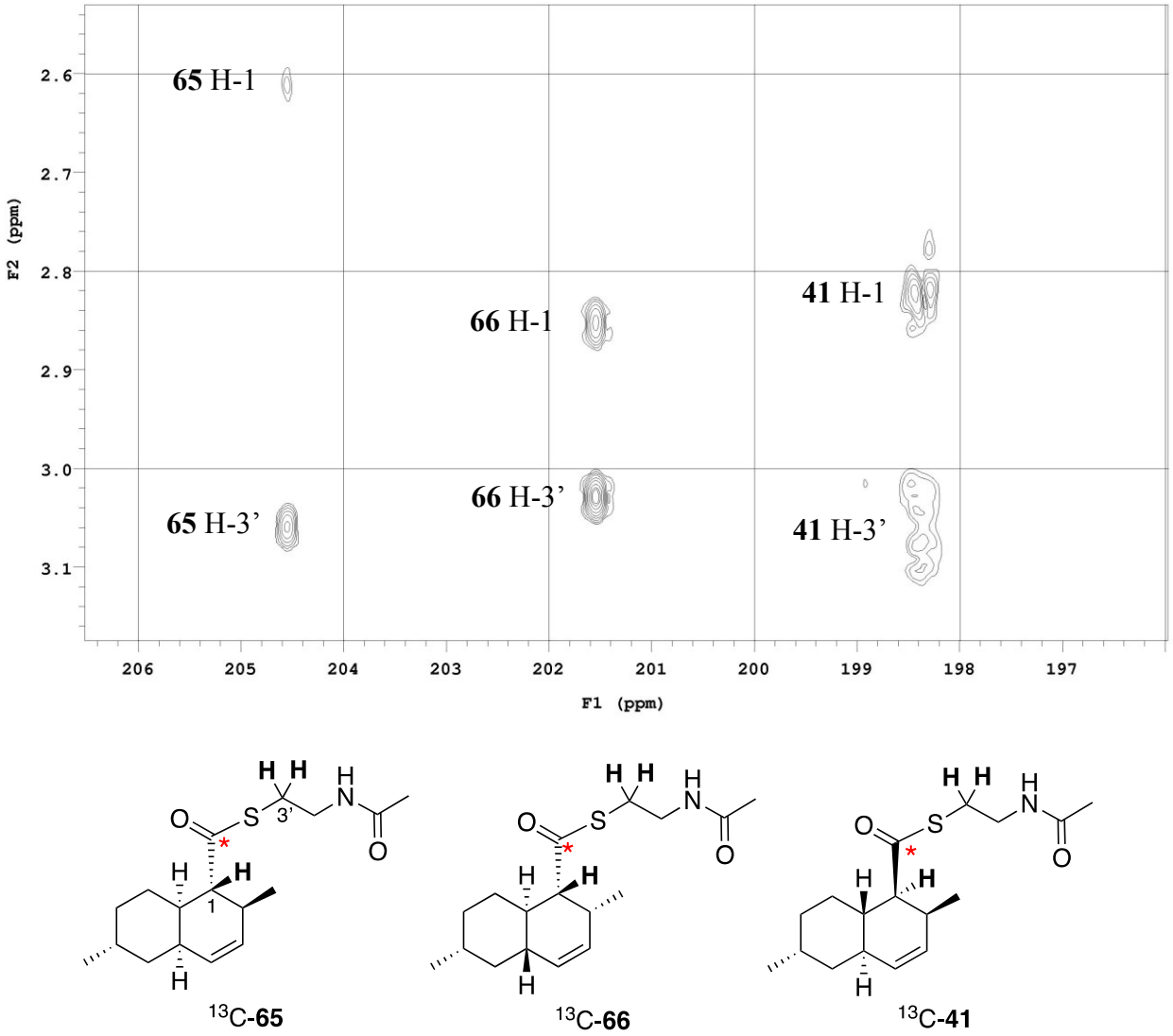

Figure 43: gHMBC of LovB catalyzed cyclization of ^{13}C-hexaketide 40

Conclusion and Future Outlook

In conclusion, I demonstrated that both LovB and LovBΔCON catalyze the cyclization of linear hexaketide triene **40** to decalin **41**, a product not found in the absence of enzyme or in the presence of the LovB CON or DH domains. The stereochemistries of the products were determined based on comparison to previously reported chemical shifts.[49,96] In the process I developed three different NMR-based assays for the detection of the products of the cyclization

reaction. HSQC and CSSF-TOCSY were useful for distinguishing the products of the background reaction from one another, however it was my assay employing a ^{13}C-labelled substrate and bsgHMBC that was able to localize the Diels-Alderase activity to LovBΔCON and not CON. All three techniques may prove to be useful in the future for studying this reaction, or other enzymatic reactions where the product and starting material possess the same molecular formula, where LC-MS is less useful. Strategic placement of the isotope label could make a combination of the three techniques powerful for determining the products of such enzymatic reactions.

It was our hypothesis that the CON domain is the Diels-Alderase within the multidomain megasynthase that is LovB, however the results reported here refute that. With intact LovB serving as a successful positive control, it was found that in the presence of CON alone only the background cyclization occurred. The discovery of enzymatic product **41** in the reaction containing LovBΔCON confirmed that the Diels-Alderase activity is present in this fragment of LovB, and refutes the possibility that CON is simply not active stand-alone. Within the LovBΔCON fragment, the DH domain was selected for the exploration of Diels-Alderase activity, the DH domain does not convert triene **40** to decalin **41**. LovBΔCON contains six other domains, KS, AT, MT, ER^0, KR and ACP, which could be investigated systematically in turn. Many of these domains work by general acid activation of the thioester carbon, and thus would be feasible Diels-Alderases.

Another objective of this chapter was to determine the true intermediate that undergoes the Diels-Alder reaction during the assembly of DHML (**11**). While the ability of LovB to cyclize triene **40** to product **41** has been confirmed and reproduced herein, this could be a promiscuous activity, as supported by the steric hindrance observed at the carbonyl carbon of

this decalin system. This work has ruled out the intermediacy of heptaketide tetraene **89**, which did not cyclize in the presence or absence of LovB. However, the β-keto heptaketide that would be present immediately following the KS-catalyzed Claisen condensation of malonyl-CoA and the hexaketide is a highly plausible substrate for the Diels-Alder reaction (see Figure 33). Due to time constraints, the synthesis of the SNAC version of this substrate (**98**) was not undertaken. It could be made using the Crimmins-inspired chemistry of Figure 44.[15]

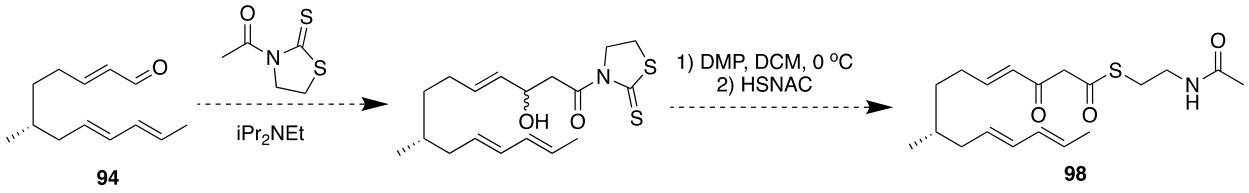

Figure 44: Proposed synthesis of β-ketoheptaketide SNAC thioester (98)

Knowing that the Diels-Alderase domain is contained in the LovBΔCON fragment but is not the DH domain, the next hypothesis I would explore is that the KR catalyzes the cyclization. KRs are highly versatile domains that perform the stereocontrolled reduction of the β-keto group using NADPH as a co-factor. They occasionally have the additional activity of epimerizing the substituents at the α position.[97] The β-keto functionality is activated by a conserved active site tyrosine acting as a general acid, with support from neighbouring serine and lysine residues. This activates the carbonyl for nucleophilic hydride attack in the case of reduction, or α-deprotonation in the case of epimerization. If the Diels-Alder reaction were to take place at the β-ketoheptaketide stage, as proposed, this tyrosine would be ideally placed to act as a general acid to catalyze the Diels-Alder reaction (Figure 45). To achieve this, the enzyme would need to delicately balance the reaction kinetics; the Diels-Alder cyclization would need to be faster than the ketoreduction, which would occur subsequently. Performing two reactions in tandem could

also improve catalytic efficiency; a primary concern regarding a true Diels-Alderase, is that the catalytic turnover would be limited by product inhibition, due to the product-like transition state of the Diels-Alder reaction. Therefore, reduction could help in product release, similar to the decarboxylation step of macrophomate synthase.[82]

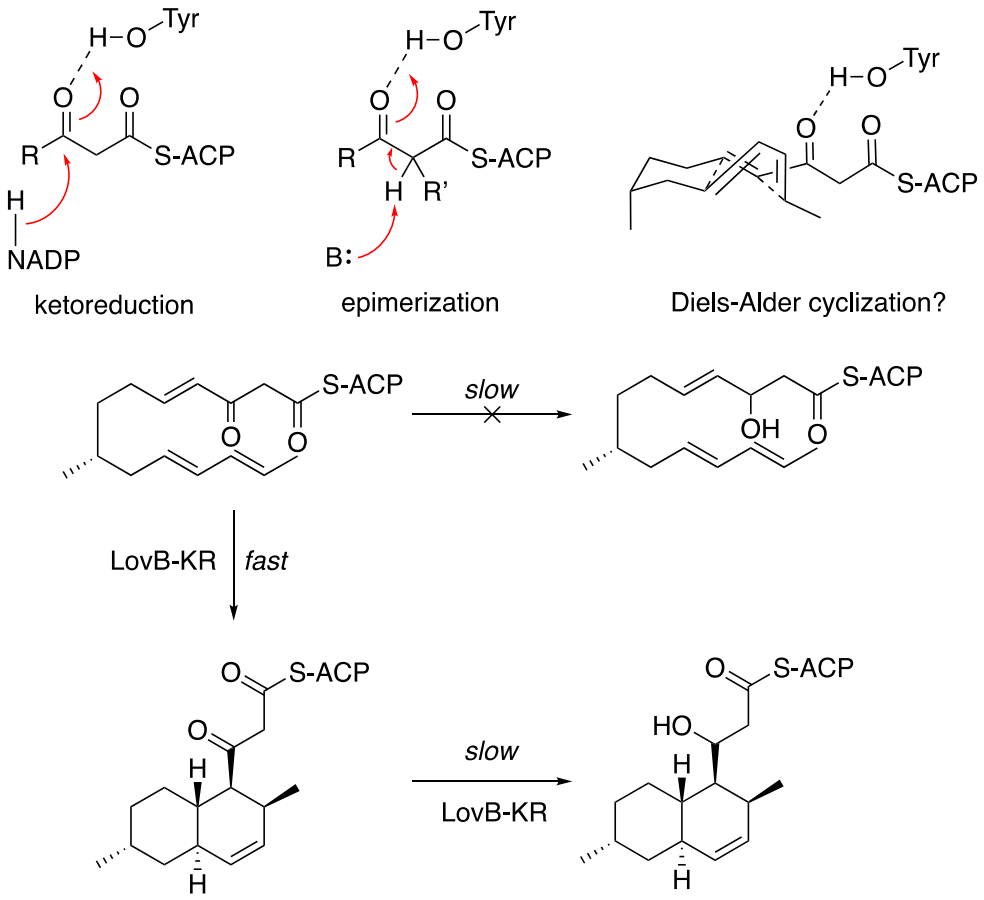

Figure 45: Basis for the proposal that LovB-KR could be the Diels-Alderase domain

This proposal is supported as well by a key literature finding. In the introduction to this chapter, I discussed a key publication involving the combinatorialization of PKS-NRPS systems that seemed to implicate the CON domain in the Diels-Alder reaction.[89] In this work, the authors isolated another key pre-Diels-Alder product that was not discussed to the same extent. They

expressed a construct of the equisetin PKS (EqxS) with the KR domain swapped for the KR domain of LovB, for which the product was the tetraene **99** (Figure 46, shown here with a *cis* double bond, as represented in the publication. This is presumably a *trans* alkene, though no evidence was provided for either stereochemistry in the publication). It is likely that, if LovB-KR were the Diels-Alderase, it would have some difficulty catalyzing the cyclization of the equisetin intermediate for two reasons: First, the α-methyl group is not present in the lovastatin equivalent. Secondly, the decalin stereochemistry of the product, trichosetin (**100**), differs from that of DHML (**11**), as it is a *trans*-decalin containing an equatorial methyl group at position 6 (similar to the non enzymatic product **66**). These factors could alter the kinetics such that ketoreduction takes place at a faster rate than cyclization, leading to a dead end product.

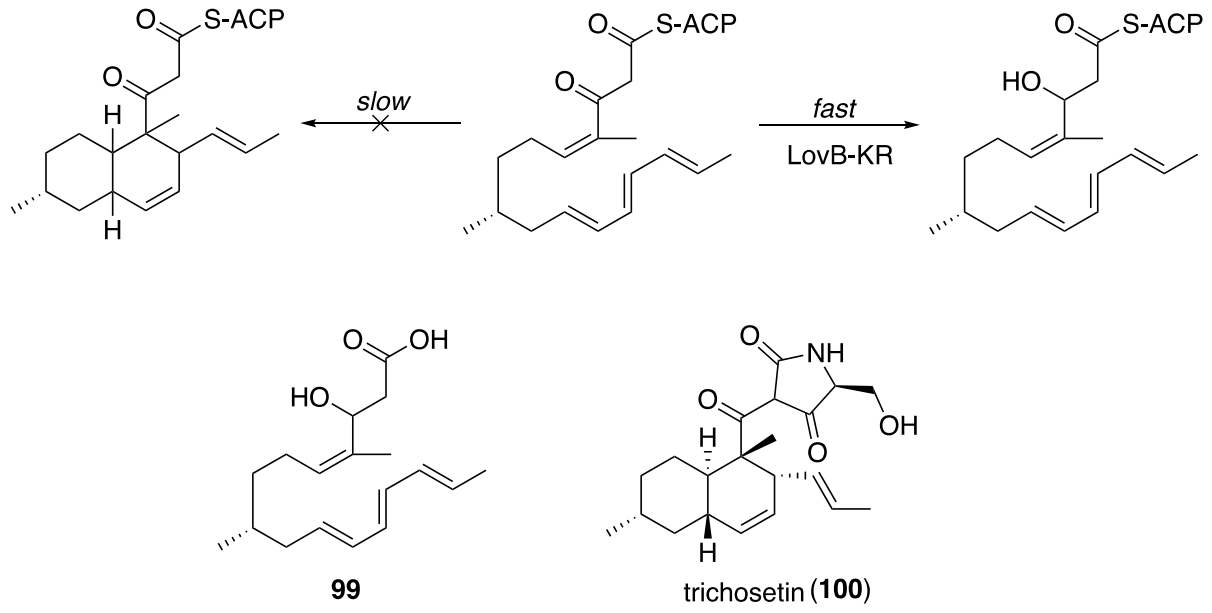

Figure 46: Product of EqxS, when the KR domain has been swapped with LovB-KR

Finally, the CON domain still has no known function, except that it is essential for LovB assembly of DHML.[25] With this work excluding it as the Diels-Alderase, its function is still unknown and must be elucidated to fully understand LovB as a molecular factory. One possibility worthy of investigation is the similarity between the LovB CON domain and the X-domain of NRPSs. X-domains are found at the C-terminus of some NRPSs, and appear to be the remnant condensation domains of a terminal module lost throughout evolution.[98] They possess a further notable similarity to LovB: the active site motif required of functional condensation domains (HHxxxDG) is mutated to HRxxxDD. The active site arginine, the same mutation found in CON, was found to alter the structure in a notable way, as the crystal structure shows this residue now projects directly into the cavity normally occupied by the donor phosphopantetheine arm in peptide bond formation.[98] In a recent letter to Nature, Cryle and coworkers demonstrated that, instead of having a catalytic activity of its own, the X-domain played a crucial role in recruitment of *trans*-acting oxygenases in glycopeptide biosynthesis.[98] I believe the next step in the search for the function of the LovB CON domain would be to investigate if it recruits LovC, the *trans*-acting ER of LovB, a role analogous to that of the X-domain. I would use gel filtration chromatography and native gel electrophoresis to investigate if CON forms a stable complex with LovC. A co-crystal structure could also be pursued.

CHAPTER 4: ACYL CARRIER PROTEIN DOMAINS OF HIGHLY REDUCING POLYKETIDE SYNTHASES

Introduction

Chapter 1 introduced the fundamental principles of polyketide biosynthesis and the nature of PKS enzymes. A key point was that, with the exception of type III PKSs, the growing acyl chain remains enzyme bound throughout the assembly of the product. This chapter explores the nature of the acyl carrier protein (ACP), the domain to which the growing chain is covalently linked. The principle role of the ACP, which can be a discrete globular protein or a domain in a megasynthase, is to shuttle the growing substrate between the various catalytic domains.[99] However, these small proteins of 70-100 residues are much more than passive carriers; they are central to their biosynthetic processes, serving a variety of roles from mediating protein-protein interactions to sequestering intermediates. Only through understanding ACPs will chemists be able to reliably engineer combinatorial biosynthetic pathways.[99]

Acyl carrier proteins were first studied in the context of *E. coli* fatty acid biosynthesis, a type II system.[100] One can easily understand Nature's need for a carrier protein in such a system; the intermediate fatty acids are insoluble and have very little functionality available for enzyme recognition, and so the ACP can sequester the hydrophobic intermediates and provide crucial hydrogen-bonding sites for substrate docking. As the knowledge of ACPs grew, it was discovered that PKS and NRPS systems also employ carrier proteins.

Ubiquitous among ACPs, whether from FA, PK or NRP biosynthesis, is the phosphopantetheine (ppant) prosthetic group. The structure of this group was introduced in Chapter 2 (Figure 14), which described the rationale for the use of the *N*-acetylcysteamine as a ppant mimic in PKS feeding studies. The structure is shown again in Figure 47, demonstrating its

origins from coenzyme A (CoA, **101**).[101] Ppant is transferred from CoA (**101**) to the *apo*-ACP active site serine through the catalysis of a ppant transferase, such as Sfp or NpgA, to form *holo*-ACP. The ppant group of holo-ACP functions as a flexible and water-soluble 20 Å linker to shuttle the substrate into the various active sites. As well, the terminal thiol is essential. By linking the growing acyl chain using a labile thioester linkage, this covalent bond can be transient, permitting transthioesterification and release from the enzyme. Furthermore, the pKa of thioester alpha proteins are substantially reduced compared to esters, permitting the enolization of the malonate extender unit, while the electrophilicity of the carbonyl carbon of the growing chain is increased, lowering the activation energy required for the Claisen condensation.

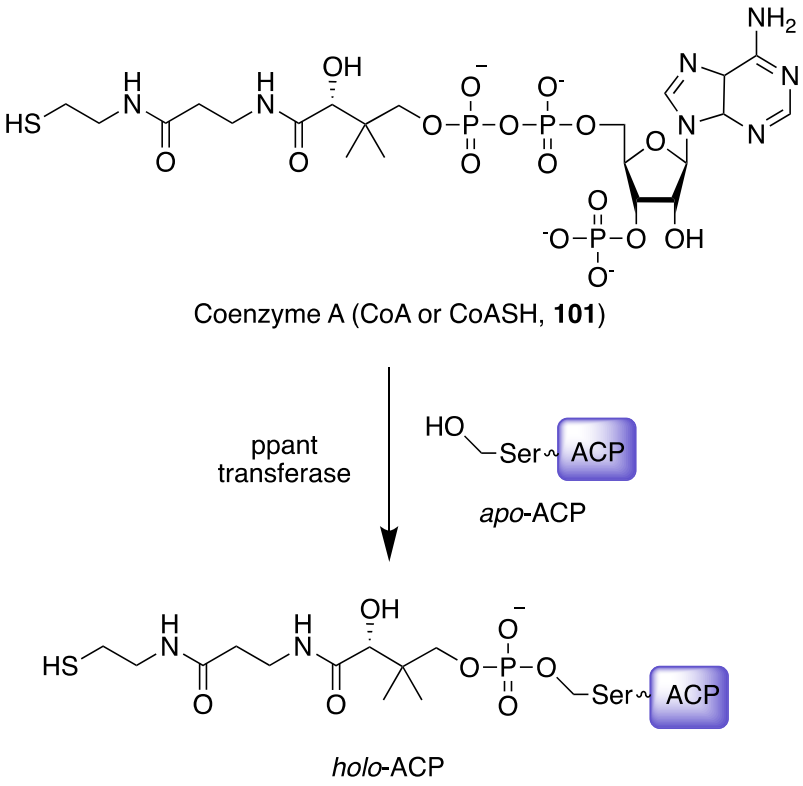

Figure 47: Phosphopantetheinylation of an ACP

Research on the role of ACPs as mediators of protein-protein interactions has been the focus of carrier protein research since the first NMR-solution structure was elucidated, that of *E. coli* FAS ACP in 1988.[102] ACPs are highly flexible and do not generally crystallize, and therefore NMR has been the method of choice to obtain structural information. Many NMR structures have been solved since, the majority show the ACP adopting a "helix bundle" tertiary structure of 3-4 helices, of which helix 2 provides a binding surface.[103] It has been exceedingly challenging to study these interactions, however, as not only are ACPs highly flexible, their protein-protein interactions are transient to allow for enzymatic turn-over as well. For example, in order to crystallize the mammalian fatty acid synthase, Ban and co-workers needed to express a construct with the ACP removed from the C-terminus and solve the structure in its absence.[104] In 2014 there were 2 major developments in this area, with two groups independently solving structures of ACP co-crystalized with synthase enzymes. First, Masoudi *et al.* took advantage of the unusually strong interaction between the ACP and acyltransferase, LpxD, in Lipid A biosynthesis.[105] By solving the structure in 3 different stages of the catalytic cycle, the researchers were able to provide insight into how the ACP docks on to LpxD, transfers the acyl group to the acyl acceptor, and releases from the enzyme. However, since LpxD is an unusually strong ACP binder, it's possible the findings cannot be extrapolated to other systems. In contrast, Nguyen *et al.* functionalized the *E. coli* FAS ACP, AcpP, with a mechanism-based inhibitor to covalently link it to the enoyl reductase, FabA.[106] Interestingly, the complex crystalized as a heterodimer, with each AcpP-FabA complex in a different conformation. The authors interpret this as two different snapshots of the AcpP docking. The reorganization of the helices support the "switchblade" mechanism, in which the hydrophobic substrate is first sequestered within the

ACP, and then presented to the active site. Because the authors were able to circumvent the low binding affinity between the ACP and the ER, their method could be applied to other systems.

Both ACPs crystallized in the above mentioned studies are from Type II systems, where the ACPs are stand-alone proteins. Type I modular systems have also been extensively studied, using DEBS as a model (see Figure 4 in Chapter 1 for a description of DEBS). The crystal structure of DEBS ACP2 was solved in 2007, and one of the notable differences in comparison to Type II system ACPs was the overall reduction in surface charge.[107] As Type I ACPs are not free in solution, hydrophilicity is not as important as with Type II ACPs, but this causes issues during their expression as stand-alone proteins. In their NMR study of the rat FAS ACP, researchers found that as a stand-alone domain, the ACP did not sequester the growing acyl chain, suggesting this function is not needed in the megasynthase.[108] The first NMR structure of a fungal iterative PKS, the ACP from norsolorinic acid synthase (NSAS), lead researchers to the same conclusion, as very few changes were observed following the functionalization of *holo*-ACP with a hexanoyl group, and there were no NOEs observed to the hydrophobic chain.[109] NSAS is a non-reducing iterative PKS, and the only other ACP NMR structure published of a fungal iterative PKS is that of CalE8.[110] CalE8 is the polyketide synthase of calicheamicin biosynthesis, an enediyne natural product, and in addition to lacking an ER domain, CalE8's ACP domain shows little homology to other ACPs. Therefore, there is a clear gap in the research that could be filled through the study of our highly reducing PKS systems, LovB and Hpm8. These ACPs, in comparison the modular systems which act for one round of chain extension, would have to carry a larger variety of acyl substrates of various chain lengths. In contrast to both the FAS and NR-PKS systems, the HR-PKS ACPs must not only carry acyl groups of varying polarity, but also delivery the intermediates to the correct domains as per the inherent

"program" of the system. Thus, I undertook the expression of the LovB and Hpm8 ACPs as stand-alone domains with the intentions of pursuing NMR structures that may provide insight into how the ACPs can accomplish these roles.

Goals of this Chapter

Originally, the goals of this chapter were to elucidate the structures of LovB-ACP and Hpm8-ACP using NMR. However, as will be discussed, this proved to be challenging due to the inherent properties of the ACPs themselves. Thus, the objectives changed to characterizing these stand-alone domains as much as possible while pursuing other uses for these tools.

Results and Discussion

Expression of Hpm8-ACP

Expression of Hpm8-ACP started with the cloning of the ACP domain from a plasmid containing the entire Hpm8 gene, working towards a construct I will refer to as Hpm8-ACP1. (The Yi Tang group at UCLA, provided the Hpm8 plasmid.) The primers used are show in Table 2. The 300 base pair insert that results was ligated into pET30b, and the resulting plasmid was used to transform *E. coli* BL21(DE3) for expression. The sequence of the resulting peptide is also shown in Table 2.

Table 2: Primers for Hpm8-ACP1 expression

Primer	Description	Sequence
Forward primer	NdeI-N-His-forward	aaCATATGCATCACCATCATCATCACtctgctgtctcgctcgcctc
Reverse primer	EcoRI-reverse	aaGAATTCttaaacagtaaccaacttgctcttc
Resulting peptide, Hpm8-ACP1: MHHHHHHSAVSLASRLSKVSTKDEAAEIITDALVNKTADILQMPPSEVDPGRPL YRYGVDSLVALEVRNWITREMKANMALLEILAAVPIESFAVKIAEKSKLVTV		

The resulting protein was largely insoluble, and in expression at 37 °C no soluble protein was produced after induction with IPTG. If the cultures instead were incubated overnight at 16 °C following induction, while still providing primarily insoluble protein, approximately 4 mg of soluble protein per 500 mL culture could be obtained following Ni-NTA affinity chromatography. In an attempt to pursue NMR analysis, the natural abundance peptide was exchanged into various NMR-suitable buffers, using the buffers from the previously published ACP structures as a guide.[107,109] Unfortunately, concentrated samples, or those in acidic buffer, would precipitate. I was able to prepare a sample for NMR with an approximate concentration of 0.5 mM in pH 7.5 20 mM phosphate buffer (10% D_2O) for preliminary NMR analysis (Figures 48 and 49). A second ^{1}H-NMR was measured after 16 hours of leaving the same at room temperature to assess that sample stability and amenability to long duration experiments. We observed a significant reduction in signal intensity, suggesting the sample would be not stable for the time courses required for NMR data collection.

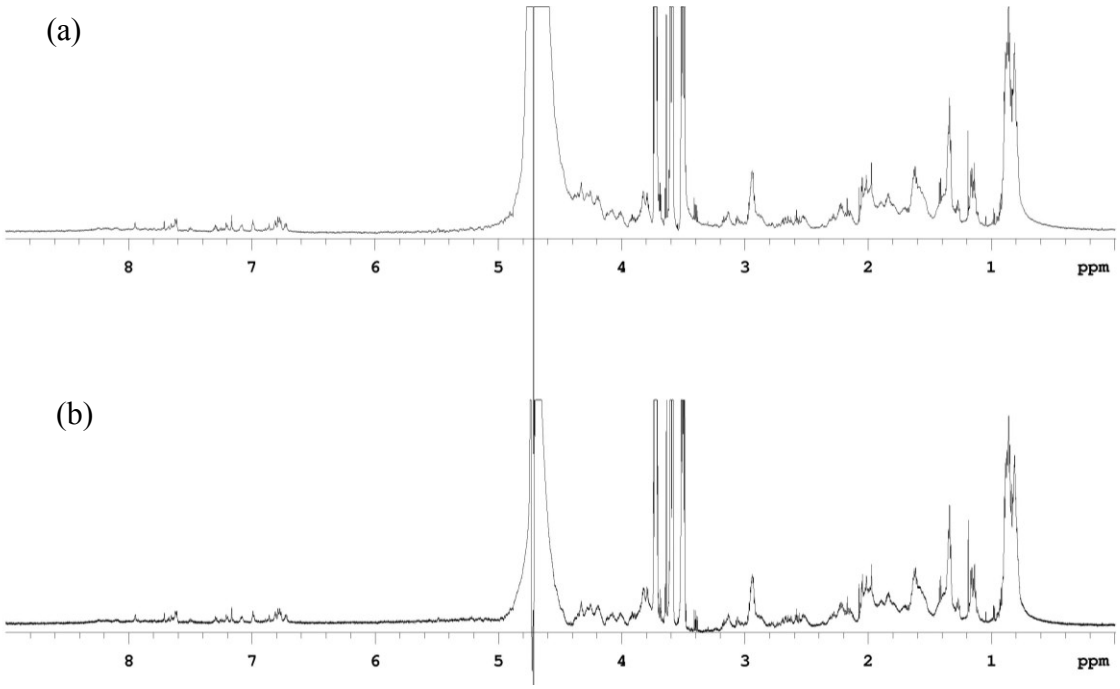

Figure 48: ^{1}H-NMR of Hpm8-ACP1 at 0 h (a) and 16 h (b)

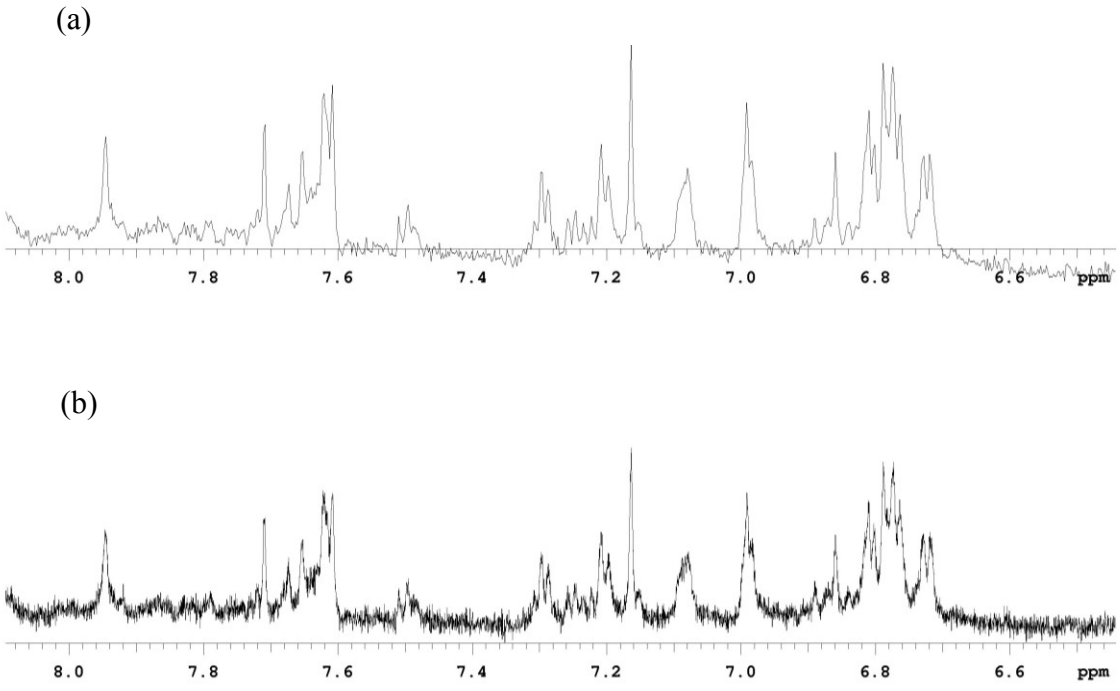

Figure 49: Expansion of the amide/aromatic region of Hpm8-ACP1 at 0 h (a) and 16 h (b), showing the notable increase in signal to noise over time

Following this disappointing result, I pursued strategies that had that potential to improve the solubility and stability. Firstly, the new construct would have a cleavable hexahistidine tag. For shorter proteins like Hpm8-ACP, the unnaturalness of six histidine residues in a row is a larger proportion of the protein than is typical, and therefore it is not unreasonable to suggest it may have been contributing to the insolubility or instability. Next, through comparison with helix boundaries in known ACP structures, we decided that the sequenced could be shortened at the N-terminus. By removing nine residues from the start of the sequence (SAVSLASRL), the predicted average hydrophobicity was reduced substantially. Average hydrophobicity is a calculation published by Kyte and Doolittle in 1982, and has since been referenced nearly 17,000 times.[111] The calculation assigns a hydrophobicity index to each amino acid, and sums the indices of the amino acid over a window of residues (a window of nine was chosen for my analysis). By plotting the sum in a graph one can visualize the overall pattern of hydrophobicity along the protein, and assign an average score (positive scores are hydrophobic, negative for hydrophilic) (Figure 50). The removal of the nine residues from the start of the protein eliminated the N-terminal hydrophobic region and reduced the predicted average hydrophobicity, also called a grand average of hydrophobicity or "GRAVY" score, from 1.61 to 0.86. To put this value in context, the average protein has a GRAVY score of -2.67, while proteins with values above 0.1 are considered to be highly hydrophobic. [112] This analysis further highlights the challenges of working with ACPs from type I systems; for comparison, the GRAVY score of *E. coli* FAS ACP, a type II ACP, is a highly negative value, -3.75.

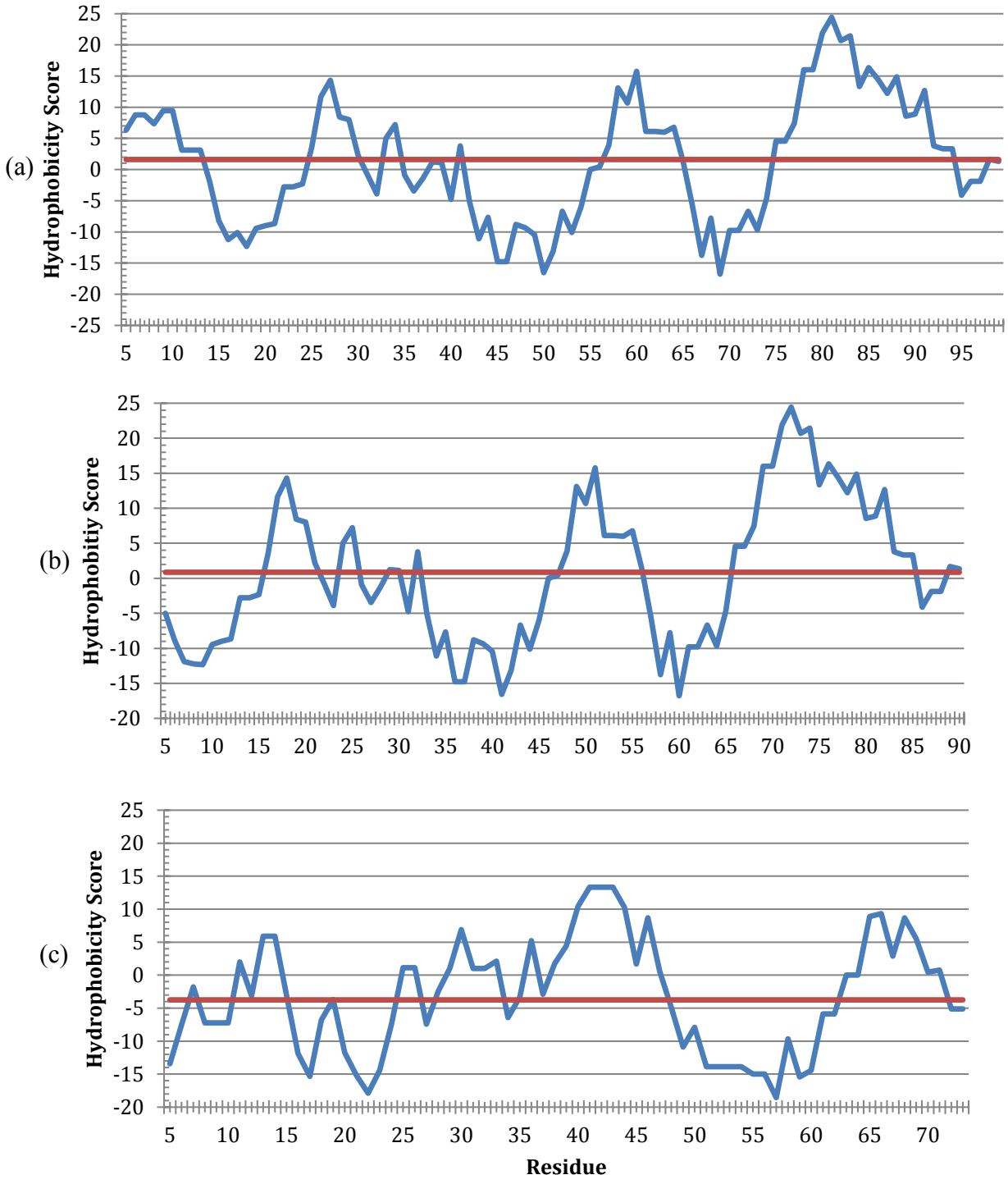

Figure 50: The Kyte and Doolittle plot for tagless Hpm8 constructs of (a) 103 residues and (b) 94 residues, and (c) for *E. coli* FAS ACP for comparison. Average hydrophobicity is traced in red.

To express this new ACP construct (called Hpm8-ACP2 herein), the gene was synthesized by Biobasic Inc. and subcloned into pET28a for expression in *E. coli*. The expected products of expression are shown in Table 3, both before and after thrombin removal of the purification tag.

Table 3: Amino Acid Sequence for Hpm8-ACP2

Identifier	Sequence	Molecular weight (Da)
His_6-Hpm8-ACP2	MGSSHHHHHHSSGLVPRGSHMSKVSTKDEAAEIITDALVNKTADILQMPPSEVDPGRPLYRYGVDSLVALEVRNWITREMKANMALLEILAAVPIESFAVKIAEKSKLVTV *His-tag *Thrombin Cleavage Site	12178.05
Hpm8-ACP2	GSHMSKVSTKDEAAEIITDALVNKTADILQMPPSEVDPGRPLYRYGVDSLVALEVRNWITREMKANMALLEILAAVPIESFAVKIAEKSKLVTV	10296.34

The expression at first seemed to proceed smoothly, yielding 3-5 mg per litre of bacterial culture, which was a single band by SDS-PAGE. However, when monitoring the thrombin cleavage reaction with MALDI, three main signals were observed, the expected peak (m/z = 10296), a peak corresponding to a loss of twelve C-terminal amino acids (m/z = 8999), and a peak corresponding to a loss of twenty C-terminal amino acids (m/z = 8185) (Figure 51). In order to determine if non-specific cleavage was taking place during the thrombin reaction, I then checked the MALDI of the pre-cleavage sample. The equivalent three peaks were observed, and when calibrated to the molecular weight of the full peptide, these peaks correspond exactly with losses of twelve (VKIAEKSKLVTV) and twenty (AVPIESFAVKIAEKSKLVTV) amino acids from the C-terminus.

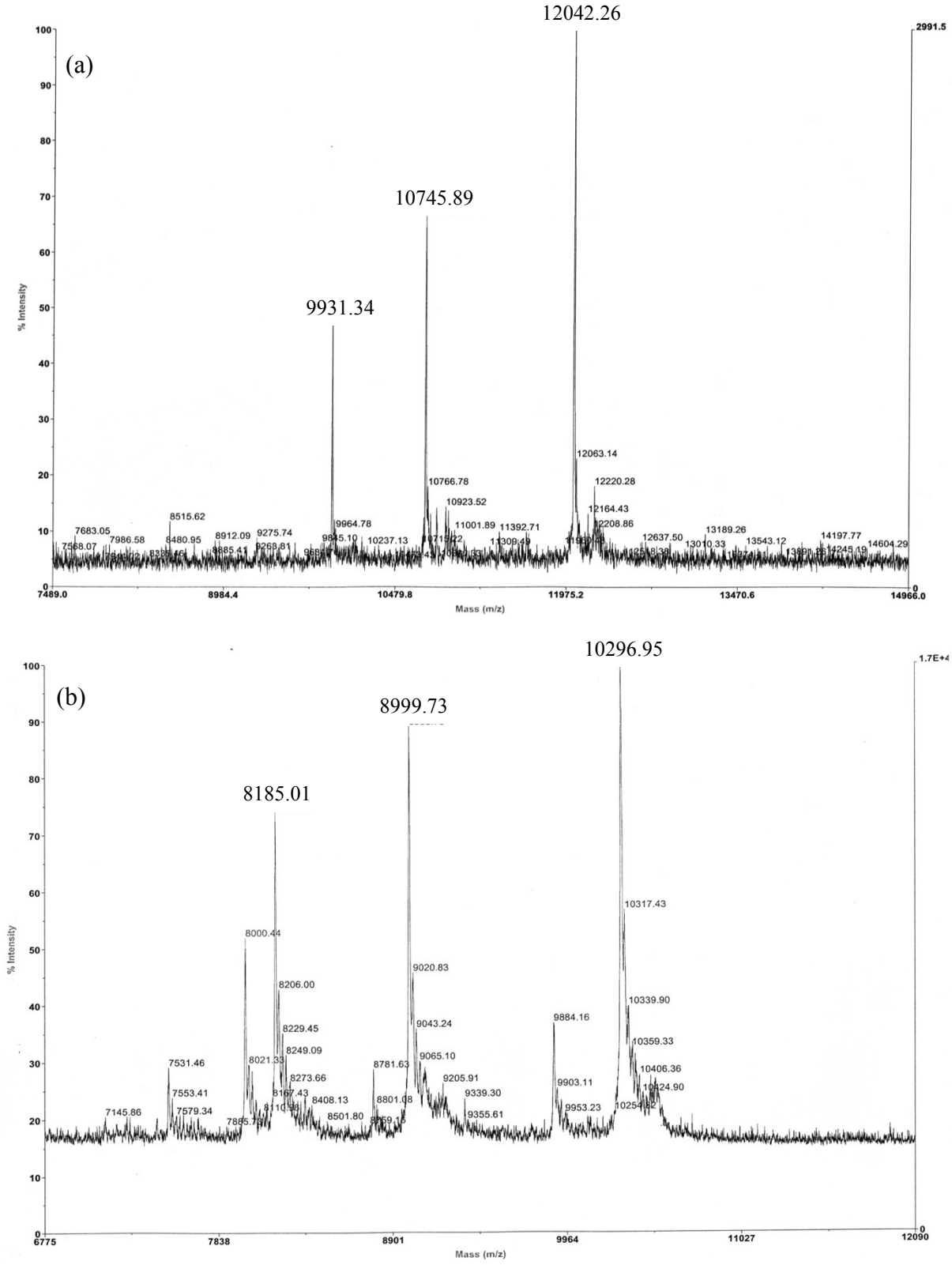

Figure 51: MALDI-MS analysis of (a) His_6-Hpm8-ACP2 and (b) Hpm8-ACP2

At this stage, I attempted the expression and purification under various conditions to try to prevent protein cleavage. However, none of the typical techniques, such as changing expression time and temperature, use of protease inhibitors during lysis and purification, varying cell lysis techniques, and diligent temperature control, were able to provide pure, intact protein. As the insolubility of inclusion bodies have the potential to make the protein resistant to proteases, I also recovered protein from the insoluble fractions for MALDI analysis. However, this sample also contained the three different species. This led me to postulate that perhaps there has been incomplete translation of the protein. Based on the Kyte-Doolittle plot shown in Figure 50, we can see that around residue 70, there is a section of hydrophobicity that is both long and intensely hydrophobic. It is a possibility that aggregation of this region could destabilize the peptide-ribosome complex, leading to the observed fragments of 74 and 82 residues. It remains unclear, however, how Hpm8-ACP1 could be spared from this phenomenon, as it was purified as a single peptide. Unfortunately, this result led me to abandon the pursuit of an Hpm8-ACP NMR structure at this stage.

Expression of LovB-ACP

As with Hpm8-ACP, prior to expression of LovB-ACP we needed to define the boundaries of the domain. Because the ACP precedes the CON domain at the C-terminus, both termini of the protein needed to be defined. We chose two different constructs to be synthesized and subcloned into pET28a by Biobasic Inc, which were designed to have N-terminal hexahistidine tags and thrombin cleavage sites. First, we expressed a slightly longer version with the homologous boundaries to Hpm8-ACP1, named LovB-ACP1. The second construct, LovB-ACP2, is homologous to Hpm8-ACP2, and therefore its boundaries were defined by comparison

to the helix boundaries in the literature. A notable difference is the addition of five residues to the C-terminus relative to LovB-ACP1, though it is still slightly shorter than LovB-ACP1 due to the elimination of 10 residues from the N-terminus. The protein sequences of the resulting peptides are show in Table 4.

Table 4: LovB-ACP constructs

Identifier	Sequence	Molecular Weight pre and post tag cleavage
(His_6)-LovB-ACP1	MGSSHHHHHHSSGLVPR|GSHMSKGSVKEQLL QATNLDQVRQIVIDGLSAKLQVTLQIPDGESVH PTIPLIDQGVDSLGAVTVGTWFSKQLYLDLPLL KVLGGASITDLANEAAAR	pre: 12243.9 post: 10361.88
(His_6)-LovB-ACP2	MGSSHHHHHHSSGLVPR|GSHMQATNLDQVRQ IVIDGLSAKLQVTLQIPDGESVHPTIPLIDQGVD SLGAVTVGTWFSKQLYLDLPLLKVLGGASITD LANEAAARLPPSS	pre: 11655.23 post: 9773.18

Similarly to Hpm8-ACPs, the LovB-ACPs were expected to be highly hydrophobic. Kyte-Doolittle analysis, graphed in Figure 52, showed this to be true. LovB-ACP is even more hydrophobic than Hpm8-ACP, and shortening of the N-terminus appears to worsen the GRAVY score from 1.35 to 1.85. Good solubility was not expected, but as this is only a prediction, the proteins were expressed and studied.

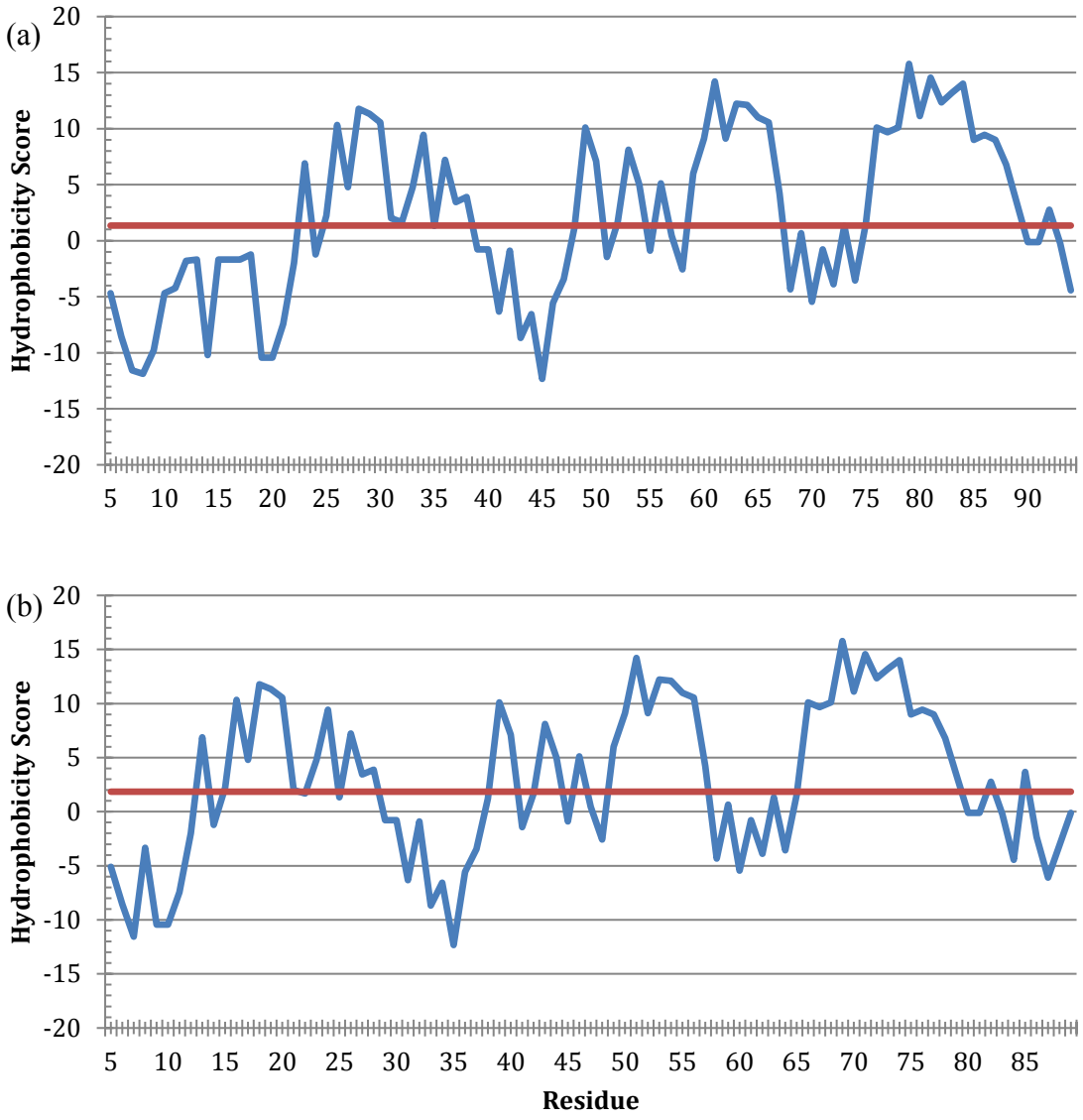

Figure 52: Kyte-Doolittle plot of LovB-ACP1 (a) and LovB-ACP2 (b)

Early small-scale trial expressions showed a significant amount of protein is expressed as inclusion bodies for both constructs, with no noticeable difference between constructs. I then proceeded with LovB-ACP2, as the shorter peptide would be preferable for NMR analysis. Due to the insolubility, isolation and renaturation of the protein from the inclusion bodies was pursued, using a procedure adapted from literature.[113] Circular dichroism spectroscopy showed

that the protein secondary structure was random coil (Figure 53), and so optimization of soluble expression needed to be pursued instead.

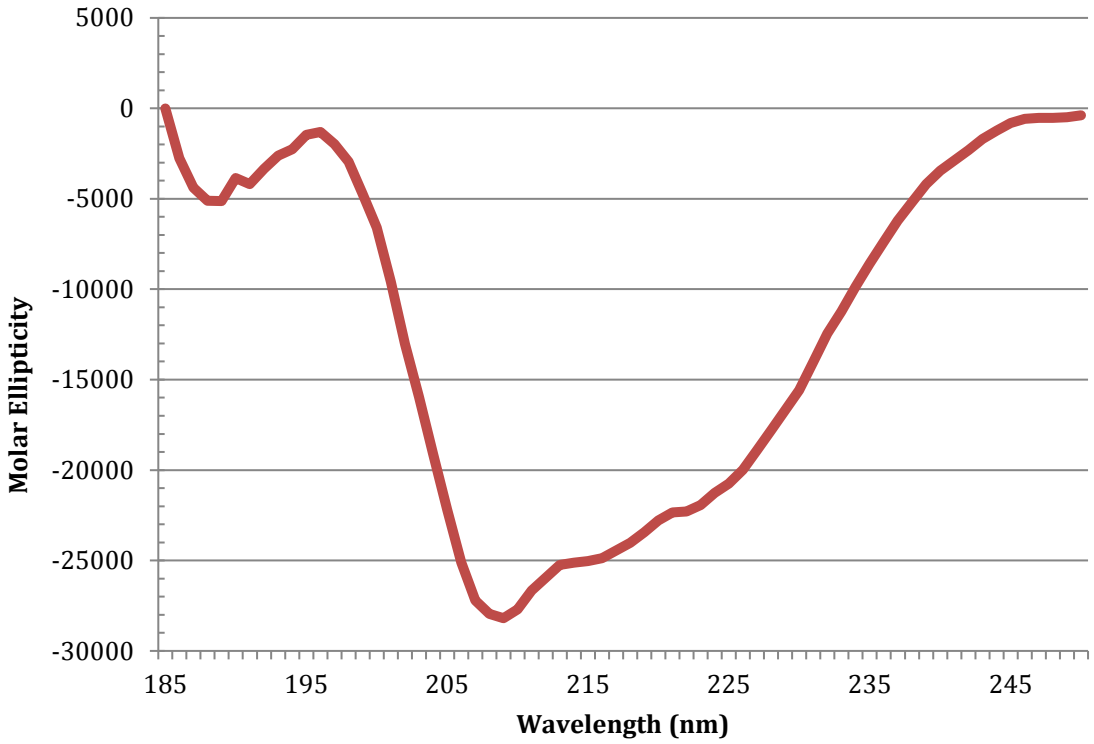

Figure 53: CD spectrum of LovB-ACP2, showing a characteristic random coil pattern, where molar ellipticity values are negative across all wavelengths

The optimal conditions, expression at 30 °C for 6 hours, following induction with 1 mM IPTG at OD_{600} 0.4-0.6, yielded approximately 2 mg of LovB-ACP2 per litre of culture. The protein appeared as single peak by LC-MS analysis, with a m/z of 9773.15 as calculated. The protein was stable in solution at very low concentrations, but would precipitate upon concentrating. The resulting supernatant would have a concentration around 1 mg/mL (0.1 mM), which is insufficient for NMR analysis. Buffer optimization (modifying pH, ionic strength,

buffer identity and organic co-solvents) was not fruitful, and thus the pursuit of an NMR structure was abandoned and other uses for LovB-ACP were explored.

Phosphopantetheinylation with Sfp and NpgA

As discussed in the introduction, one motivation for studying ACP is advancing our understanding of how carrier proteins interact with their cognate enzymes. LovB-ACP could therefore be used towards this end through the study of its interactions with the CON and DH domains previously expressed. However, at this stage, only *apo*-LovB-ACP was available. It is probable that protein-protein interactions rely on the phosphopantetheine prosthetic group. Therefore, the next goal was to phosphopantetheinylate LovB-ACP1.

One possible way to obtain *holo*-LovB-ACP is to use an *E. coli* host with a chromosomal copy of a phosphopantetheinyl transferase gene, typically *sfp* from *B. subtilis*.[114] However, ideally the procedure would be amenable to the use of unnatural analogues of CoA, and therefore an *in vitro* method was sought.

Our lab had on hand some heterologously expressed Sfp, and I attempted the ppant transferase with this enzyme. LovB-ACP2 was reacted with Coenzyme A in the presence of Sfp and $MgCl_2$. Monitoring the reaction using MALDI, there was low conversion, and after leaving it overnight, residual apoprotein remained. Because the *apo*- and *holo*-ACP would be impossible to separate based on traditional protein purification methods, this was inadequate. Sfp is from a bacterial source, and so it was believed that a ppant transferase from a fungal source would be better matched with LovB-ACP for this reaction. Thus, an expression plasmid containing for *npgA* was acquired from our collaborator Shiou-Chuan Tsai at UC Irvine. NpgA is a ppant transferase from the fungus *Aspergillus nidulans*,[53] and has been successfully employed for

fungal carrier proteins where Sfp was inadequate. It is the ppant transferase used in the yeast expression of LovB in Chapter 3, and therefore is known to be effective *in vivo* for this purpose. I heterologously expressed and purified NpgA from *E. coli*, and employed it in a phosphopantetheinylation reaction. As predicted, the reaction proceeded cleanly and was complete following overnight reaction (Figure 54).

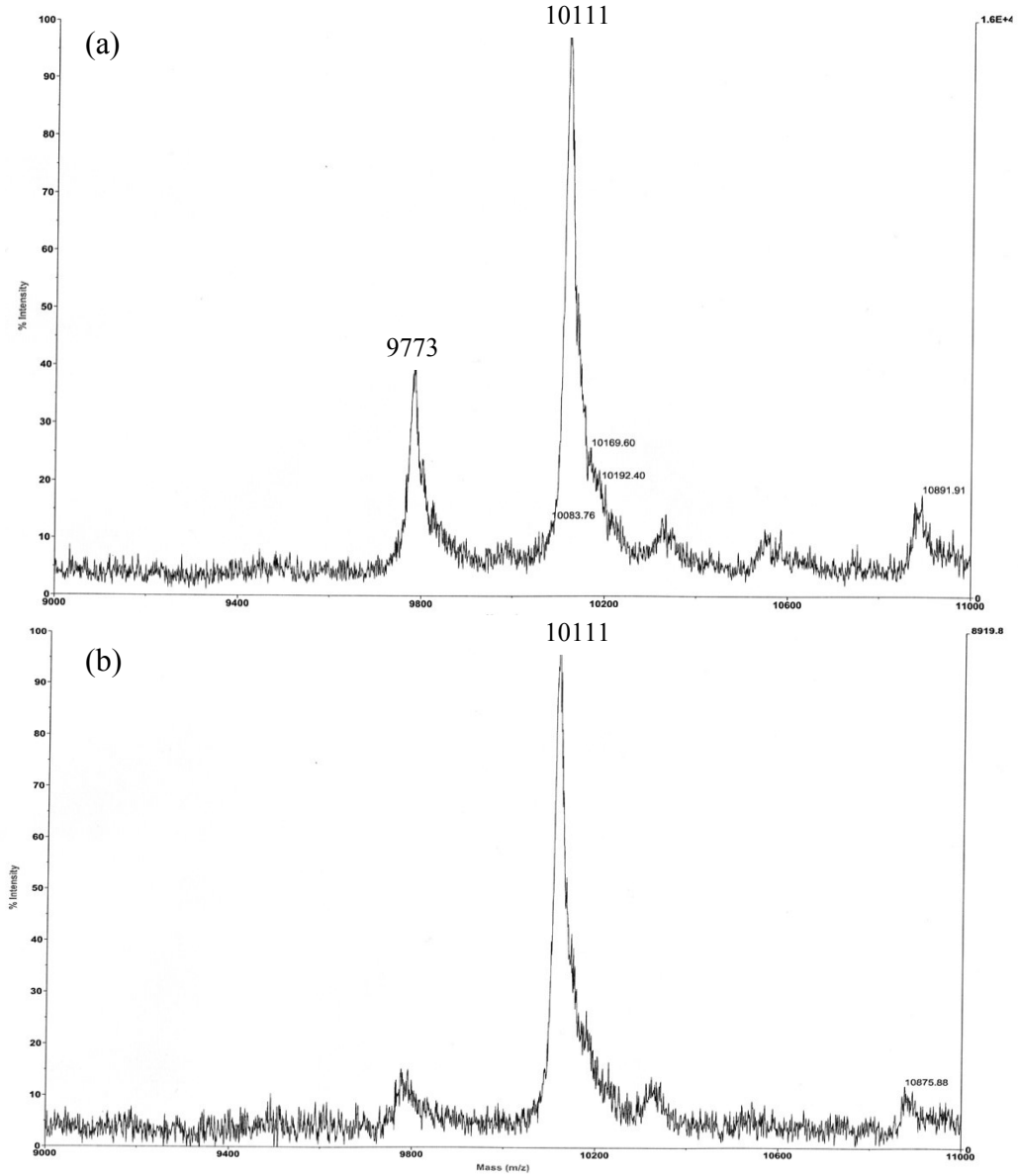

Figure 54: MALDI showing the improvement from using Sfp (a) for phosphopantetheinylation, to using NpgA (b)

Conclusion and Future Work

It has become evident through this work that the ACPs from fungal Type I PKS systems are challenging to work with and may not be amenable to NMR solution structure elucidation. While I was unable to solve the structures for Hpm8-ACP or LovB-ACP, their heterologous expression was accomplished in *E. coli*. LovB-ACP was successfully phosphopantetheinylated, and having *holo*-ACP in hand could prove to be a useful tool for understanding LovB function. My next step would be to assess the interactions of LovB-ACP with other stand-alone domains that were expressed. Using native gel electrophoresis, I could assess qualitatively if *holo*-LovB-ACP binds to DH and/or CON, and these interactions could quantitatively be assessed with isothermal calorimetry. If *holo*-ACP did not interact with CON, or the interaction was relatively weaker than its interaction with DH, this would support the theory discussed in Chapter 3 that the CON does not have a catalytic role for the growing acyl chain.

Our group also has a long-term goal of obtaining more structural information about LovB throughout the assembly of DHML (**11**). PhD student Randy Sanichar has successfully modified Coenzyme A to amino-CoA, an analogue that carries a terminal amino group in place of the free thiol. This free amine can be coupled to various acyl chains, such as ketides or mechanism-based inhibitors. Functionalizing LovB-ACP with amino-CoA derived phosphopantetheine analogues would provide useful tools for the structural analysis of LovB. The goal would be to produce crystal structures with the ACP bound to different domains of LovB to freeze the enzyme in one step of the assembly line at a time. This would help us understand the role the ACP plays in shuttling the intermediates around the molecular factory that is LovB, and shed light on the programming of this complex megasynthase.

CHAPTER 5: CONCLUSION

Fungal Iterative Highly Reducing Polyketide Synthases (HR-PKSs) are large, complicated, multi-domain proteins that catalyze the assembly of biologically potent, pharmaceutically relevant and financially important natural products. The overall aim of this thesis was to contribute to our collective knowledge of how these molecular factories operate.

In Chapter 1, polyketides were introduced with the intention of conveying the importance these molecules have in chemistry and in health care. I discussed the knowledge in the literature prior to this thesis regarding the assembly of hypothemycin (**12**) and lovastatin (**1**), the two molecules at the centre of this work.

In Chapter 2, I explored the nature of the many intermediates found the biosynthesis of hypothemycin (**12**) and lovastatin (**1**). Prior to our publication in the Journal of the American Chemical Society,[38] the proposed intermediates of HR-PKS enzymes had not been proven experimentally. The synthesis of the series of LovB/C intermediates was also completed, so that the results found in the Hpm system can be validated and extended to another subtype of fungal HR-PKS.

In Chapter 3, the highly elusive and controversial subject of natural Diels-Alderase enzymes was broached, in the context of such activity of LovB. To our surprise, it was found that the CON domain does not catalyze the cyclization of the SNAC analogue of the hexaketide triene (**40**). Throughout the study I developed new ways to analyze the results of this reaction, which have the potential to improve detection and ease of future studies in this area. While the details of the Diels-Alder reaction, including the active domain and the true substrate, have not been characterized as of yet, the work in this thesis provided compelling evidence for where to explore next. In particular, the potential of a KR-catalyzed cyclization of the β-ketoheptaketide

98 is a promising avenue for investigation that would not have been explored without the results of this thesis.

In Chapter 4, we learned of the inherent difficulties of working with the ACP domains of fungal iterative HR-PKSs. The ACP domain is not a passive carrier, but rather an important player in polyketide biosynthesis, and we wish to understand its role in the HR-PKS. Despite the challenges of working with intensely hydrophobic proteins that are not designed to stand alone, I believe my work has laid the foundations for future investigations into the structural biology of LovB.

EXPERIMENTAL PROCEDURES

Chemical Synthesis

Reagents, Solvents and Purification

All reactions requiring an inert atmosphere (air or moisture sensitive), where conducted under positive pressure of anhydrous argon. Solvents were distilled under argon as follows: tetrahydrofuran and diethyl ether were distilled over sodium and benzophenone; acetonitrile, dichloromethane, chloroform, methanol, and triethylamine were distilled over calcium hydride, while methanol and triethylamine were further dried over activated molecular sieves. All other solvents and chemicals were reagent grade and used as supplied, unless otherwise indicated. Chemical reagents were purchased from Sigma Aldrich, with the exception of ^{13}C-labeled reagents, which were purchased from Cambridge isotope laboratories. Deionized water was obtained from a Milli-Q reagent water system. Brine refers to a saturated solution of NaCl. Removal of solvent was performed under reduced pressure using a Büchi rotary evaporator. Flash chromatography was performed using silica gel (EM Science, 60 Å, 230-400 mesh), while fractions were monitored using Thin Layer Chromatography (TLC). TLC was performed on glass plates, coated with 0.25 mm silica (Merck 60, F_{254}). Compounds were visualized under UV when possible, or stained by dipping the plates in 1% $Ce(SO_4)•4H_2O$ or 2.5% $(NH_4)Mo_7O_{24})•4H_2O$ in 10% H_2SO_4, followed by heating with a heat gun.

Characterization

Infrared spectroscopy (IR) was performed on a Nicolet Magna 750 or a 20SX FT-IR spectrometer. Cast film method refers to the evaporation of a solution containing the analyte on a NaCl plate. Nuclear magnetic resonance (NMR) spectra were acquired on Varian Inova 400

MHz, Varian Inova 500 MHz, Varian 500 (equipped with cryo-probe) and VNMRS 700 MHz spectrometers. ^{1}H NMR chemical shifts are reported in parts per million (ppm), referencing to the residual proton resonances of the deuterated chloroform (7.26 ppm). ^{13}C NMR chemical shifts are referenced to $CDCl_3$ (77.0 ppm). Optical rotations were measured on a Perkin Elmer 241 polarimeter with a microcell (10 cm, 1 mL) at 23 °C. High resolution mass spectrometry was performed on a ZabSpec IsoMass VG (electrospray ionization (ES)).

Synthesis and Characterization of Compounds

Dihydromonacolin L (11)

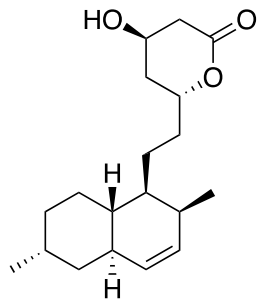

11

Dihydromonacolin L was isolated from a strain of *Aspergillus nidulans* expressing the *lovB* and *lovC* genes (stored at the University of Alberta Microfungus Collection and Herbarium, accession number 9442),[24] using the procedure of John Sorensen.[64] A spore suspension was made from plated mycelia using sterile water, and was used to inoculate 1 L of *A. nidulans* growth media (see recipe in biological methods). The culture was incubated at 30 °C and 200 rpm for 4 days. The mycelia were harvested by filtration through sterile cheesecloth and were thoroughly rinsed with 2 L of a 1% lactate solution. The harvested mycelia were divided in 4 equal portions to inoculate 4 x 1 L of *A. nidulans* growth media (see recipe in biological

methods). Cultures were incubated for 2 days at 30 °C and 200 rpm, after which point the growth media was supplemented with 1 g/L of sodium acetate daily for an additional 5 days. The broth was isolated by removing the mycelia using vacuum filtration, and all 4 litres were combined. The combined broth was acidified with 2 N HCl (to a pH of less than 2) and extracted with CH_2Cl_2 (2 x 1.5 L). The combined organic layers were dried over sodium sulfate, and the solvent was removed *in vacuo*. The residue was purified by column chromatography (10% acetone in CH_2Cl_2) to yield on average 300 mg of pure **11**. Spectral data was in accordance with published data.

^{1}H NMR (500 MHz, $CDCl_3$) δ 5.57 (ddd, 1H, J = 9.8, 4.9, 2.7 Hz, H-3), 5.28 (d, 1H, J = 9.8 Hz H-4), 4.67 (m, 1H, H-11), 4.38 (m, 1H, H-13), 2.72 (dd, 1H, J = 17.6, 5.13 Hz, Ha-14), 2.60 (ddd, 1H, J = 17.6, 3.7, 1.6 Hz, Hb-14), 2.21 (m, 1H, H-2), 2.00 (m, 1H, H-6), 1.95 (m, 1H, Ha-12), 1.89 (m, 1H, H-4a), 1.80-1.73 (m, 2H, Ha-10 and Hb-12), 1.62 (m, 2H, H-9), 1.58-1.42 (m, 5H, H-5, H-7, H-8a and Hb-10), 1.07 (m, 1H, Ha-8), 0.97 (m, 1H, Hb-8), 0.96 (d, 3H, J = 7.3 Hz, 6-CH_3), 0.82 (d, 3H, J = 6.9 Hz, 2-CH_3). ^{13}C NMR (125 MHz, $CDCl_3$) δ 170.7 (C-15), 132.6 (C-3), 131.7 (C-4), 76.2 (C-11), 62.8 (C-13), 41.4 (C-8a), 40.0 (C-8), 39.0 (C-5), 38.7 (C-14), 37.3 (C-4a), 36.1 (C-12), 33.2 (C-10), 32.3 (C-7), 32.0 (C-2), 27.5 (C-6), 23.7 (C-1), 23.6 (C-9), 18.2 (6-CH_3), 15.0 (2-CH_3).

[1-^{13}C]-(*S*,*E*)-*S*-2-acetamidoethyl 5-hydroxyhex-2-enethioate (30)

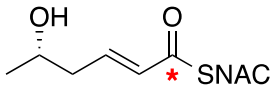

To a solution of AcOH/H_2O/THF (3:3:1, 7 mL) was added compound **35** (225 mg, 0.650 mmol). The mixture was stirred at room temperature for 19 hours, after which the volatile components

were removed under high vacuum. The residue was diluted with 5 mL water, and the solution was extracted with EtOAc (3x5 mL). The combined organic portions were washed with brine (20 mL) and dried over Na_2SO_4, filtered and concentrated under reduced pressure to give **30** as a white solid (125 mg, 83%). IR (cast film) 3295, 3086, 2968, 2930, 1650, 1617, 1553 cm^{-1}; ^1H NMR (500 MHz, $CDCl_3$) δ 6.92 (dddd, 1H, J =15.4, 7.3, 7.3 Hz, $J_{1H\text{-}13C}$ = 7.30 Hz, H-3), 6.20 (ddt, 1H, J = 15.4, 1.5 Hz, $J_{1H\text{-}13C}$ = 6.10 Hz, H-2), 6.00 (br s, 1H, NH), 3.96 (sextet, 1H, J = 6.10 Hz, H-5), 3.46 (dt, 2H, J = 6.1, 6.1 Hz, H-1'), 3.10 (dt, 2H, $J_{1H\text{-}13C}$ = 5.6 Hz, J = 4.9 Hz, H-2'), 2.34 (t, 2H, J = 7.4 Hz, H-4), 1.94 (s, 3H, H-5'), 1.22 (d, 3H, J = 6.2 Hz, H-6); ^{13}C NMR (125 MHz, $CDCl_3$) δ 190.3 (enriched, C-1), 170.6 (C-4'), 142.6 (C-3), 130.5 (d, $J_{13C\text{-}13C}$ = 61.3 Hz, C-2), 66.6 (C-5), 41.8 (d, $J_{13C\text{-}13C}$ = 6.7 Hz), 39.7, 28.3, 23.4, 23.2; α_D^{25}= 0.0944 (c = 0.780, $CHCl_3$); HRMS (ES) m/z calculated for $C_9[^{13}C]H_{18}NO_3S$ 233.1035, found 233.1034 $[M+H]^+$.

[1-^{13}C]-Diethyl phosphonoacetate N-acetylcysteamine thioester (32)

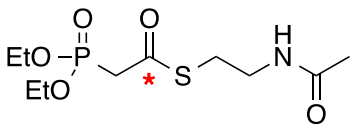

To a stirred solution of 1M NaOH (3.6 mL), ethyl-(diethoxyphosphono)-[1-^{13}C]-acetate (**31**) dropwise. After 3 hours at room temperature, ethanol produced in the reaction was removed under reduced pressure. The remaining aqueous solution was acidified to pH = 1 using concentrated HCl and extracted with ethyl acetate (3x5 mL). The combined organic extracts were washed with brine (10 mL), dried with sodium sulfate, filtered and concentrated under reduced pressured to give diethyl phosphonoacetic acid as a colourless liquid (450 mg, 73% yield). IR ($CHCl_3$, cast film) 2987, 1689, 1224 cm^{-1}; ^1H NMR (500 MHz, $CDCl_3$) δ 9.48 (br s,

1H, COO<u>H</u>), 4.22-4.15 (m, 4H, OC<u>H</u>$_2$CH$_3$), 2.98 (dd, 2H, $J_{1H\text{-}13C}$ = 7.3 Hz, $J_{1H\text{-}31P}$ = 21.8 Hz, H-1), 1.34 (t, 6H, J = 7.1 Hz, OCH$_2$C<u>H</u>$_3$); ^{13}C NMR (125 MHz, $CDCl_3$) δ 167.8 (enriched, d, $J_{13C\text{-}31P}$ = 5.4 Hz), 63.2 (d, $J_{13C\text{-}31P}$ = 6.5 Hz), 34.2 (dd, $J_{13C\text{-}31P}$ = 134.5 Hz, $J_{13C\text{-}13C}$ = 55.2 Hz), 16.3; HRMS calculated for $C_5[^{13}C]H_{12}O_5P$ 196.0461, Found 196.0464 $[M\text{-}H]^-$.

The isotopically labeled version of known compound **32** was synthesized by a literature method.[28] In a flame-dried flask under argon, [1-^{13}C]-diethylphosphonoacetic acid (330 mg, 1.70 mmol) was dissolved in 10 mL of CH_2Cl_2 and cooled to 0 °C. Dimethylaminopyridine (20.0 mg, 0.163 mmol) and dicyclohexylcarbodiimide (DCC) (385 mg, 1.85 mmol) were added, followed by an excess of *N*-acetylcysteamine (0.500 mL, 4.70 mmol). The reaction mixture was stirred at 0 °C for 30 min, then warmed to room temperature and stirred for an additional 22 hours. The solvent was removed under reduced pressure, and the crude reaction mixture was redissolved in ethyl acetate/diethyl ether = 1:1 (10 mL) and filtered to remove precipitated *N,N'*-dicyclohexylurea. The filtrate was concentrated under reduced pressure, and then purified by flash column chromatography (EtOAc to 10% MeOH/EtOAc) to give **32** as a white solid (315 mg, 62% yield). IR ($CHCl_3$, cast film) 3294, 2983, 1648, 1548, 1255 cm^{-1}; ^{1}H NMR (500 MHz, $CDCl_3$) δ 6.65 (br s, 1H, N<u>H</u>), 4.20 (m, 4H, OC<u>H</u>$_2$CH$_3$), 3.45 (dt, 2H, J = 6.2, 6.2 Hz, H-4), 3.22 (dd, 2H, $J_{1H\text{-}31P}$ = 21.2 Hz, $J_{1H\text{-}13C}$ = 6.4 Hz, H-1), 3.09 (2H, dt, J = 6.5 Hz, $J_{1H\text{-}13C}$ = 5.6 Hz, H-3), 2.00 (s, 3H, H-6), 1.34 (t, 6H, J = 7.1 Hz, OCH$_2$CH$_3$); ^{13}C NMR (125 MHz, $CDCl_3$) δ 190.5 (enriched, d, $J_{13C\text{-}31P}$ = 7.0 Hz), 170.5, 62.9 (d, $J_{13C\text{-}31P}$ = 6.2 Hz), 43.0 (dd, $J_{13C\text{-}31P}$ = 131.0 Hz, $J_{13C\text{-}13C}$ = 44.7 Hz), 39.0, 29.5, 23.1, 16.3 (d, $J_{13C\text{-}31P}$ = 6.2 Hz); HRMS (ES) m/z calculated for $C_9[^{13}C]H_{21}NO_5PS$ 299.0906, found 299.0909 $[M+H]^+$.

4-Tertbutyldimethylsilyl-butyryl aldehyde (33)

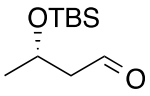

The known aldehyde was synthesized by a literature procedure, and characterization matched published data. [58]

[1-^{13}C]-(*S*,*E*)-*S*-2-acetamidoethyl 5-(*tert*-butyldimethylsilyloxy)hex-2-enethioate (35)

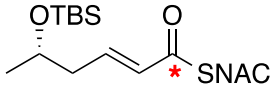

To a stirred solution of LiBr (252 mg, 3.00 mmol) in THF, compound **32** (280 mg, 0.950 mmol) was added. The solution was stirred for 10 min at 25 °C, followed by the addition of Et_3N (0.400 mL, 3.00 mmol). The solution was stirred for an additional 10 min and then aldehyde 33 (404 mg) in 2 mL dry THF was added. After 12 hours at room temperature, the reaction was quenched by the addition of 15 mL of water, and the resulting solution was extracted with EtOAc (3x10 mL). The combined organic extracts were washed with brine (20 mL), dried over Na_2SO_4 and concentrated under reduced pressure. The residue was purified by flash column chromatography (1:1 EtOAc/hexanes to 2:1 EtOAc/hexanes) to give **35** as a yellow oil (241 mg, 76 % yield). IR ($CHCl_3$, cast film) 3289, 2956, 2929, 1651, 1619, 1552, 1462; ^{1}H NMR (500 MHz, $CDCl_3$) δ 6.94 (dddd, 1H, J = 15.6, 7.3, 7.3 Hz, $J_{1H\text{-}13C}$ = 7.3 Hz, H-4), 6.14 (ddt, 1H, J = 15.6, 1.3 Hz, $J_{1H\text{-}13C}$ = 6.1 Hz, H-5), 6.1 (br s, 1H, N<u>H</u>), 3.95 (sextet, 1H, J = 6.1 Hz, H-2), 3.46 (dt, 2H, J = 6.1, 6.1 Hz, H-8), 3.10 (dt, 2H, J = 6.6, 4.9 Hz, H-7), 2.32 (t, 2H, J = 6.6 Hz, H- 3), 1.97 (s, 3H, H-10), 1.17 (d, 3H, J = 6.1 Hz, H-1), 0.88 (s, 9H, Si-C(C<u>H</u>$_3$)$_3$), 0.05 (s, 3H, Si-C<u>H</u>$_3$), 0.04 (s, 3H, Si-C<u>H</u>$_3$); ^{13}C NMR (125 MHz, $CDCl_3$) δ 190.3 (enriched), 170.4, 143.6, 130.1 (d, $J_{13C\text{-}13C}$ = 61.4

Hz), 67.5, 42.5 (d, $J_{13C\text{-}13C}$ = 6.7 Hz), 39.9, 28.2, 25.8, 23.9, 23.1, 18.0, -4.80; α_D^{25} = 7.88 (c = 0.510 g/100 mL, $CHCl_3$); HRMS (ES) m/z calculated for $C_{15}[^{13}C]H_{32}NO_3SSi$ 347.19, found 347.1896 $[M+H]^+$.

[9-^{13}C]-(*R*,6*E*,8*E*)-*S*-2-acetamidoethyl 4-methyldeca-6,8-dienethioate (^{13}C-39)

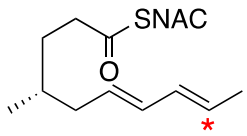

The following stock solution was prepared: 16 mL tBuOH, 1.06 mL 2-methyl-2-butene, 194 mg sodium chlorite, 148.3 mg NaH_2PO_4 in 4.5 mL H_2O. 5 mL of the stock solution was added to 12 mg of aldehyde ^{13}C-**51** and the reaction was stirred until completed by TLC (3 hours). The reaction was diluted with 12 mL of water, acidified to below pH 6 and extracted with 3x EtOAc. The combined organic layers were washed with brine, dried over $MgSO_4$, filtered and concentrated under reduced pressure, yielding acid ^{13}C-**52**. The acid ^{13}C-**52** was then used without further purification in the coupling to *N*-acetylcysteamine. ^{1}H NMR (500 MHz, $CDCl_3$) δ 6.10-5.98 (m, 2H), 5.85-5.71 (m, 1H), 5.69-5.41 (m, 1H), 2.49-2.32 (m, 2H), 2.20-1.92 (m, 2H), 1.80-1.65 (m, 4H), 1.60-1.45 (m, 2H), 0.92 (d, 3H, J = 6.5 Hz); ^{13}C NMR (125 MHz, $CDCl_3$) δ 177.1, 131.5 (d, J = 71 Hz, C-8), 129.7 (C-7), 129.4 (d, J = 10 Hz, C-6), 127.3 (C-9, enriched), 39.8, 32.9, 31.8, 31.3,19.2, 18.1 (d, J = 44 Hz, C-10).

The acid ^{13}C-**52** was dissolved in 1 mL distilled dichloromethane and cooled to 0 °C. 1.7 mg of DMAP and 29.3 mg DCC were added, following by 14.9 µL *N*-acetylcysteamine. The reaction was stirred overnight, allowing the ice to melt. The reaction was applied directly to a silica column and purified using neat EtOAc. (2.6 mg, 23 % yield over two steps). ^{1}H NMR (500 MHz,

$CDCl_3$) δ 6.1-6.0 (m, 2H), 5.85-5.71 (m, 1H), 5.68-5.43 (m, 1H, H-9), 3.46 (q, 2H, J = 6.0 Hz, C$\underline{H}_2$N), 3.05 (t, 2H, J = 6.1 Hz), 2.69-2.55 (m, 2H), 2.18-1.86 (m, 2H), 2.0 (s, 3H), 1.80-1.65 (m, 4H), 1.60-1.45 (m, 2H), 0.92 (d, 3H, 6.5 Hz); ^{13}C NMR (125 MHz, $CDCl_3$) δ 200.2 (C-1), 170.2 (N$\underline{C}$OCH$_3$), 131.5 (d, J = 71 Hz, C-8), 129.7 (C-7), 129.4 (d, J = 10 Hz, C-6), 127.5 (C-9, enriched), 42.0 ($\underline{C}$H$_2$N), 39.8 (C-5), 32.8, 32.1, 32.0, 28.5 ($\underline{C}$H$_2$S), 23.2 (NCO$\underline{C}$H$_3$), 19.2, 18.0 (d, J = 44 Hz, C-10); HRMS (ES) m/z calculated for [C_{14}[^{13}C]$H_{25}NO_2S$+Na] 307.1532, found 307.1530 $[M+Na]^+$.

(*R*,2*E*,8*E*,10*E*)-*S*-2-acetamidoethyl 6-methyldodeca-2,8,10-trienethioate (40) and (^{13}C-40)

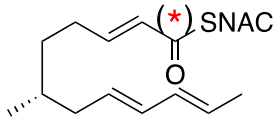

In a flame-dried flask under argon, LiBr (63 mg, 0.75 mmol) was dissolved in 1 mL THF. Horner-Wadworth-Emmons reagent **32** (150 mg, 0.5 mmol) was added in 1 mL THF, with an additional 0.5 mL to ensure complete transfer. Triethylamine (100 uL, 0.75 mmol) was added dropwise and the reaction was stirred for 10 min. Aldehyde **51** (approx. 0.25 mmol) was then added in a solution of diethyl ether and the reaction was left to stir overnight. When complete by TLC, the solvent was removed *in vacuo* and the crude mixture was redissolved in dichloromethane and distributed between 2 preparatory TLC plates for purification to provide the thioester **40** in up to 60% yield.

The same reaction was performed with ^{13}C-**51** to produce ^{13}C-**40**.

Data for natural abundance **40**: IR ($CHCl_3$, cast film) 3289 (broad), 3078, 3015, 2956, 2926, 2870, 1662, 1551 988 cm^{-1}; ^{1}H NMR (500 MHz, $CDCl_3$) δ 6.92 (dt, 1H, J = 15.5, 7.4 Hz, H-3),

6.13 (dt, 1H, J = 15.5, 1.5 Hz, H-2), 6.06-5.96 (m, 2H, H-9 and H-10), 5.63-5.55 (m, 1H, H-11), 5.53-5.46 (m, 1H, H-8), 3.46 (q, 2H, J = 6.0 Hz, H-2'), 3.09 (t, 2H, J = 6.0 Hz, H-3'), 2.30-2.14 (m, 2H, H-4), 2.10-2.20 (m, 1H, 1 x H-7), 1.96 (s, 3H, H-6'), 1.96-1.90 (m, 1H, 1 x H-7), 1.74 (d, 3H, J = 6.6 Hz, H-12), 1.55 (s, 1H, NH), 1.58-1.46 (m, 2H, 1 x H-5 and H-6), 1.31-1.24 (m, 1H, 1 x H-5), 0.88 (d, 3H, J = 6.6 Hz, 6-CH_3); ^{13}C NMR (125 MHz, $CDCl_3$) δ 199.4 (C-1), 170. 2 (C-5'), 146.8 (C-3), 132.0 (C-9), 131.6 (C-10), 129.7 (C-8), 128.3 (C-2), 127.2 (C-11), 39.9 (C-7), 39.8 (C-3'), 34.5 (C-4), 32.9 (C-6), 30.0 (C-5), 28.3 (C-2'), 23.2 (C-6'), 19.3 (C-12), 18.0 (6-CH_3); α_D^{25} = -8.82 (c = 1.0 g/100 mL, $CHCl_3$); HRMS (ES) m/z calculated for [$C_{17}H_{28}NO_2S$] 310.1835, found 310.1831 $[M+H]^+$.

Data for ^{13}C-**40**: ^{1}H NMR (500 MHz, $CDCl_3$) δ 6.92 (dt, 1H, J = 15.5, 7.4 Hz, H-3), 6.13 (ddt, 1H, J = 15.5, 6.8 Hz, 1.5 Hz, H-2), 6.06-5.96 (m, 2H, H-9 and H-10), 5.63-5.55 (m, 1H, H-11), 5.53-5.46 (m, 1H, H-8), 3.46 (q, 2H, J = 6.0 Hz, H-2'), 3.09 (t, 2H, J = 6.0 Hz, H-3'), 2.30-2.14 (m, 2H, H-4), 2.10-2.20 (m, 1H, 1 x H-7), 1.96 (s, 3H, H-6'), 1.96-1.90 (m, 1H, 1 x H-7), 1.74 (d, 3H, J = 6.6 Hz, H-12), 1.55 (s, 1H, NH), 1.58-1.46 (m, 2H, 1 x H-5 and H-6), 1.31-1.24 (m, 1H, 1 x H-5), 0.88 (d, 3H, J = 6.6 Hz, 6-CH_3); ^{13}C NMR (125 MHz, $CDCl_3$) δ 199.4 (C-1, enriched), 170. 2 (C-5'), 146.8 (C-3), 132.0 (C-9), 131.6 (C-10), 129.7 (C-8), 128.3 (d, J = 61.6 Hz, C-2), 127.2 (C-11), 39.9 (C-7), 39.8 (C-3'), 34.5 (C-4), 32.9 (C-6), 30.0 (C-5), 28.3 (d, J = 6.7 Hz, C-2'), 23.2 (C-6'), 19.3 (C-12), 18.0 (6-CH_3).

[^{13}C]-(1*S*,2*S*,4a*R*,6*R*,8a*S*)-*S*-2-acetamidoethyl 2,6-dimethyl-1,2,4a,5,6,7,8,8a-octahydronaphthalene-1-carbothioate (^{13}C-41)

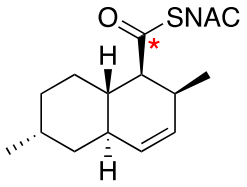

Five reactions were set up as follows, in glass falcon tubes: 2 mL reaction buffer (20 mM Tris, pH 8.0, 1 mM DTT, 1 mM sodium ascorbate), 1 mg triene ^{13}C-**40** (in a solution with 100 µL methanol) and 50 µL enzyme in storage buffer (20 mM Tris, pH 8.0, 1 mM DTT, 2 mM EDTA). Due to the low solubility of triene ^{13}C-**40**, the solutions were cloudy, and so more reaction buffer was added until the reactions were visibly clear (an additional 2 mL, for a total of 4 mL reaction buffer). The concentration of each enzyme stock solution was as follows: control, 0 mg/mL; LovB, 14 mg/mL; LovBΔCON, 8 mg/mL, CON, 6.2 mg/mL; DH, 7.5 mg/mL). The reactions were placed on an orbital shaker overnight. After 16 hours of reaction, the reactions were extracted with 3x5 mL $CHCl_3$. The $CHCl_3$ of the extracts was removed under reduced pressure, and the residues were redissolved in $CDCl_3$ for NMR analysis (as shown in Figures 41, 42 and 43). A discussion of the interpretation of these spectra can be found in the text, with the relevant signals to enzymatic product ^{13}C-**41** listed here, as found in the products of the reactions with LovB and LovBΔCON: ^{13}C NMR (700 MHz) δ 198.2 and/or 198.1. bsgHMBC (700 MHz) δ [198, 2.9] and [198, 3.6].

***S*-2-acetamidoethyl 3-((1*S*,2*S*,4a*R*,6*R*,8a*S*)-2,6-dimethyl-1,2,4a,5,6,7,8,8a-octahydronaphthalen-1-yl)propanethioate (^{2}H-42)**

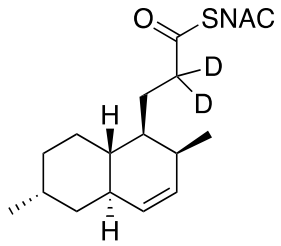

4.5 mg (0.02 mmol) of acid ^{2}H-**61** was dissolved in 200 μL of distilled CH_2Cl_2 and the solution was cooled to 0 °C in an ice-water bath. 2 mg of DMAP (0.6 eq) was added, followed by 10 μL of *N*-acetylcysteamine (4 eq), and finally 5 mg of DCC (1.2 eq). The reaction mixture was stirred for 30 min at 0 °C and then stirred overnight at room temperature. A white precipitate formed, and reaction mixture was concentrated *in vacuo*. The mixture was applied directly to a silica column for purification without further work up (gradient of 30% EtOAc in Hexanes to neat EtOAc). 2.2 mg of ^{2}H-**43** was obtained as a white solid (35% yield). ^{1}H NMR (500 MHz, $CDCl_3$) δ 5.78 (br s, 1H), 5.57 (ddd, 1H, J = 9.7, 4.9, 2.8 Hz), 5.29 (dt, 1H, J = 9.7 Hz, 1.3 Hz), 3.42 (q, 2H, J = 6.3 Hz), 3.02 (t, 2H, J = 6.5 Hz), 2.22 (m, 1H) 2.00 (m, 1H), 1.95 (s, 3H), 1.89 (m, 1H), 1.59-1.43 (m, 7H), 1.40-1.34 (m, 1H), 1.29-1.22 (m, 3H), 1.10 (dq, 1H, J = 12.1, 3.1 Hz), 0.98 (dq, 1H, J = 10.3, 2.3 Hz), 0.97 (3H, d, J = 7.0 Hz), 0.84 (3H, d, 7.4 Hz); ^{13}C NMR (125 MHz, $CDCl_3$) δ 200.4, 170.2, 132.3, 131.7, 41.0, 40.9, 39.9, 39.7, 38.86, 37.2, 32.2, 31.9, 28.5, 27.4, 24.7, 23.6, 23.2, 18.2, 14.9.

(*R*)-*S*-2-acetamidoethyl 5-((1*S*,2*S*,4a*R*,6*R*,8a*S*)-2,6-dimethyl-1,2,4a,5,6,7,8,8a-octahydronaphthalen-1-yl)-3-hydroxypentanethioate (^{2}H-43)

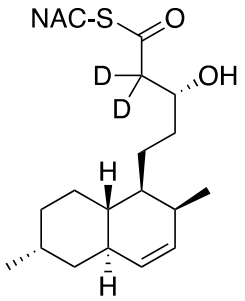

7 mg (0.025 mmol) of acid ^{2}H-**57** was dissolved in 200 µL of CH_2Cl_2 and the solution was cooled to 0 °C in an ice-water bath. 2 mg of DMAP (0.6 eq) was added, followed by 10 µL of *N*-acetylcysteamine (4 eq), and finally 6.2 mg of DCC (1.2 eq). The reaction mixture was stirred for 30 min at 0 °C and then stirred overnight at room temperature. A white precipitate formed, and reaction mixture was concentrated *in vacuo*. The mixture was applied directly to a silica column for purification without further work up (gradient of 30% EtOAc in hexanes to neat EtOAc). 2.0 mg of ^{2}H-**43** was obtained as a white solid (25% yield).

^{1}H NMR (500 MHz, $CDCl_3$) δ 5.74 ppm (br s, 1H, N<u>H</u>CH_2CH_2S), 5.57 (ddd, 1H, J = 9.8, 4.7, 2.7 Hz, H-3), 5.27 (d, 1H, 5.8 Hz, H-4), 4.04 (br s, 1H, H-3'), 3.49-3.39 (m, 2H, NHC<u>H$_2$</u>CH_2S), 3.08-2.99 (m, 2H, $NHCH_2C$<u>H$_2$</u>S), 2.55 (br s, 1H, O<u>H</u>), 2.21 (m, 1H, H-2), 2.00 (m, 1H, H-6), 1.95 (s, 3H, COC<u>H$_3$</u>), 1.88 (t, 1H, J = 11.3 Hz, H-4a), 1.60-1.42 (m, 6H, H-1, H-7, Ha-5, Ha-8, Ha-5'), 1.35-1.15 (m, 4H, Hb-5, Hb-5', H-4'), 1.07 (dq, 1H, J = 12.4, 3.7 Hz, Hb-8), 0.97 (dq, 1H, J = 10.4, 3.4 Hz, H-8a), 0.96 (d, 3H, J = 7.2 Hz, 6-CH_3), 0.82 (d, 3H, J = 7.0 Hz, 2-CH_3); ^{13}C NMR (125 MHz, $CDCl_3$) δ 199.5, 170.3, 132.7, 131.6, 69.0, 41.36, 40.0, 39.3, 38.9, 37.3, 34.2, 32.3, 31.9, 29.7, 28.8, 27.5, 24.0, 23.6, 23.2, 18.2, 14.9; HRMS (ES) m/z calculated for $C_{21}H_{34}D_2NO_3S$ 384.2536, found 384.2536 $[M+H]^+$.

(*R*)-3,7-dimethyloct-6-enyl acetate (45)

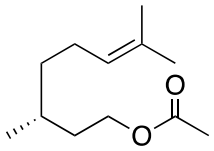

The known compound was made as per literature.[49] 5 g of *R*-(+)-β-citronellol (**44**) was dissolved in 70 mL distilled THF in a flame dried 250 mL round bottom flask, and cooled to 0 °C in an ice-water bath. Acetyl chloride (1.2 eq, 3 g, 2.74 mL) was added dropwise, followed by triethylamine (1.2 eq, 5.35 mL). The reaction was warmed to room temperature after an hour, and then stirred an additional hour at room temperature. The solvent was removed *in vacuo*, and the crude residue was redissolved in dichloromethane and transferred to a separatory funnel, where it was washed with 30 mL 1 M HCl, 2 x 30 mL water, and brine. The organic phase was dried over $MgSO_4$ and the solvent was removed *in vacuo* to provide a quantitative yield of citronellol acetate (**45**) (6.3 g). Spectroscopic data matched that previously reported. ^{1}H NMR (500 MHz, $CDCl_3$) δ 5.12 (triplet of quintets, 1H, J = 7.1, 1.4 Hz, H-6), 4.13 (m, 2H, H-1), 2.08 (s, 3H, H-2'), 2.01 (m, 2H, H-5), 1.71 (d, 3H, J = 1.2 Hz, HC=CC$\underline{H}_3$), 1.70 (m, 1H, Ha-2), 1.64 (s, 3H HC=CC$\underline{H}_3$), 1.58 (m, 1H, H-3), 1.47 (m, 1H, H-2), 1.38 (m, 1H, Ha-4), 1.22 (m, 1H, Hb-4), 0.95 (d, 3H, J = 6.6 Hz, 3-C$\underline{H}_3$); ^{13}C NMR (125 MHz, $CDCl_3$) δ 171.2 (C-1'), 131.4 (C-7), 124.6 (C-6), 63.1 (C-1), 37.0 ($\underline{C}H_2$), 35.4 ($\underline{C}H_2$), 29.5 (C-3), 25.7 (C-8), 25.4 (C-4), 21.1 (C-2'), 19.4 ($\underline{C}H_3$), 17.7 ($\underline{C}H_3$).

(*R*)-6,6-dimethoxy-3-methylhexyl acetate (46)

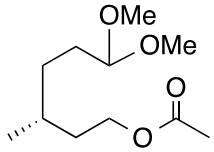

The known compound **46** was made using a modified procedure.[65] 6.3 g of citronellol acetate (**45**) was dissolved in 50 mL methanol and 50 mL dichloromethane in a three-neck round bottom flask fitted with a stopper, a drying tube and an adapter to the ozone generator. The reaction vessel was cooled to -78 °C in a dry ice/acetone bath. Ozone was bubbled through until the blue colour persisted. Oxygen was bubbled through until the solution returned to colourless. *p*-Toluenesulfonic acid (10 w%) was added, then the reaction was warmed to room temperature. After 2 hours, dimethyl sulfide (2 eq) was added and the reaction was left to stir overnight. The solvent was removed *in vacuo* and the residue was redissolved in dichloromethane. The mixture was washed with an equal portion of water. The aqueous layer was then extracted with two portions of dichloromethane. The combined dichloromethane extracts were washed with one portion of water, dried over $MgSO_4$ and concentrated *in vacuo* to yield a crude oil. This oil was purified via SiO_2 flash chromatography (20% EtOAc in hexanes) to yield **46** as a colourless oil (60%) with spectroscopic data matching that previously reported.[49]

^{1}H NMR (500 MHz, $CDCl_3$) δ 4.35 (t, 1H, J = 5.7 Hz, H-6), 4.17-4.08 (m, 2H, H-1), 3.33 (s, 6H, 2 x OC$\underline{H}_3$), 2.05, (s, 3H, H-2'), 1.74-1.52 (m, 4H, Ha-2, H-3, H-5), 1.51-1.36 (m, 2H, Hb-2, Ha-4), 1.27-1.17 (m, 1H, Hb-4), 0.94 (d, 3H, J = 6.8 Hz, 3-C$\underline{H}_3$); ^{13}C NMR (125 MHz, $CDCl_3$) δ 171.3 (C-1'), 104.8 (C-6), 62.9 (C-1), 52.7 (O$\underline{C}H_3$), 52.6 (O$\underline{C}H_3$), 35.4 ($\underline{C}H_2$), 31.5 ($\underline{C}H_2$), 30.0 ($\underline{C}H_2$), 29.8 (C-3), 21.0 (C-2'), 19.4 (3-$\underline{C}H_3$).

(*R*)-6,6-dimethoxy-3-methylhexanal (47)

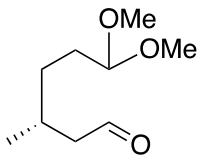

The acetate (1.26 g, 5.8 mmol) **46** was dissolved in 40 mL distilled methanol and placed under argon. NaOMe (32 mg, 10% wt/wt) was added as a powder and the reaction was stirred over night. The reaction was quenched with 10 mL water and the methanol was removed *in vacuo.* The remaining aqueous solution was extracted with ether, and the combined organic layers were washed with water then brine, and dried over $MgSO_4$. Removing the solvent *in vacuo* provides a quantitative yield of the intermediate alcohol. Spectroscopic data matched that previously reported.[49] IR ($CHCl_3$, cast film) 3427 (br), 2952, 2930, 2830, 1459, 1383, 1129 and 1059 cm^{-1}; ^1H NMR (500 MHz, $CDCl_3$) δ 4.36 (t, 1H, J = 5.7 Hz, H-6), 3.70 (m, 2H, H-1), 3.33 (s, 6H, 2xOC$\underline{H}_3$), 1.72-1.54 (m, 4H, Ha-2, H-3 and H-5), 1.14 (m, 1H, Hb-2), 1.22 (m, 1H, H-4), 0.93 (d, 3H, J = 6.6 Hz, 3-C$\underline{H}_3$); ^{13}C NMR (125 MHz, $CDCl_3$) δ 104.8 (C-6), 61.1 (C-1), 52.7 (O-$\underline{C}H_3$), 52.6 (O-$\underline{C}H_3$), 39.8 ($\underline{C}H_2$), 31.6 ($\underline{C}H_2$), 29.6 ($\underline{C}H_2$), 29.3 (C-3), 19.5 (3-($\underline{C}H_3$); α_D^{25} = 2.51 (c = 0.71 g/100 mL, $CHCl_3$); HRMS (ES) m/z calculated for $C_9H_{20}NaO_3$ 199.1305, found 199.1305. $[M+Na]^+$.

In a flame-dried flask, Dess-Martin periodinane (1.1 eq, 4.6 mmol, 1.95 g) was dissolved in 10 mL dichloromethane. The intermediate alcohol (4.1 mmol, 720 mg) was dissolved in 10 mL of dichloromethane and added dropwise to reaction. A further 5 mL of dichloromethane was used to ensure complete transfer. The reaction was monitored by TLC and was complete in about 20 minutes, at which point it was diluted with ether and 1 M NaOH was added to quench over 1 hour. The ether layer was washed with 1 M NaOH, water then brine, and the solvent was removed in vacuo to provide 683 mg of aldehyde **47** (96%). Spectroscopic data matched that previously reported.[49] IR ($CHCl_3$, cast film) 3434, 2954, 2929, 2882, 2830, 2719, 1725, 1130, 1059 cm^{-1}; ^1H NMR (500 MHz, $CDCl_3$) δ 9.76 (dd, 1H, J = 2.5, 2.0 Hz, H-1), 4.33 (t, 1H, J = 5.7 Hz, H-6), 3.32 and 3.31 (two singlets, 6H, 2xOC$\underline{H}_3$), 2.41 (ddd, 1H, J = 16.4, 5.7, 2.0 Hz, Ha-2),

2.25 (ddd, 1H, J = 16.3, 7.9, 2.5 Hz, Hb-2), 2.07 (m, 1H, H-3), 1.69-1.52 (m, 2H, H-5), 1.44-1.36 (m, 1H, Ha-4), 1.33-1.25 (m, 1H, Hb-4), 0.97 (d, 3H, J = 6.8 Hz, 3-C$\underline{H}_3$); ^{13}C NMR (125 MHz, $CDCl_3$) δ 202.6 (C-1), 104.6 (C-6), 52.9 (O$\underline{C}H_3$), 52.8 (O$\underline{C}H_3$), 51.0 (C-2), 31.6 ($\underline{C}H_2$), 30.0 ($\underline{C}H_2$), 28.0 (C-3), 19.8 (3-$\underline{C}H_3$); α_D^{25} = 9.76 (c = 1.01 g/100 mL, $CHCl_3$); HRMS (ES) m/z calculated for $C_9H_{18}NaO_3$ 197.1148, found 197.1148 $[M+Na]^+$.

(*R*,*E*)-ethyl 8,8-dimethoxy-5-methyloct-2-enoate (48)

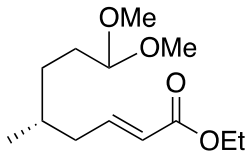

In a flame dried flask with stir bar, a solution of NaH (14.7 mmol, 588 mg of 60% mineral oil suspension) was prepared with THF (15 mL) at room temperature. Over 5 min, triethylphosphonoacetate (13.3 mmol, 2.64 mL) was added dropwise and left to deprotonate over 1 hour. Aldehyde **47** (13.3 mmol, 2.3 mg) was then added dropwise. After 2.5 hours, adding a small amount of ice directly into the reaction quenched the reaction and the mixture was stirred until the ice melted. 5 mL water was added and the THF was removed under vacuum. The resulting aqueous solution was extracted with diethyl ether, and the combined organic layers were dried over $MgSO_4$ and filtered, and the solvent of the filtrate was removed *in vacuo*. The residue was purified using silica gel flash chromatography (4:1 hexanes:EtOAc) to provide 2.49 g of ester **48** (77% yield). Spectral data corresponded that which was previously reported.[49] ^{1}H NMR (500 MHz, $CDCl_3$) δ 6.93 (dt, 1H, J = 15.6, 7.5 Hz, H-3), 5.8 (dt, 1H, J = 15.7, 1.5 Hz, H-2), 4.33 (t, 1H, J = 5.7 Hz, H-8), 4.18 (q, 2H, J = 7.2 Hz, H-1'), 3.31 (two s, 6H, 2xOC$\underline{H}_3$), 2.21

(m, 1H, Ha-4), 2.04 (m, 1H, Hb-4), 1.75-1.54 (m, 4H, H-7, H-5 and Ha-6), 1.41 (m, 1H, Hb-6), 1.29 (t, 3H, J = 7.2 Hz, H-2'), 0.94 (d, 3H, J = 6.7 Hz, 5-C$\underline{H}_3$).

(*R*,*E*)-8,8-dimethoxy-5-methyloct-2-enal (49)

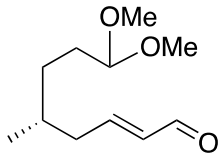

In a flame-dried flask with stir bar, a solution of ester **48** (6.8 mmol, 1.66 g) was prepared with dichloromethane (10 mL) and cooled to -78 °C in a dry ice/acetone bath. 20.4 mmol of diisobutylaluminum hydride was added as a solution in CH_2Cl_2, and within 5 min the ester was consumed, according to TLC analysis. The reaction was warmed to -20 °C in a salt water/ice bath and quenched slowly with methanol (3 mL), then diluted with 200 mL diethyl ether. The mixture was washed with saturated aqueous potassium sodium tartrate (4x100 mL), then water (100 mL) and brine (100 mL). The ether layer was dried over $MgSO_4$ and filtered, and the solvent of the filtrate was removed *in vacuo*. The residue was purified by silica flash chromatography (2:1 hexanes/EtOAc) to provide 1.29 g of the intermediate allylic alcohol (93% yield). Spectral data matched that previously reported.[49] IR ($CHCl_3$, cast film) 3409 (br), 2952, 2930, 2972, 2932, 1469, 1383, 1127, 1059 cm^{-1}; ^1H NMR (500 MHz, $CDCl_3$) δ 5.69 (m, 2H, H-2 and H-3), 4.37 (t, 1H, J = 5.7 Hz, H-8), 4.13 (d, 2H, J = 4.4 Hz, H-1) 3.35 (s, 6H, 2xOC$\underline{H}_3$), 2.10 (m, 1H, Ha-4), 1.95 (m, 1H, Hb-4), 1.73-1.49 (m, 4H, H-7, H-5, OH), 1.41 (m, 1H, Ha-6), 1.21 (m, 1H, Hb-6), 0.92 (d, 3H, J = 6.7 Hz, 5-C$\underline{H}_3$); ^{13}C NMR (125 MHz, $CDCl_3$) δ 131.6 (C$\underline{H}$=CH), 130.4 (C$\underline{H}$=CH), 104.8 (C-8), 63.7 (C-1), 52.7 (OC$\underline{H}_3$), 52.6 (OC$\underline{H}_3$), 39.6 (C-4), 32.8 (C-5), 31.2 ($\underline{C}H_2$), 30.1 ($\underline{C}H_2$), 19.4 (5-C$\underline{H}_3$); α_D^{25} = 0.51 (c = 1.60 g/100 mL, $CHCl_3$).

In a flame-dried flask with stir bar, Dess-Martin periodinane (105.3 mg, 1.1 eq) was suspended in 1 mL of distilled dichloromethane. With stirring, a solution of intermediate allylic alcohol (0.23 mmol, 42.5 mg) in CH_2Cl_2 (0.5 mL) was added slowly to reaction mixture, and an addition 0.5 mL of CH_2Cl_2 was used to ensure complete transfer. The reaction was stirred at room temperature and monitored by TLC. When completed, the reaction was diluted with ether and 1 M NaOH was added to quench over 1 hour. The ether layer was washed with 1 M NaOH, water then brine, and the solvent was removed in vacuo to provide aldehyde **49** (90%). Spectroscopic data matched that previously reported.[49]

IR ($CHCl_3$, cast film) 2954, 2932, 2830, 1693, 1173 cm^{-1}; ^1H NMR (500 MHz, $CDCl_3$) δ 9.53 (d, 2H, J = 7.9 Hz, H-1), 6.84 (dt, 1H, J = 15.4, 7.4 Hz, H-3), 6.14 (ddt, 1H, J = 15.6, 8.1, 1.4 Hz, H-2), 4.35 (t, 1H, J = 5.7 Hz, H-8), 3.34 (two s, 6H, 2 x OC$\underline{H}_3$), 2.38 (m, 1H, Ha-4), 2.22 (m, 1H, Hb-4), 1.76-1.55 (m, 3H, H-5 and H-7), 1.44 (m, 1H, Ha-6), 1.27 (m, 1H, Hb-6), 0.97 (d, 3H, J = 6.7 Hz); ^{13}C NMR (125 MHz, $CDCl_3$) δ 193.9 (C-1), 157.2 (C-3), 134.3 (C-2), 104.6 (C-8), 52.9 (O$\underline{C}H_3$), 52.7 (O$\underline{C}H_3$), 40.1 (C-4) , 32.5 (C-5), 31.3 ($\underline{C}H_2$), 30.1 ($\underline{C}H_2$), 19.5 (5-$\underline{C}H_3$); α_D^{25} = 0.12 (c = 1.72 g/100 mL, $CHCl_3$).

(*R*,2*E*,4*E*)-10,10-dimethoxy-7-methyldeca-2,4-diene (50) and (^{13}C-50)

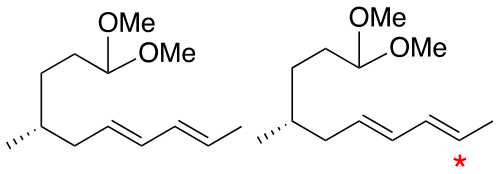

The known compound **50** was prepared using the literature procedure.[49,62] Ethyl triphenylphosphonium iodide (1.02 g, 2.44 mmol) was suspended in 30 mL 1:1 THF/ether in a 250 mL flame-dried round bottom flask with stir bar under an Argon atmosphere. At room

temperature, n-butyl lithium (1 eq, 1.02 mL of a 2.39 M solution in hexanes) was slowly added. The suspension turned yellow, then gradually darkened to orange/red, and then was stirred ten minutes to fully deprotonate. Next, the reaction was cooled to -78 °C in a dry ice/acetone bath. The aldehyde **49** (487 mg, 2.44 mmol) was slowly added as a solution of diethyl ether (5 mL), with an additional 5 mL of solvent to rinse, and the reaction faded back to yellow. After 5 min, a second equivalent of n-butyl lithium (1.02 mL of 2.39 M solution) was added dropwise, bringing the colour back to red. After 10 min, 1.1 eq of HCl in dioxane (4 M, 671 uL) was added dropwise, immediately followed by a rapid addition of KOtBu/BuOH (1.5 M solution, 2.44 mL). The vessel was removed from the cooling bath and stirred at room temperature for an additional 2 hours. The mixture was diluted with 40 mL diethyl ether and washed twice with 25 mL water. The organic layer was dried with $MgSO_4$ and rotovapped gently to prevent product loss. The diene **50** was purified by silica chromatography (5% diethyl ether in petroleum ether) and a yield of 80% was achieved (9:1 *trans*/*cis*). Spectroscopic data matched that previously reported. IR ($CHCl_3$, cast film) 3016, 2953, 2930, 2829, 1697, 1659, 1625, 1457, 1379, 1126, 1059 cm^{-1}; ^1H NMR (500 MHz, $CDCl_3$) δ 6.06-5.94 (m, 2H, H-3 and H-4), 5.62-5.48 (m, 2H, H-2 and H-5), 4.33 (t, 1H, J = 5.8 Hz, H-10), 3.31 (s, 6H, 2xOC$\underline{H}_3$), 2.07 (m, 1H, Ha-6), 1.90 (m, 1H, Hb-6), 1.73 (d, 3H, J = 6.5 Hz, H-1), 1.68-1.45 (m, 3H, H-9, H-7), 1.37 (m, 1H, Ha-8), 1.16 (m, 1H, Hb-8), 0.87 (d, 3H, J = 6.7 Hz, 7-C$\underline{H}_3$); ^{13}C NMR (125 MHz, $CDCl_3$) δ 131.7 (C-3), 131.7 (C-4), 130.2 (C-5), 126.9 (C-2), 104.8 (C-10), 52.7 (O$\underline{C}H_3$), 52.6 (O$\underline{C}H_3$), 40.0 (C-6), 33.2 (C-7), 31.2 ($\underline{C}H_2$), 30.1 ($\underline{C}H_2$), 19.5 (7-$\underline{C}H_2$), 18.0 (C-1); α_D^{25} = -0.91 (c = 0.95 g/100mL, $CHCl_3$); HRMS (ES) m/z calculated for $C_{13}H_{24}NaO_2$ 235.1669, found 235.1668 $[M+Na]^+$.

The same reaction was performed with ^{13}C ethyl triphenylphosphonium iodide to produce ^{13}C-**50**. ^1H NMR (500 MHz, $CDCl_3$) δ 6.06-5.94 (m, 2H, H-3 and H-4), 5.76-5.38 (m, 2H, H-2 and

H-5), 4.33 (t, 1H, J = 5.8 Hz, H-10) 3.31 (s, 6H, 2xOC$\underline{H}_3$), 2.07 (m, 1H, Ha-6), 1.90 (m, 1H, Hb-6), 1.73 (d, 3H, J = 6.5 Hz, H-1), 1.68-1.45 (m, 3H, H-9, H-7), 1.37 (m, 1H, Ha-8), 1.16 (m, 1H, Hb-8), 0.87 (d, 3H, 6.7 Hz, 7-C$\underline{H}_3$); ^{13}C NMR (125 MHz, $CDCl_3$) δ 131.7 (C-3), 131.7 (d, J = 57.7 Hz, C-4), 130.2 (d, J = 9.5 Hz, C-5), 126.9 (enriched, C-2), 104.8 (C-10), 52.7 (O$\underline{C}H_3$), 52.6 (O$\underline{C}H_3$), 40.0 (C-6), 33.2 (C-7), 31.2 ($\underline{C}H_2$), 30.1 ($\underline{C}H_2$), 19.5 (7-$\underline{C}H_2$), 18.0 (d, J = 43.8 Hz, C-1).

(*R*,6*E*,8*E*)-4-methyldeca-6,8-dienal (51) and (^{13}C-51)

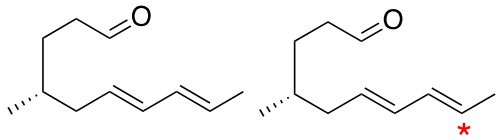

The known compound **51** was prepared as per literature.[49] 250 mg of the acetal **50** was dissolved in 15 mL of THF. 5 mL of saturated aqueous oxalic acid was added and the reaction was stirred at room temperature overnight. In the morning, an additional 3 mL of oxalic acid solution was added and it was stirred for an addition 3 hours. The reaction was then diluted with diethyl ether (20 mL), washed with water (2x15 mL) and brine (15 mL) and dried over $MgSO_4$. The solvent was removed carefully to prevent product loss (yield: 90%). Product was not purified or fully characterized due to volatility, though spectroscopic data obtained was consistent with that which was previously reported. ^{1}H NMR (700 MHz, $CDCl_3$) δ 9.74 (t, 1H, J = 1.9 Hz, H-1), 6.03-5.93 (m, 2H, H-7 and H-8), 5.62-5.44 (m, 2H, H-6 and H-9), 2.48-2.36 (m, 2H, H-2), 2.04 (m, 1H, Ha-5), 1.92 (m, 1H, Hb-5), 1.72 (d, 3H, J = 6.6 Hz, H-10), 1.70-1.65 (m, 1H, Ha-3), 1.51 (m, 1H, H-4), 1.43 (m, 1H, Hb-3), 0.87 (d, 3H, J = 6.6 Hz, 4-C$\underline{H}_3$); ^{13}C NMR (125 MHz, $CDCl_3$) δ 202.8 (C-1), 132.0 ($\underline{C}$H=CH), 131.5 ($\underline{C}$H=CH), 129.5 ($\underline{C}$H=CH), 127.3 ($\underline{C}$H=CH), 41.7 ($\underline{C}H_2$), 39.8 ($\underline{C}H_2$), 32.9 (C-4), 28.4 ($\underline{C}H_2$), 19.3 (4-$\underline{C}H_3$), 18.0 (C-10).

The same reaction was performed with ^{13}C-**50** to produce ^{13}C-**51**. ^{1}H NMR (500 MHz, $CDCl_3$) δ 9.74 (t, 1H, J = 1.9 Hz, H-1), 6.06-5.93 (m, 2H, H-7 and H-8), 5.79-5.40 (m, 2H, H-6 and H-9), 2.51-2.35 (m, 2H, H-2), 2.17-1.86 (m, 2H, H-5), 1.72 (d, 3H, J = 6.6 Hz, H-10), 1.70-1.65 (m, 1H, Ha-3), 1.58-1.38 (m, 2H, Hb-3 and H-4), 0.87 (d, 3H, J = 6.6 Hz, 4-CH_3); ^{13}C NMR (125 MHz, $CDCl_3$) δ 202.8 (C-1), 132.0 (CH=CH), 131.5 (d, J = 71.3 Hz, CH=CH), 129.5 (d, J = 9.5 Hz, CH=CH)), 127.3 (enriched, C-9), 41.7 (CH_2), 39.8 (CH_2), 32.9 (C-4), 28.4 (CH_2), 19.3 (4-CH_3), 18.0 (d, J = 43.8 Hz, C-10).

^{13}C-(*R*,6*E*,8*E*)-4-methyldeca-6,8-dienoic acid (^{13}C-52)

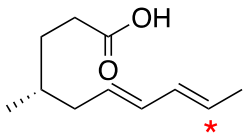

The following stock solution was prepared: 16 mL tBuOH, 1.06 mL 2-methyl-2-butene, 194 mg sodium chlorite, 148.3 mg NaH_2PO_4 in 4.5 mL H_2O. 5 mL of the stock solution was added to 12 mg of aldehyde ^{13}C-**51** and the reaction was stirred until completed by TLC (3 hours). The reaction was diluted with 12 mL of water, acidified to below pH 6 and extracted with 3x EtOAc. The combined organic layers were washed with brine, dried over $MgSO_4$, filtered and concentrated under reduced pressure, yielding acid ^{13}C-**52**. The acid ^{13}C-**52** was then used without further purification in the coupling to N-acetylcysteamine (see synthesis of compound ^{13}C-**39**.) ^{1}H NMR (500 MHz, $CDCl_3$) δ 6.10-5.97 (m, 2H), 5.83-5.42 (m, 2H), 2.49-2.33 (m, 2H), 2.11 (m, 1H), 1.97 (m, 1H), 1.76 (d, 3H, J = 7.0 Hz), 1.83-1.69 (m, 1H), 1.65-1.44 (m, 2H), 0.93, (d, 3H, J = 6.8 Hz); ^{13}C NMR (125 MHz, $CDCl_3$) δ 177.4, 132.0, 131.6 (d, J = 70.1 Hz), 129.5 (d, J = 9.5 Hz), 127.2 (enriched), 39.7, 32.8, 31.4, 31.2, 19.3, 18.0 (d, J = 43.9 Hz).

(4*R*,6*R*)-6-(2-((1*R*,2*R*,3*S*,4*S*,4a*S*,6*R*,8a*R*)-3,4-dibromo-2,6-dimethyldecahydronaphthalen-1-yl)ethyl)-4-hydroxytetrahydro-2*H*-pyran-2-one (53)

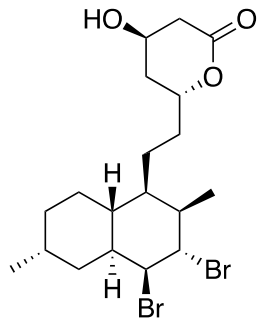

Dibromide **53** was prepared using the method of John Sorensen.[64] 247 mg (0.8 mmol) of dihydromonacolin L (**11**) was dissolved in 10 mL $CHCl_3$, and 1.25 mL of glacial acetic acid was added with stirring. Bromine (1.5 eq, 1.2 mmol) was added dropwise as a 10 mmol/mL solution in $CHCl_3$. The reaction was stirred at room temperature for 1 hour, at which point sodium dithionate dihydrate was added (20 mL of a 10% solution). The biphasic mixture was diluted with 10 mL of CH_2Cl_2 and transferred to a separatory funnel. The organic layer was separated and washed with sodium bicarbonate, water and brine, then dried over sodium sulfate. The product was concentrated by rotary evaporation and the residue was purified by column chromatography (40% EtOAc in hexanes) to yield 283 mg of dibromide **53** (75% yield). Spectroscopic data matched that which was previously reported. IR ($CHCl_3$, cast film) 3435 (br), 2956, 2924, 2852, 1714, 1258, 1070 cm^{-1}; ^1H NMR (400 MHz, $CDCl_3$) δ 4.95 (t, J = 2.0 Hz, H-4), 4.68 (m, 1H, H-11), 4.46 (m, 1H, H-3), 4.38 (m, 1H, H-13), 2.72 (dd, 1H, J = 17.6 Hz, 4.8 Hz, Ha-14), 2.61 (ddd, 1H, J = 17.6, 3.6, 1.7 Hz, Hb-14), 2.34 (m, 1H, H-2), 2.14 (m, 1H, H-4a), 2.09-2.01 (m, 1H, H-1), 1.99-1.88 (m, 2H, H-6, Ha-12), 1.81-1.61 (m, 4H, Ha-5, H-8, Hb-12), 1.57-1.1 (m, 8H, Hb-5, H-7, H-8a, H-9, H-10), 1.27 (d, 3H, J = 7.8 Hz, 2-C$\underline{H}_3$), 1.02 (d, 3H, J = 7.2 Hz, 6-C$\underline{H}_3$); ^{13}C NMR (125 MHz, $CDCl_3$) δ 170.1, 75.6, 62.9, 60.3, 60.1, 39.5, 38.9, 38.7,

38.4, 36.3, 34.9, 37.7, 32.8, 31.1, 27.0, 23.7, 23.6, 18.0, 17.7; α_D^{25} = 44.4 (c = 0.24 g/100 mL, $CHCl_3$); HRMS (ES) m/z calculated for $C_{19}H_{30}Br_2NaO_3$ 487.0454, found 487.0461 $[M+Na]^+$.

(*R*)-6-(2-((1*R*,2*R*,3*S*,4*S*,4a*S*,6*R*,8a*R*)-3,4-dibromo-2,6-dimethyldecahydronaphthalen-1-yl)ethyl)-5,6-dihydro-2*H*-pyran-2-one (54)

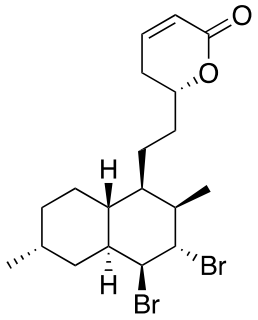

Unsaturated dibromide **54** was prepared using the method of John Sorensen.[64] In a round bottom flask under argon, 260 mg (0.56 mmol) of dibromide **53** was dissolved in 5 mL freshly distilled CH_2Cl_2 and cooled to 0 °C. 195 µL (2.5 eq,1.4 mmol) of triethylamine was added, followed by 47 µL (1.1 eq, 0.62 mmol) of methanesulfonylchloride. The reaction was stirred for 1 hour and then quenched with 20 mL 1 N HCl and stirred for 10 minutes. The biphasic mixture was then diluted with 50 mL CH_2Cl_2 and the layers were separated. The organic phase was washed with water, saturated sodium bicarbonate, water and brine, and then dried over sodium sulfate and concentrated under reduced pressure. The crude product was purified by column chromatography (30% EtOAc in hexanes) to yield 175 mg of product **54** (70%). Spectroscopic data matched that which was previously reported. ^{1}H NMR (600 MHz, $CDCl_3$) δ 6.89 (ddd, 1H, J = 9.9, 4.4, 3.5 Hz, H-13), 6.05 (dt, 1H, J = 9.7, 1.7 Hz, H-14), 4.98 (t, 1H, J = 2.0 Hz, H-4), 4.49 (m, 1H, H-3), 4.43 (m, 1H, H-11), 2.39-2.34 (m, 3H, H-2, H-12), 2.16 (tt, J = 11.3, 3.2 Hz, H-4a), 2.08 (m, 1H, H-6), 1.96 (tt, 1H, J = 11.1, 4.0 Hz, H-1), 1.83-1.74 (m, 4H, Ha-5, H-8a, H-10), 1.60-1.49 (m,

3H, Ha-7, H-9), 1.44 (dd, 1H, J = 11.2, 4.0 Hz, Hb-7), 1.36 (m, 1H, Ha-8), 1.31 (d, 3H, J = 7.8 Hz, 2-CH_3), 1.28-1.23 (m, 1H, Hb-5), 1.19 (dd, 1H, J = 11.8, 4.6 Hz, Hb-8), 1.04 (d, 3H, J = 7.2 Hz, 6-CH_3); ^{13}C NMR (125 MHz, $CDCl_3$) δ 164.4, 144.9, 121.5, 78.0, 60.3, 60.0, 39.5, 38.8, 38.4, 34.9, 34.7, 32.1, 31.1, 29.7, 26.9, 23.7, 23.5, 18.0, 17.7.

(*R*)-methyl 5-((1*R*,2*R*,3*S*,4*S*,4a*S*,6*R*,8a*R*)-3,4-dibromo-2,6-dimethyldecahydronaphthalen-1-yl)-3-hydroxypentanoate (55)

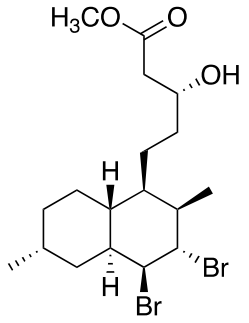

Dibromooctaketide methyl ester **55** was prepared using the method of John Sorensen.[64] A three neck round bottom flask was fitted with a glass stopped, O_3 inlet, and $CaCl_2$ drying tube outlet, and loaded with a solution of 306 mg (0.65 mmol) of compound **54** in 70 mL CH_2Cl_2. 7 mL of a methanolic 2.5 M NaOH solution was added, and the vessel was cooled to -78 °C. O_3 was vigourously bubbled through, and the reaction instantly turned orange. The stream of O_3 was continued under a persistent blue colour developed, at which point O_2 was bubbled through for 5 min to purge the solution of excess O_3. The reaction was warmed to room temperature, diluted with 100 mL of $CHCl_3$ and acidified with 100 mL 2N HCl. The organic layer was separated and washed with water, saturated sodium bicarbonate, water and brine. It was then dried over sodium sulfate and concentrated under reduced pressure. The crude product was purified by column chromatography (10% EtOAc in hexanes) to yield 160 mg of **55** (52%). Spectroscopic data

matched that which was previously reported. IR ($CHCl_3$, cast film) 3466 (br), 2953, 2924, 2874, 2853, 1737, 1438, 1175 cm^{-1}; ^1H NMR (500 MHz, $CDCl_3$) δ 4.96, (t, 2H, J = 2.1 Hz, H-4), 4.47 (m, 1H, H-3), 4.00 (m, 1H, H-11), 3.71 (s, 3H, O$\underline{CH_3}$), 2.89 (br s, 1H, O$\underline{H}$), 2.51 (dd, 1H, J = 16.6, 3.5 Hz, Ha-12), 2.43 (dd, 1H, J = 16.5 Hz, 8.8, Hb-12), 2.35 (m, 1H, H-2), 2.14 (tt, 1H, J = 11.5, 3.4 Hz, H-4a), 2.01 (m, 1H, H-6), 1.93 (m, 1H, H-1), 1.81-1.67 (m, 3H, Ha-5, H-8), 1.60-1.48 (m, 4H, Hb-5, H-9, Ha-10) 1.31-1.11 (m, 4H, H-7, H-8a, Hb-10), 1.27 (d, 3H, J = 7.8 Hz, 2-C$\underline{H_3}$), 1.02 (d, 3H, J = 7.3 Hz, 6-C$\underline{H_3}$); ^{13}C NMR (125 MHz, $CDCl_3$) δ 173.4, 77.4, 68.0, 60.3, 51.8, 41.2, 39.4, 38.8, 38.4, 35.0, 34.8, 33.5, 31.1, 27.0, 23.9, 23.7, 18.0, 17.7. α_D^{25} = 24.45 (c = 0.31 g/100 mL, $CHCl_3$); HRMS (ES) m/z calculated for $C_{18}H_{30}Br_2NaO_3$ 475.0454, found 475.0453 $[M+Na]^+$.

(*R*)-methyl 5-((1*S*,2*S*,4a*R*,6*R*,8a*S*)-2,6-dimethyl-1,2,4a,5,6,7,8,8a-octahydronaphthalen-1-yl)-3-hydroxypentanoate (56)

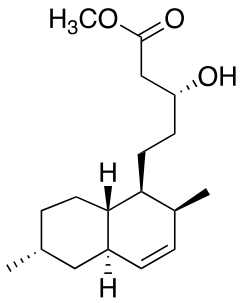

Octaketide methyl ester **56** was prepared using the method of John Sorensen.[64] In a round bottom flask with stir bar, 50 mg of protected compound **55** was dissolved in 5 mL CH_2Cl_2. To this was added 0.5 mL glacial acetic acid and 25 mg of zinc powder. The reaction was stirred overnight at room temperature, the diluted with CH_2Cl_2, filtered, and transferred into a separatory funnel. The solution was washed with saturated sodium bicarbonate and water, then dried over sodium

sulfate, filtered and concentrated under reduced pressure. The crude product was purified with column chromatography (5% EtOAc in hexanes) to provide 31.5 mg of **56** (97%). Spectroscopic data matched that which was previously reported. ^{1}H NMR (500 MHz, $CDCl_3$) δ 5.62 (ddd, 1H, J = 9.8, 4.8, 2.7 Hz, H-3), 5.32 (dt, 1H, J = 10.0, 1.6 Hz, H-4), 4.04 (m, 1H, H-11), 3.74 (s, 3H, $OC\underline{H}_3$), 2.55 (dd, 1H, J = 16.5, 3.3 Hz, Ha-12), 2.47 (dd, 1H, J = 16.4, 8.9 Hz, Hb-12), 2.26 (m, 1H, H-2), 2.04 (m, 1H, H-6), 1.93 (m, 1H, H-4a), 1.69-1.45 (m, 8H, H-1, H-4a, Ha-5, Ha-7, H-9, H-10), 1.38-1.20 (m, 3H, Hb-5, Hb-7, Ha-8), 1.12 (dq, 1H, J = 12.4 Hz, 4.1 Hz, Hb-8), 1.06-0.96 (m, 1H, H-8a), 1.00 (d, 3H, J = 7.2 Hz, 6-$C\underline{H}_3$), 0.87 (d, 3H, J = 7.1 Hz, 2-$C\underline{H}_3$); ^{13}C NMR (125 MHz, $CDCl_3$) δ 173.5, 132.8, 131.6, 68.3, 51.8, 41.4, 41.2, 40.1, 39.0, 37.4, 34.1, 32.3, 32.0, 27.5, 24.1, 23.7, 18.2, 15.0.

[^{2}H]-(*R*)-5-((1*S*,2*S*,4a*R*,6*R*,8a*S*)-2,6-dimethyl-1,2,4a,5,6,7,8,8a-octahydronaphthalen-1-yl)-3-hydroxypentanoic acid (^{2}H-57)

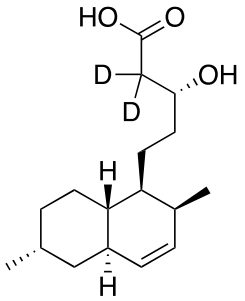

Octaketide methyl ester **56** (9 mg, 0.03 mmol) was dissolved in 0.5 mL THF-d_8. 4 mg of potassium *tert*-butoxide was dissolved in 1 mL of methanol-d_4 in a reaction vial with stir bar. The substrate solution was added dropwise to base solution with stirring at room temperature, and was subsequently heated to 65 °C and monitored by NMR. After 4 hours, the deuteration was complete and approximately 10% of the substrate had hydrolyzed to acid **57**. At this point, a

few drops of D_2O and an additional 2 mg of potassium *tert*-butoxide were added to complete the saponification. After stirring at room temperature overnight, the saponification was complete, and the reaction was acidified to pH 2 with 1 M HCl. The methanol-d_4 and THF-d_8 were then removed by rotary evaporation. The concentrate was diluted with water and extracted three times with CH_2Cl_2. The combined organic layers were washed with water and brine, and dried over sodium sulfate. The solvent was removed under reduced pressure to provide 6.5 mg of acid **57** as a white solid (75% yield). ^{1}H NMR (500 MHz, $CDCl_3$) δ 5.57 (ddd, 1H, J = 9.7, 4.8, 2.8 Hz, H-3), 5.27 (dt, 1H, J = 10.0, 1.5 Hz, H-4), 4.02 (br s, 1H, OH), 2.22 (m, 1H, H-2), 2.00 (m, 1H, H-6), 1.89 (m, 1H, H-4a), 1.65-1.42 (m, 7H, H-1, H-4a, Ha-7, H-9, H-10), 1.36-1.30 (m, 1H, Ha-5), 1.28-1.16 (m, 3H, Hb-5, Hb-7, Ha-8), 1.08 (dq, 1H, J = 12.4, 3.7 Hz, Hb-8), 0.97 (dq, 1H, J = 10.4, 3.4 Hz, H-8a), 0.96 (d, 3H, J = 7.2 Hz), 0.82 (d, 3H, J = 7.0 Hz); ^{13}C NMR (125 MHz, $CDCl_3$) δ 178.9, 132.7, 131.6, 68.1, 41.3, 40.0, 38.9, 37.3, 34.0, 32.3, 32.3, 31.9, 27.4, 24.0, 23.6, 18.2, 14.9.

(*E*)-methyl 5-((1*R*,2*R*,3*S*,4*S*,4a*S*,6*R*,8a*R*)-3,4-dibromo-2,6-dimethyldecahydronaphthalen-1-yl)pent-2-enoate (58)

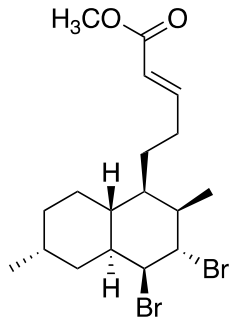

Unsaturated octaketide **58** was prepared using the method of John Sorensen.[64] In a round bottom flask with stir bar under argon, a solution of 90.3 mg (0.2 mmol) of compound **55** was prepared

with 5 mL of CH_2Cl_2, and then cooled to 0 °C. To this was added 81 μL (3 eq, 0.6 mmol) of triethylamine, then 30 μL (2 eq, 0.4 mmol) of methanesulfonyl chloride. The reaction was slowly warmed to room temperature and stirred for 3 days. Following this, the reaction was quenched by the addition of 10 mL 1 N HCl with stirring over 10 minutes. The mixture was diluted with 25 mL of CH_2Cl_2 and the layers were separated. The organic layer was washed with water, saturated sodium bicarbonate, water and brine, then dried over sodium sulfate, filtered and concentrated under reduced pressure. The product **58** (43 mg, 51% yield) could be separated from unreacted starting material **55** (20 mg) by column chromatography (20% EtOAc in hexanes). Spectroscopic data matched that which was previously reported. ^{1}H NMR (500 MHz, $CDCl_3$) δ 6.98 (dt, 1H, J = 15.7, 7.2 Hz, H-11), 5.86 (d, 1H, J = 15.7 Hz, H-12), 4.97 (s, 1H, H-4), 4.49 (s, 1H, H-3), 3.75 (s, 3H, OC$\underline{H_3}$), 2.41 (m, 1H, H-2), 2.31-2.01 (m, 4H, Ha-5, H-6, H-10), 1.97 (tt, 1H, J = 11.0, 4.2 Hz, H-4a), 1.86-1.70 (m, 3H, H-1, Hb-5, Ha-9), 1.63-1.49 (m, 2H, H-8), 1.43 (dq, 1H, J = 10.7, 3.66 Hz, H-1), 1.30 (d, 3H, J = 7.7 Hz, 2-CH_3), 1.26-1.16 (m, 3H, H-7, Hb-9), 1.05 (d, 3H, J = 7.3 Hz, 6-CH_3); ^{13}C NMR (125 MHz, $CDCl_3$) δ 167.1, 149.0, 121.2, 60.2, 59.9, 51.5, 39.2, 38.5, 38.4, 34.9, 34.7, 31.2, 29.4, 26.9, 26.7, 23.6, 18.0, 17.7.

Methyl 3-((1*R*,2*R*,3*S*,4*S*,4a*S*,6*R*,8a*R*)-3,4-dibromo-2,6-dimethyldecahydronaphthalen-1-yl)propanoate (59)

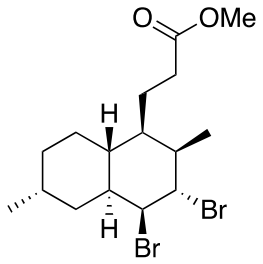

Heptaketide dibromide **59** was prepared using the method of John Sorensen.[64] A three neck round bottom flask was fitted with a glass stopped, O_3 inlet, and $CaCl_2$ drying tube outlet, and loaded with a solution of 76 mg (0.17 mmol) of compound **58** in 20 mL CH_2Cl_2. 7.5 mL of a methanolic 2.5 M NaOH solution was added, and the vessel was cooled to -78 °C. O_3 was vigourously bubbled through, and the reaction instantly turned orange. The stream of O_3 was continued under a persistent blue colour developed, at which point O_2 was bubbled through for 5 min to purge the solution of excess O_3. The reaction was warmed to room temperature, diluted with 60 mL $CHCl_3$ and acidified with 10 mL 2N HCl. The organic layer was separated and washed with water, saturated sodium bicarbonate, water and brine. It was then dried over sodium sulfate and concentrated under reduced pressure. The crude product was purified by column chromatography (5% EtOAc in hexanes) to yield 35.5 mg of **59** (49%). Spectroscopic data matched that which was previously reported. ^{1}H NMR (600 MHz, $CDCl_3$) δ 4.96 (t, 1H, J = 1.7 Hz, H-4), 4.48 (m, 1H, H-3), 3.69 (s, 3H, OCH_3), 2.38 (m, 1H, H-2), 2.32 (ddd, 1H, J = 15.6, 10.3, 5.5 Hz, Ha-10), 2.22-2.13 (m, 2H, Hb-10 and H-4a), 2.11-2.02 (m, 2H, H-6 and H-1), 1.94 (m, 1H, Ha-5), 1.79 (m, 2H, H-8), 1.59-1.50 (m, 2H, H-7), 1.48-1.18 (m, 4H, H-8a, Hb-5, H-9), 1.29 (d, 3H, J = 7.7 Hz, 2-CH_3), 1.04 (d, 3H, J = 7.3 Hz, 6-CH_3); ^{13}C NMR (150 MHz, $CDCl_3$) δ 176.7, 62.7, 62.5, 56.1, 41.8, 41.3, 41.0, 37.5, 37.3, 34.2, 33.8, 29.6, 26.4, 26.3, 20.7, 20.3.

Methyl 3-((1*S*,2*S*,4a*R*,6*R*,8a*S*)-2,6-dimethyl-1,2,4a,5,6,7,8,8a-octahydronaphthalen-1-yl)propanoate (60)

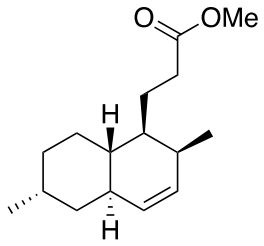

A reaction vial with stir bar was loaded with 35 mg (0.09 mmol) of heptaketide dibromide **59** dissolved in 2.5 mL freshly distilled CH_2Cl_2. 18 mg of zinc dust was added, along with 0.25 mL of glacial acetic acid. The reaction was stirred overnight at room temperature, then filtered and diluted with an additional 10 mL CH_2Cl_2. The solution was transferred to a separatory funnel to be washed with saturated sodium bicarbonate, water and brine. The organic phase was dried over sodium sulfate, filtered, and concentrated under reduced pressure. The crude product was purified by column chromatography (5% EtOAc in hexanes) to yield 13 mg (62%) of deprotected product **60**. ^{1}H NMR (600 MHz, $CDCl_3$) δ 5.61 (ddd, 1H, J = 9.7, 4.8, 2.8 Hz, H-3), 5.31 (dt, 1H, J = 9.6, 1.6 Hz, H-4), 3.69 (s, 3H, OCH_3), 2.41 (ddd, 1H, J = 15.5, 10.4, 5.2 Hz, Ha-10), 2.28-2.18 (m, 2H, H-2 and Hb-10), 2.08-2.00 (m, 1H, H-4a), 1.99-1.89 (m, 2H, H-6 and Ha-9), 1.66-1.45 (m, 4H, H-1, Hb-9, H-7), 1.39 (m, 1H, H-8a), 1.33-1.25 (m, 2H, H-5), 1.14 (dq, 1H, J = 12.5, 3.3 Hz, Ha-8), 1.06-0.96 (m, 1H, Hb-8) 1.00 (d, 3H, J = 7.2 Hz, 6-CH_3), 0.86 (d, 3H, J = 7.0 Hz, 2-CH_3); ^{13}C NMR (150 MHz, $CDCl_3$) δ 177.2, 135.2, 134.3, 56.09, 43.8, 42.6, 41.6, 39.9, 34.9, 34.7, 34.5, 30.1, 26.7, 26.3, 20.9, 17.6.

[^{2}H]-3-((1*S*,2*S*,4a*R*,6*R*,8a*S*)-2,6-dimethyl-1,2,4a,5,6,7,8,8a-octahydronaphthalen-1-yl)propanoic acid (^{2}H-61)

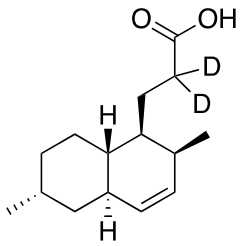

Heptaketide methyl ester **60** (12 mg, 0.05 mmol) was dissolved in 0.5 mL THF-d_8. 4 mg of potassium *tert*-butoxide was dissolved in 1 mL of methanol-d_4 in a reaction vial with stir bar. The substrate solution was added dropwise to base solution with stirring at room temperature, and was subsequently heated to 50 °C and monitored by NMR. After 4 hours, the deuteration was complete. At this point, a few drops of D_2O and an additional 2 mg of potassium *tert*-butoxide were added to complete the saponification to acid **61**. After stirring at room temperature overnight, the saponification was complete, and the reaction was acidified to pH 2 with 1 M HCl. The methanol-d_4 and THF-d_8 were then removed by rotary evaporation. The concentrate was diluted with water and extracted three times with CH_2Cl_2. The combined organic layers were washed with water and brine, and dried over sodium sulfate. The solvent was removed under reduced pressure to provide 10 mg of acid **57** as a white solid (90% yield). IR ($CHCl_3$, cast film) 3020, 2953, 2915, 2860, 2661, 1692, 1294; ^{1}H NMR (700 MHz, $CDCl_3$) δ 5.57 (ddd, 1H, J = 9.7, 4.8, 2.7 Hz, H-3), 5.28 (d, 1H, J = 9.6 Hz, H-4), 2.22 (m, 1H, H-2), 2.00 (m, 1H, H-4a), 1.96-1.86 (m, 2H, H-6 and Ha-9), 1.62-1.41 (m, 5H, H-1, H-7, H-8, Hb-9), 1.29-1.21 (m, 2H, H-5), 1.12 (dq, 1H, J = 12.8, 4.1 Hz, Ha-8), 1.02-0.95 (m, 1H, Hb-8), 0.97 (d, 3H, J = 7.2 Hz, 6-CH_3), 0.83 (d, 3H, J = 7.0 Hz, 2-CH_3); ^{13}C NMR (175 MHz, $CDCl_3$) δ 178.5, 132.4, 131.6, 53.4, 40.9,

31.8, 39.9, 38.9, 37.2, 32.3, 30.9, 27.4, 23.5, 18.2, 14.9; α_D^{25} = 74.26 (c = 0.22 g/100 mL, $CHCl_3$);

(1*R*,2*S*,4a*R*,6*R*,8a*R*)-*S*-acetamidomethyl 2,6-dimethyl-1,2,4a,5,6,7,8,8a-octahydronaphthalene-1-carbothioate) (65)

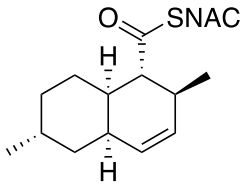

and **(1*R*,2*R*,4a*S*,6*R*,8a*R*)-*S*-acetamidomethyl 2,6-dimethyl-1,2,4a,5,6,7,8,8a-octahydronaphthalene-1-carbothioate (66)**

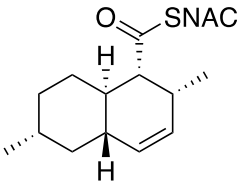

5 mg of triene **41** was dissolved in 0.8 mL 1:1 tetrahydrofuran and H_2O, and allowed to react for 12 hours. The tetrahydrofuran was removed under reduced pressure, and the cloudy aqueous solution that resulted was extracted with 3x $CHCl_3$. The combined organic extracts were dried over magnesium sulfate, and the solvent was removed under reduced pressure. The residue was dissolved in $CDCl_3$ to acquire the HSQC and CSSF-TOCSY spectra shown in Figures 37 and 38, which were interpreted in Chapter 3, with reference to the reported NMR data. [49]

(*R*,2*E*,4*E*,10*E*,12*E*)-*S*-2-acetamidoethyl 8-methyltetradeca-2,4,10,12-tetraenethioate (89)

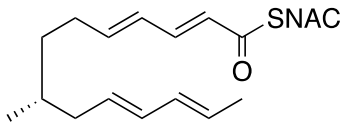

HWE reaction with aldehyde **95**:

Lithium bromide (oven dried, 27 mg, 4.0 eq) was added to a flame-dried 10 mL round bottom with stir bar. Horner-Wadsworth-Emmons reagent **32** (3.6 eq, 56 mg) was added in 2 mL THF, and the mixture was stirred for 10 minutes. Triethylamine (44 μL, 6.0 eq) was then added, and 10 minutes was allotted for deprotonation. Next, aldehyde **95** (10 mg, 0.05 mmol) was added in a tetrahydrofuran solution, and the mixture was allowed to react overnight. The solvent was removed *in vacuo* and the crude residue was applied directly to a silica column for purification (gradient of 25% EtOAc in hexanes to neat EtOAc), to yield 2 mg of tetraene **89** (11%).

Coupling to acid **97**:

In a flame-dried flask with stir bar, 31 mg (0.13 mmol) of acid **97** was dissolved in 10 mL freshly distilled CH_2Cl_2. 56 μL (4 eq, 0.53 mmol) of *N*-acetylcysteamine was added, followed by 54 mg (2 eq, 0.26 mmol) of dicyclohexylcarbodiimide. The reaction was stirred at room temperature, and monitored by TLC. After two hours, the reaction was complete, and the solvent was removed *in vacuo*. The crude mixture was resuspended in ice-cold 1:1 EtOAc:Et_2O, and filtered through a pipette packed with a small amount of cotton and sand. The filtrate, following concentration under reduced pressure, was purified using column chromatography (gradient of 50% EtOAc in pentane to neat EtOAc), to yield 27 mg (62%). IR ($CHCl_3$, cast film) 3287 (br), 3016, 2954, 2927, 2853, 1655, 1637, 1554, 989; ^{1}H NMR (700 MHz, $CDCl_3$) δ 7.19 (dd, 1H, J = 15.2, 10.8 Hz, H-3), 6.21 (m, 1H, H-5), 6.13 (m, 1H, H-4), 6.08 (d, 1H, J = 15.2 Hz, H-2), 6.04-5.95 (m, 2H, H-12 and H-11), 5.91 (br s, 1H, NH), 5.58 (m, 1H, H-13), 5.49 (m, 1H, H-10), 3.45

(q, 2H, J = 6.7 Hz, H-2'), 3.09 (t, 2H, J = 6.3 Hz, H-1'), 2.22 (m, 1H, Ha-6), 2.16 (m, 1H, Hb-6). 2.04 (m, 1H, Ha-9), 1.95 (s, 3H, COC$\underline{H}_3$), 1.91 (m, 1H, Hb-9), 1.72 (d, 3H, J = 6.6 Hz, H-14), 1.55-1.41 (m, 2H, H-8 and Ha-7), 1.28 (m, 1H, Hb-7), 0.87 (d, 3H, J = 6.7 Hz, 8-CH_3); ^{13}C NMR (175 MHz, $CDCl_3$) δ 193.1 (C-1), 173.0 (C-3'), 150.0 (C-5), 144.7 (C-3), 134.5 (C-12), 134.2 (C-11), 132.6 (C-10), 130.7 (C-4), 129.8 (C-13), 128.5 (C-2), 42.6 (C-9), 42.5 (C-2'), 37.9 (C-7), 35.5 (C-8), 33.5 (C-6), 31.0 (C-1'), 25.9 (C-4'), 22.0 (8-CH_3), 20.7 (C-14); α_D^{25} = -12.32 (c = 0.49 g/100 mL, $CHCl_3$); HRMS (ES) m/z calculated for $C_{19}H_{30}NO_2S$ 336.1992, found 336.2003 $[M+H]^+$.

(*R*,8*E*,10*E*)-6-methyldodeca-8,10-dien-1-ol (91)

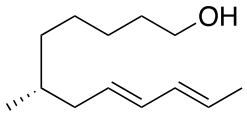

Procedure using DIBAL-H:

10 mg (0.032 mmol) of triene **41** was dissolved in 0.5 mL freshly distilled CH_2Cl_2 and cooled to -78 °C, after which 70 μL (2.1 eq, 0.07 mmol) of a 1M solution of diisobutylaluminum hydride in CH_2Cl_2 was added dropwise. After two hours, TLC analysis showed a significant amount of triene remained, so an addition 2 equivalents of diisobutylaluminum hydride were added. No change was observed after an additional hour, at which point the reaction was warmed to room temperature. The reaction was quenched slowly with methanol (0.5 mL), then diluted with 10 mL diethyl ether. The mixture was washed with saturated aqueous potassium sodium tartrate (4x10 mL), then water (10 mL) and brine (10 mL). The ether layer was dried over $MgSO_4$ and filtered, and the solvent of the filtrate was removed *in vacuo*. Purification by column

chromatography (50% EtOAc in pentane) produced an inseparable mixture of undesired saturated alcohol **91** and desired unsaturated alcohol **93**.

Luche reduction method:

3.0 mg (0.01 mmol) of triene **41** was dissolved in 0.3 mL of methanol and 11 mg (3 eq, 0.03 mmol) of $CeCl_3 \bullet 7H_2O$ was added. The mixture was stirred for 10 min at room temperature, and then cooled to -78 °C. A methanolic solution of sodium borohydride (1 mg in 0.5 mL methanol, 3 eq, 0.03 mmol), was prepared, and then added dropwise to the reaction. After one hour of reaction, starting material remained by TLC, and thus another equivalent of sodium borohydride was added. After an additional hour, the reaction was quenched with 0.5 mL water, and the methanol was removed *in vacuo*. The aqueous solution was extracted three times with 0.5 mL $CHCl_3$, and the combined organic layers were washed with water and brine, then dried over sodium sulfate and concentrated under reduced pressure. Purification by column chromatography (50% EtOAc in pentane) produced an inseparable mixture of undesired saturated alcohol **91** and desired unsaturated alcohol **93**. NMR data for alcohol **91**: ^{13}C NMR (175 MHz, $CDCl_3$) δ 131.7, 131.43, 130.6, 126.7, 63.1, 40.1, 36.5, 33.2, 32.8, 26.7, 25.9, 19.5, 18.0.

(*R*,2*E*,8*E*,10*E*)-ethyl 6-methyldodeca-2,8,10-trienoate (92)

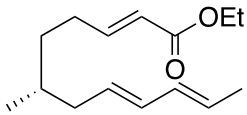

125 mg of sodium metal was reacted with 50 mL anhydrous EtOH (prepared over molecular sieves), to make NaOEt solution of approximately 0.1 M. 3 mL of this solution was added to 74 mg (0.24 mmol) of triene **41**. After 30 minutes of stirring at room temperature, starting material was consumed, as per the TLC. The reaction was neutralized with 0.1 M HCl, then extracted

three times with CH_2Cl_2. The combined organic layers were washed with brine, dried over sodium sulfate and concentrated under reduced pressure. The residue was purified by column chromatography (10% Et_2O in hexanes), to yield 18 mg of **92** (32%). ^1H NMR (700 MHz, $CDCl_3$) δ 6.94, (dt, 1H, J = 15.7, 6.9 Hz, H-3). 6.05-5.94 (m, 2H, H-10 and H-9), 5.80 (dt, 1H, J = 15.7, 1.6 Hz, H-2), 5.57 (dd, 1H, J = 13.8, 6.5 Hz, H-11), 5.49 (dt, 1H, J = 14.6, 7.4 Hz, H-8), 4.17 (q, 2H, J = 7.2 Hz, H-1'), 2.22 (m, 1H, Ha-4), 2.16 (m, 1H, Hb-4), 2.04 (m, 1H, Ha-7), 1.91 (m, 1H, Hb-7), 1.72 (d, 3H, J = 6.6 Hz. H-12), 1.56-1.43 (m, 2H, Ha-5 and H-6), 1.26-1.20 (m, 1H, H-5), 1.29 (t, 3H, J = 6.6 Hz, H-2'), 0.90 (d, 3H, J = 6.3 Hz, 6-CH_3); ^{13}C NMR (175 MHz, $CDCl_3$) δ 166. (C-1), 149.4 (C-3), 131.8 (C-9), 131.5 (C-10), 129.8 (C-8), 127.1 (C-11), 123.9 (C-2), 60.1 (C-1'), 39.9 (C-7), 34.6 (C-5), 32.8 (C-6), 28.9 (C-4), 19.3 (6-C<u>H</u>$_3$), 17.9 (C-12), 14.3 (C-2').

(*R*,2*E*,8*E*,10*E*)-6-methyldodeca-2,8,10-trien-1-ol (93)

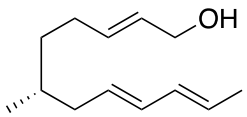

Ester **92** (0.08 mmol, 18 mg) was dissolved in 2 mL freshly distilled CH_2Cl_2 and cooled to -78 °C. Dropwise, 240 μL of a 1 M diisobutylaluminum hydride in CH_2Cl_2 (3 eq, 0.24 mmol) was added. The reaction was stirred for 1 hour, at which point the reaction was quenched slowly with methanol (0.5 mL) then diluted with 10 mL diethyl ether. The mixture was washed with saturated aqueous potassium sodium tartrate (4 x 10 mL), then water (10 mL) and brine (10 mL). The ether layer was dried over $MgSO_4$ and filtered, and the solvent of the filtrate was removed *in vacuo*. Purification by column chromatography (50% EtOAc in pentane) produced desired unsaturated alcohol **93** (10 mg, 64% yield). ^1H NMR (500 MHz, $CDCl_3$) δ 6.04-5.90 (2H, m, H-

10 and H-9), 5.70-5.60 (m, 2H, H-3 and H-2), 5.57 (m, 1H, H-11), 5.50 (dt, 1H, J = 14.6, 7.4 Hz, H-8), 4.07 (t, 2H, J = 5.4 Hz, H-1) 2.11-1.98 (m, 3H, H-4, Ha-7), 1.89 (m, 1H, Hb-7), 1.72 (d, 3H, J = 6.5 Hz, H-12), 1.50 (m, 1H, H-6), 1.41 (m, 1H, Ha-5), 1.26 (m, 1H, Hb-6), 0.86 (d, J = 6.7 Hz, 6-CH_3); ^{13}C NMR (175 MHz, $CDCl_3$) δ 133.5, 131.7, 131.2, 130.2, 128.7, 127.0, 63.9, 40.0, 36.0, 27.7, 29.8, 19.4, 17.9.

(*R*,2*E*,8*E*,10*E*)-6-methyldodeca-2,8,10-trienal (94)

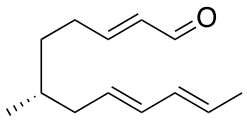

A 10 mL flame dried flask with stir bar was loaded with 5 mg (1.1 eq) sodium bicarbonate, 24 mg (1.1 eq) DMP and 1 mL CH_2Cl_2. 10 mg of alcohol **93** was dissolved in 1 mL freshly distilled CH_2Cl_2 and the solution was added to the DMP solution dropwise. The reaction was complete, as per the TLC, in 30 minutes, at which point the reaction was quenched by the addition of 2 mL concentrated aqueous $NaHCO_3$/NaS_2O_3, and stirred for 15 minutes. The organic layer was then separated, and washed with saturated sodium bicarbonate, water and brine, dried over magnesium sulfate and concentrated under reduced pressure. Aldehyde **94** did not need further purification (quantitative yield). ^{1}H NMR (700 MHz, $CDCl_3$) δ 9.49 (d, 1H, J = 7.9 Hz, H-1), 6.83 (dt, 1H, J = 15.9, 6.8 Hz, H-3), 6.11 (ddt, 1H, J = 15.6, 7.8, 1.5 Hz, H-10), 6.04-5.94 (m, 2H, H-2 and H-9), 5.58 (m, 1H, H-11), 5.49 (dt, 1H, J = 14.2, 7.4 Hz, H-8), 2.36 (m, 1H, Ha-4), 2.30 (m, 1H, Hb-4), 2.05 (m, 1H, Ha-7), 1.94 (m, 1H, Hb-7), 1.72 (d, 3H, J = 6.6 Hz, H-12), 1.60-1.49 (m, 2H, Ha-5 and H-6), 1.31 (m, 1H, Hb-5), 0.89 (d, 3H, J = 6.5 Hz, 6-CH_3); ^{13}C NMR (175 MHz, $CDCl_3$) δ 194.1 (C-1), 159.0 (C-3), 132.9 (C-10), 132.0 (C-9), 131.5 (C-2), 129.6 (C-8), 127.3 (C-11), 39.8 (C-7), 34.4 (C-5), 32.8 (C-6), 30.4 (C-4), 19.3 (6-CH_3), 18.0 (C-12).

(*R*,2*E*,4*E*,10*E*,12*E*)-ethyl 8-methyltetradeca-2,4,10,12-tetraenoate (96)

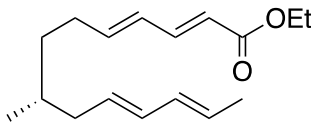

Extended HWE reagent **95** (0.4 mmol, 100 mg) was dissolved in 8 mL freshly distilled tetrahydrofuran in a 3 neck flame-dried flask, fitted with an argon inlet, separate argon outlet and a septum. The vessel was cooled to -78 °C using a finely controlled cooling system and lithium bis(trimethylsilyl)amide (0.37 mmol, 370 μL of a 1.0 M solution in tetrahydrofuran) was added dropwise. Aldehyde **51** (0.40 mmol, 66 mg) was added dissolved in 2 mL tetrahydrofuran. The temperature was reset to -40 °C and the reaction was stirred overnight. To quench, 1 mL of a 1 M ammonium chloride solution was added, and the mixture was extracted three times with Et_2O, and dried by filtering through pipette loaded with magnesium sulfate. The filtrate was concentrated under reduced pressure, and the crude mixture was purified using column chromatography (5% Et_2O in pentane) to yield 25 mg of triene **96** (25%). IR ($CHCl_3$, cast film) 3016, 2957, 2927, 2914, 2873, 1715, 1643, 1259, 1139, 988 cm^{-1}; ^1H NMR (700 MHz, $CDCl_3$) δ 7.24 (dd, 1H, J = 15.3, 10.6 Hz, H-3), 6.16 (dd, 1H, J = 15.2, 10.7 Hz, H-4), 6.09 (dt, 1H, J = 15.0, 6.8 Hz, H-5), 6.05-5.94 (m, 2H, H-11 and H-12), 5.77 (d, 1H, J = 15.4 Hz, H-2), 5.57 (m, 1H, H-13), 5.49 (dt, 1H, J = 14.7, 7.4 Hz, H-10), 4.19 (q, 2H, J = 7.2 Hz, H-1'), 2.20 (m, 1H, Ha-6), 2.13 (m, 1H, Hb-6), 2.04 (m, 1H, Ha-9), 1.91 (dt, 1H, J = 13.8, 7.3 Hz, Hb-9), 1.72 (d, 3H, J = 6.4 Hz, H-14), 1.53-1.41 (m, 2H, Ha-7 and H-8), 1.28 (t, 3H, J = 7.3 Hz, H-2'), 1.22 (m, 1H, Hb-7), 0.87 (d, 3H, J = 6.6 Hz, 8-CH_3); ^{13}C NMR (175 MHz, $CDCl_3$) δ 167.3 (C-1), 145.0 (C-3), 144.6 (C-5), 131.7 (C-12), 131.6 (C-11), 130.0 (C-10), 128.3 (C-4), 127.0 (C-13), 119.2 (C-2), 60.1 (C-1'), 39.9 (C-9), 35.4 (C-7), 32.8 (C-8), 30.6 (C-6), 19.33 (8-CH_3), 18.0 (C-14), 14.3 (C-

2'); α_D^{25} = -15.84 (c = 0.50 g/100 mL, $CHCl_3$); HRMS (ES) m/z calculated for $C_{17}H_{26}NaO_2$ 285.1825, found 285.1822 $[M+Na]^+$.

(*R*,2*E*,4*E*,10*E*,12*E*)-8-methyltetradeca-2,4,10,12-tetraenoic acid (97)

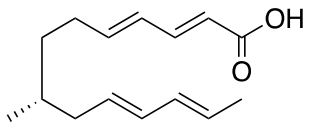

A portion of ethyl ester **96** (20 mg, 0.07 mmol) was mixed with 250 μL of 2 M KOH. Tetrahydrofuran was added dropwise until a clear solution was formed. The reaction was then warmed to 60 °C and stirred, unsealed, while reaction progression was monitored by TLC. After completed reaction (48 hours), the solution was neutralized with 0.5 mL of 1 M HCl, and extracted with Et_2O. The combined organic layers were dried by filtering through a pipette filled with magnesium sulfate, and the filtrate was concentrated under reduced pressure to provide 14 mg of acid **97** (80% yield). ^{1}H NMR (700 MHz, $CDCl_3$) δ 7.24 (dd, 1H, J = 15.3, 10.5 Hz, H-3), 6.16 (dd, 1H, J = 15.4, 10.9 Hz, H-4), 6.09 (dt, 1H, J = 15.3, 6.8 Hz, H-5), 6.05-5.94 (m, 2H, H-11 and H-12), 5.77 (d, 1H, J = 15.4 Hz. H-2), 5.57 (m, 1H, H-13), 5.49 (dt, 1H, J = 14.6, 7.5 Hz. H-10), 2.19 (m, 1H, Ha-6), 2.13 (m, 1H, Hb-6), 2.04 (m, 1H, Ha-9), 1.91 (dt, 1H, J = 13.9, 7.2 Hz, Hb-9), 1.72 (d, 3H, J = 6.6 Hz, H-14), 1.50 (m, 1H, H-8), 1.46 (m, 1H, Ha-7), 1.24 (m, 1H, Hb-7), 0.87 (d, 3H, J = 6.7 Hz, 8-CH_3); ^{13}C NMR (175 MHz, $CDCl_3$) δ 172.5 (C-1), 147.5 (C-3), 146.2 (C-5), 131.8 (C-12), 131.6 (C-11), 129.9 (C-10), 128.2 (C-4), 127.0 (C-2), 39.9 (C-9), 35.2 (C-7), 32.8 (C-8), 30.7 (C-6), 19.3 (8-CH_3), 18.0 (C-14); HRMS (ES) m/z calculated for $C_{15}H_{21}O_2$ 233.1547, found 233.1549 $[M-H]^+$.

Biological Methods

General Techniques for DNA Manipulation

E. coli DH5α (Invitrogen) was used for cloning following standard techniques. DNA restriction enzymes (Thermo Scientific) were used as directed. PCR was performed with a Platinum Taq High Fidelity DNA polymerase (Invitrogen).

Media Recipes

YPD media is made from 20 g/L bactopeptone, 10 g/L yeast extract, both from Becton, Dickonson and Company, dissolved in deionized water and sterilized by autoclaving. LB medium is made from 10 g/L bacto-tryptone, 5 g/L yeast extract, both from Becton, Dickonson and Company, and 10 g/L NaCl, dissolved in deionized water and sterilized by autoclaving.

Aspergillus nidulans growth media is composed of 20 g of glucose, 20 g of yeast extract, 1 g of peptone and 1 mg of para-aminobenzoic acid in 1 L of distilled, deionized water.

Aspergillus nidulans production media is prepared by dissolving in 1 L of distilled deionized water 1 mL trace elements solution (1.0 g $FeSO_4 \bullet 7H_2O$, 8.8 g $ZnSO_4 \bullet 7H_2O$, 0.4 g $CuSO_4 \bullet 5 H_2O$, 0.15 g $MnSO_4 \bullet 4H_2O$, 0.1 g $Na_2B_7O_7 \bullet 10H_2O$, 0.05 g $(NH_4)_6Mo_7O_{24} \bullet 4H_2O$, 0.5 mL concentrated hydrochloric acid dissolved in 1 L H_2O), 100 mL of 10X AMM salts (60 g $NaNO_3$, 5.2 g KCl, 15.2 g KH_2PO_4 dissolved in 1 L of H_2O and adjusted to pH 6.5), 1 mL of 1 mg/mL para-aminobenzoic acid solution, and 0.9 mL cyclopentanone and autoclaving. After cooling to room temperature, 2.5 mL of filter sterilized 20 % $MgSO_4 \bullet 7H_2O$ and 25 mL filter sterilized 40% lactose was added.

Procedures for Heterologous Expression of Proteins

Expression of LovB and LovBΔCON in *S. cerevisiae* strain BJ5464-NpgA

Two strains of *S. cerevisiae* BJ5464-NpgA, one transformed with a plasmid containing the *lovB* gene, and one transformed with a plasmid containing the *lovBΔCON* gene, were received from the Yi Tang group at UCLA.[25] Each protein was expressed using the same method, as follows. 1 L of YPD media with 1% dextrose was inoculated with the yeast cells, and incubated at 30 °C at 200 rpm for 72 hours. The cells were harvested by centrifugation (30 min, 4 °C, 8000 rpm on JA-10 rotor), resuspended in 30 mL lysis buffer (50 mM sodium phosphate, 0.5 mM NaCl, 10 mM imidazole), and cells were lysed using sonication on ice. Cellular debris was removed by centrifugation (15000 g, 1 hour, 4 °C). The supernatant was mixed with 2 mL Ni-NTA resin (QIAGEN), and shaken for 2 hours at 4 °C. Using a gravity flow column, the protein was purified using increasing amounts of imidazole in Buffer A (50 mM Tris, pH 7.9, 2 mM EDTA, 2 mM DTT). The fractions were analysed by SPS-PAGE (4-20% acrylamide, BIO-RAD), and fractions containing pure LovB or pure LovBΔCON were combined, concentrated, and buffer exchanged into Buffer A + 10% glycerol, then flash frozen by submerging microcentrifuge tube in dry ice/acetone, and stored at -80 °C.

Expression of CON in *E. coli* BL21(DE3)

Plasmid pSMa61 (*con* cloned into pET28a) was obtained from the Yi Tang group.[25] The plasmid was transformed into BL21(DE3) using the heat shock method. Expression was performed as follows: 1L of LB medium + 30 μg/mL kanamycin (Fisher Scientific) was inoculated with cells from an overnight culture, to an initial OD_{600} of approximately 0.1. The cells were grown at 37 °C and 200 rpm until an OD_{600} of 0.4, at which point the cultures were placed in an ice-water

bath for 10 minutes. Expression was induced with 0.1 mM isopropyl thio-β-D-galactoside (IPTG, Fisher Scientific), and incubation was continued at 16 °C for 16 hours. The cells were then harvested by centrifugation (30 min, 4 °C, 8000 rpm on JA-10 rotor), resuspended in 20 mL lysis buffer. Lysozyme (to 1 mg/mL) and DNaseI (to 5 ug/L) were added, and the cells were lysed using a cell disruptor. Cellular debris was removed by centrifugation (30000 g, 30 min, 4 °C), and the supernatant was incubated with 1 mL Ni-NTA resin (QIAGEN) at 4 °C for 1 hour. Using a gravity flow column, the CON domain was purified using increasing amounts of imidazole in Buffer A (50 mM Tris, pH 7.9, 2 mM EDTA, 2 mM DTT). The fractions were analysed by SPS-PAGE (4-20% acrylamide, BIO-RAD), and fractions containing pure CON were combined, concentrated, and buffer exchanged into Buffer A + 10% glycerol, flash frozen in dry ice/acetone, and stored at -80 °C.

Expression of DH in *E. coli* BL21(DE3)

The dehydratase gene was purchased as a synthetic gene product from Biobasic Inc., with codon usage optimized for expression in *E. coli*. The gene was subcloned into the pET28a vector at the NdeI and EcoRI restriction sites, to such that expression would produce the following construct, with an N-terminal His_6-tag:

MGSSHHHHHHSSGLVPRGSHMHLLLGKLSEYSTPLSFQWLNFVRPRDIEWLDGHALQG
QTVFPAAGYIVMAMEAALMIAGTHAKQVKLLEILDMSIDKAVIFDDEDSLVELNLTADV
SRNAGEAGSMTISFKIDSCLSKEGNLSLSAKGQLALTIEDVNPRTTSASDQHHLPPPEEEH
PHMNRVNINAFYHELGLMGYNYSKDFRRLHNMQRADLRASGTLDFIPLMDEGNGCPLL
LHPASLDVAFQTVIGAYSSPGDRRLRCLYVPTHVDRITLVPSLCLATAESGCEKVAFNTI
NTYDKGDYLSGDIVVFDAEQTTLFQVENITFKPFSPPDAST

Expression and purification were performed using the same method that was used for the CON domain, as above.

Cloning and Expression of Hpm8-ACP1 in *E. coli* BL21(DE3)

The first Hpm8-ACP construct, Hpm8-ACP1, was cloned as a standalone protein with the primer pair show in Table 2 (Chapter 4). A plasmid containing the entire Hpm8 gene, obtained from Yi Tang,[28] was used as the template and the PCR product was ligated into a PCR blunt vector for amplification. The amplified plasmid was digested using NdeI and EcoRI to obtain the Hpm8-ACP1 insert with sticky ends, which was ligated into pET28a to yield the expression plasmid. This plasmid was used to transform BL21(DE3) cells for expression. Hpm8-ACP1 was expressed and purified using the same method as for the CON domain, as above.

Cloning and Expression of Hpm8-ACP2 in *E. coli* BL21(DE3)

The gene for Hpm-ACP2 was synthesized and subcloned into pET28a by Biobasic Inc. (sequence in Chapter 4), and the plasmid was transformed into BL21(DE3) for expression. The protein was expressed and purified using the same method as for the CON domain, except that expression was performed at 30 °C for 6 hours. The His_6 tag was removed using the Thrombin Cleavage Capture kit (Novagen).

Cloning and Expression of LovB-ACP2 in *E. coli*

The gene for Hpm-ACP2 was synthesized and subcloned into pET28a by Biobasic Inc. (sequence in Chapter 4), and the plasmid was transformed into BL21(DE3) for expression. The protein was expressed and purified using the same method as for the CON domain, except that

expression was performed at 30 °C for 6 hours. The His_6 tag was removed using the Thrombin Cleavage Capture kit (Novagen).

Expression of NpgA

An expression plasmid containing the *npgA* gene was obtained from Shiou-Chuan Tsai, and was transformed into BL21(DE3) for expression. The protein was expressed using the same method as for the CON domain (see above), except that 1 mM IPTG was used for induction, and the expression was performed at 20 °C for 16 hours. The construct contained a Strep-tag purification tag, and thus the protein was purified using Strep-trap HP system (GE Healthcare Life Sciences).

Phosphopantetheinylation Procedure

Phosphopantetheinylation of LovB-ACP2

The following reactions were set up in 0.3 mL Eppendorf tubes:

Volume added	Reagent	Stock concentration	Final concentration
20 µL	LovB-ACP2	130 µM	26 µM
2 µL	Coenzyme A	200 mM	4 mM
0.5 µL	$MgCl_2$	2 M	10 mM
0.5 µL	DTT	1 M	5 mM
0.5 µL	Sfp or NpgA	4 mM	20 µM
80 µL	Sterile water		

The reactions were left for 16 hours at room temperature, at which point MALDI-MS analysis was performed, to provide the spectra shown in Figure 54, demonstrating the superiority of the NpgA for phosphopantetheinylation of LovB-ACP2.

REFERENCES

1. Weissman, K. J.; Leadlay, P. F. Combinatorial biosynthesis of reduced polyketides. *Nat. Rev. Microbiol.* **2005***, 3*, 925-936.

2. Birch, A. J.; Massywestropp, R. A.; Moye, C. J. Studies in Relation to Biosynthesis .7. 2-Hydroxy-6-Methylbenzoic Acid in Penicillium Griseofulvum Dierckx. *Aust. J. Chem.* **1955***, 8*, 539-544.

3. Staunton, J.; Weissman, K. J. Polyketide biosynthesis: a millennium review. *Nat. Prod. Rep.* **2001***, 18*, 380-416.

4. Cox, R. J.; Simpson, T. J. 1.09 - Fungal Type I Polyketides. In *Comprehensive Natural Products II*; Liu, H., Mander, L., Eds.; Elsevier: Oxford, 2010; pp 347-383.

5. Dewick, P. M. *Medicinal natural products : a biosynthetic approach;* Wiley: Chichester, U.K., 2009.

6. Smith, S.; Tsai, S. The type I fatty acid and polyketide synthases: a tale of two megasynthases. *Nat. Prod. Rep.* **2007***, 24*, 1041-1072.

7. Shen, B. Polyketide biosynthesis beyond the type I, II and III polyketide synthase paradigms. *Curr. Opin. Chem. Biol.* **2003***, 7*, 285-295.

8. Cortes, J.; Haydock, S. F.; Roberts, G. A.; Bevitt, D. J.; Leanly, P. F. An Unusually Large Multifunctional Polypeptide in the Erythromycin-Producing Polyketide Synthase of Saccharopolyspora-Erythraea. *Nature* **1990***, 348*, 176-178.

9. Donadio, S.; Staver, M. J.; McAlpine, J. B.; Swanson, S. J.; Katz, L. Modular Organization of Genes Required for Complex Polyketide Biosynthesis. *Science* **1991***, 252*, 675-679.

10. Katz, L. The Debs Paradigm for Type I Modular Polyketide Synthases and Beyond. *Methods Enzymol.* **2009***, 459*, 113-142.

11. Chen, H.; Du, L. Iterative polyketide biosynthesis by modular polyketide synthases in bacteria. *Appl. Microbiol. Biotechnol.* **2016***, 100*, 541-557.

12. Keatinge-Clay, A. T. A tylosin ketoreductase reveals how chirality is determined in polyketides. *Chem. Biol.* **2007***, 14*, 898-908.

13. Weissman, K. J. Genetic engineering of modular PKSs: from combinatorial biosynthesis to synthetic biology. *Nat. Prod. Rep.* **2016***, 33*, 203-230.

14. Zhou, H.; Gao, Z.; Qiao, K.; Wang, J.; Vederas, J. C.; Tang, Y. A fungal ketoreductase domain that displays substrate-dependent stereospecificity. *Nat. Chem. Biol.* **2012***, 8*, 331-333.

15. Cacho, R. A.; Thuss, J.; Xu, W.; Sanichar, R.; Gao, Z.; Nguyen, A.; Vederas, J. C.; Tang, Y. Understanding Programming of Fungal Iterative Polyketide Synthases: The Biochemical Basis for Regioselectivity by the Methyltransferase Domain in the Lovastatin Megasynthase. *J. Am. Chem. Soc.* **2015***, 137*, 15688-15691.

16. Chooi, Y.; Tang, Y. Navigating the Fungal Polyketide Chemical Space: From Genes to Molecules. *J. Org. Chem.* **2012**, *77*, 9933-9953.

17. Crawford, J. M.; Thomas, P. M.; Scheerer, J. R.; Vagstad, A. L.; Kelleher, N. L.; Townsend, C. A. Deconstruction of iterative multidomain polyketide synthase function. *Science* **2008**, *320*, 243-246.

18. Ray, L.; Moore, B. S. Recent advances in the biosynthesis of unusual polyketide synthase substrates. *Nat. Prod. Rep.* **2016**, *33*, 150-161.

19. Crawford, J. M.; Korman, T. P.; Labonte, J. W.; Vagstad, A. L.; Hill, E. A.; Kamari-Bidkorpeh, O.; Tsai, S.; Townsend, C. A. Structural basis for biosynthetic programming of fungal aromatic polyketide cyclization. *Nature* **2009**, *461*, U243.

20. Dimroth, P.; Walter, H.; Lynen, F. Biosynthesis of 6-Methylsalicylic Acid. *Eur. J. Biochem.* **1970**, *13*, 98-110.

21. Spencer, J. B.; Jordan, P. M. Purification and Properties of 6-Methylsalicylic Acid Synthase from Penicillium-Patulum. *Biochem. J.* **1992**, *288*, 839-846.

22. Parascandolo, J. S.; Havemann, J.; Potter, H. K.; Huang, F.; Riva, E.; Connolly, J.; Wilkening, I.; Song, L.; Leadlay, P. F.; Tosin, M. Insights into 6-Methylsalicylic Acid Bio-assembly by Using Chemical Probes. *Angew. Chem. Int. Ed. Engl.* **2016**, *55*, 3463-3467.

23. Campbell, C. D.; Vederas, J. C. Biosynthesis of Lovastatin and Related Metabolites Formed by Fungal Iterative PKS Enzymes. *Biopolymers* **2010**, *93*, 755-763.

24. Kennedy, J.; Auclair, K.; Kendrew, S. G.; Park, C.; Vederas, J. C.; Hutchinson, C. R. Modulation of polyketide synthase activity by accessory proteins during lovastatin biosynthesis. *Science* **1999**, *284*, 1368-1372.

25. Ma, S. M.; Li, J. W. -.; Choi, J. W.; Zhou, H.; Lee, K. K. M.; Moorthie, V. A.; Xie, X.; Kealey, J. T.; Da Silva, N. A.; Vederas, J. C.; Tang, Y. Complete Reconstitution of a Highly Reducing Iterative Polyketide Synthase. *Science* **2009**, *326*, 589-592.

26. Hendrickson, L.; Davis, C. R.; Roach, C.; Nguyen, D. K.; Aldrich, T.; McAda, P. C.; Reeves, C. D. Lavastatin biosynthesis in Aspergillus terreus: characterization of blocked mutants, enzyme activities and a multifunctional polyketide synthase gene. *Chem. Biol.* **1999**, *6*, 429-439.

27. Xu, W.; Chooi, Y.; Choi, J. W.; Li, S.; Vederas, J. C.; Da Silva, N. A.; Tang, Y. LovG: The Thioesterase Required for DihydromonacolinL Release and Lovastatin Nonaketide Synthase Turnover in Lovastatin Biosynthesis. *Angew. Chem. Int. Ed. Engl.* **2013**, *52*, 6472-6475.

28. Zhou, H.; Qiao, K.; Gao, Z.; Meehan, M. J.; Li, J. W. -.; Zhao, X.; Dorrestein, P. C.; Vederas, J. C.; Tang, Y. Enzymatic Synthesis of Resorcylic Acid Lactones by Cooperation of Fungal Iterative Polyketide Synthases Involved in Hypothemycin Biosynthesis. *J. Am. Chem. Soc.* **2010**, *132*, 4530-4531.

29. Hertweck, C. The Biosynthetic Logic of Polyketide Diversity. *Angew. Chem. Int. Ed. Engl.* **2009***, 48*, 4688-4716.

30. Malpartida, F.; Hopwood, D. A. Molecular-Cloning of the Whole Biosynthetic-Pathway of a Streptomyces Antibiotic and its Expression in a Heterologous Host. *Nature* **1984***, 309*, 462-464.

31. Morita, H.; Abe, I.; Noguchi, H. *Plant Type III PKS;* Elsevier Science BV: Amsterdam, 2010; pp 225.

32. Agatsuma, T.; TakahashiI, A.; Kabuto, C.; Nozoe, S. Revised Structure and Stereochemistry of Hypothemycin. *Chem. Pharm. Bull.* **1993***, 41*, 373-375.

33. Reeves, C. D.; Hu, Z.; Reid, R.; Kealey, J. T. Genes for the biosynthesis of the fungal polyketides hypothemycin from Hypomyces subiculosus and radicicol from Pochonia chlamydosporia. *Appl. Environ. Microbiol.* **2008***, 74*, 5121-5129.

34. Wee, J. L.; Sundermann, K.; Licari, P.; Galazzo, J. Cytotoxic hypothemycin analogues from Hypomyces subiculosus. *J. Nat. Prod.* **2006***, 69*, 1456-1459.

35. Shen, W.; Mao, H.; Huang, Q.; Dong, J. Benzenediol Lactones: A Class Of Fungal Metabolites With Diverse Structural Features And Biological Activities. *Eur. J. Med. Chem.* **2015***, 97*, 747-777.

36. Fukazawa, H.; Ikeda, Y.; Fukuyama, M.; Suzuki, T.; Hori, H.; Okuda, T.; Uehara, Y. The Resorcylic Acid Lactone Hypothemycin Selectively Inhibits the Mitogen-Activated Protein Kinase Kinase-Extracellular Signal-Regulated Kinase Pathway in Cells. *Biol. Pharm. Bull.* **2010***, 33*, 168-173.

37. Sharma, S. V.; Agatsuma, T.; Nakano, H. Targeting of the protein chaperone, HSP90, by the transformation suppressing agent, radicicol. *Oncogene* **1998***, 16*, 2639-2645.

38. Gao, Z.; Wang, J.; Norquay, A. K.; Qiao, K.; Tang, Y.; Vederas, J. C. Investigation of Fungal Iterative Polyketide Synthase Functions Using Partially Assembled Intermediates. *J. Am. Chem. Soc.* **2013***, 135*, 1735-1738.

39. Dietrich, D.; Vederas, J. C. Lovastatin, Compactin, and Related Anticholesterolemic Agents. In *Biosynthesis and Molecular Genetics of Fungal Secondary Metabolites*; Martin, JF GarciaEstrada, C Zeilinger,S., Ed.; Springer: New York; 233 Spring Street, New York, NY 10013, United States, 2014; pp 263-287.

40. Alberts, A. W.; Chen, J.; Kuron, G.; Hunt, V.; Huff, J.; Hoffman, C.; Rothrock, J.; Lopez, M.; Joshua, H.; Harris, E.; Patchett, A.; Monaghan, R.; Currie, S.; Stapley, E.; Albersschonberg, G.; Hensens, O.; Hirshfield, J.; Hoogsteen, K.; Liesch, J.; Springer, J. Mevinolin - a Highly Potent Competitive Inhibitor of Hydroxymethylglutaryl-Coenzyme-a Reductase and a Cholesterol-Lowering Agent. *Proc Natl Acad Sci U S A* **1980***, 77*, 3957-3961.

41. Endo, A.; Kuroda, M.; Tsujita, Y. Ml-236a, Ml-236b, and Ml-236c, New Inhibitors of Cholesterogenesis Produced by Penicillium Citrinum. *J. Antibiot.* **1976***, 29*, 1346-1348.

42. Genest, J.; McPherson, R.; Frohlich, J.; Anderson, T.; Campbell, N.; Carpentier, A.; Couture, P.; Dufour, R.; Fodor, G.; Francis, G. A.; Grover, S.; Gupta, M.; Hegele, R. A.; Lau, D. C.; Leiter, L.;

Lewis, G. F.; Lonn, E.; Mancini, G. B. J.; Ng, D.; Pearson, G. J.; Sniderman, A.; Stone, J. A.; Ur, E. 2009 Canadian Cardiovascular Society/Canadian guidelines for the diagnosis and treatment of dyslipidemia and prevention of cardiovascular disease in the adult-2009 recommendations. *Can. J. Cardiol.* **2009***, 25*, 567-579.

43. ENDO, A. The Discovery and Development of Hmg-Coa Reductase Inhibitors. *J. Lipid Res.* **1992***, 33*, 1569-1582.

44. Stone, N. J.; Robinson, J. G.; Lichtenstein, A. H.; Goff, D. C. J.; Lloyd-Jones, D. M.; Smith, S. C. J.; Blum, C.; Schwartz, J. S. Treatment of Blood Cholesterol to Reduce Atherosclerotic Cardiovascular Disease Risk in Adults: Synopsis of the 2013 American College of Cardiology/American Heart Association Cholesterol Guideline. *Annals of Internal Medicine* **2014***, 160*, 339-343.

45. Leading causes of death, by sex (Both sexes). *http://www.statcan.gc.ca/tables-tableaux/sum-som/l01/cst01/hlth36a-eng.htm* (accessed August,19, 2015).

46. Prevalence of statin treatment, recommended statin treatment, risk of cardiovascular disease (CVD) events, number needed to treat (NNT) and CVD events avoided, by CVD risk category, household population aged 20 to 79, Canada excluding territories, 2007 to 2011. *http://www.statcan.gc.ca/pub/82-003-x/2016001/article/14305/tbl/tbl02-eng.htm* (accessed August 19, 2016).

47. Chan, J. K.; Moore, R. N.; Nakashima, T. T.; Vederas, J. C. Biosynthesis of Mevinolin - Spectral Assignment by Double-Quantum Coherence Nmr After High C-13 Incorporation. *J. Am. Chem. Soc.* **1983***, 105*, 3334-3336.

48. Moore, R. N.; Bigam, G.; Chan, J. K.; Hogg, A. M.; Nakashima, T. T.; Vederas, J. C. Biosynthesis of the Hypocholesterolemic Agent Mevinolin by Aspergillus-Terreus - Determination of the Origin of Carbon, Hydrogen, and Oxygen-Atoms by C-13-Nmr and Mass-Spectrometry. *J. Am. Chem. Soc.* **1985***, 107*, 3694-3701.

49. Witter, D. J.; Vederas, J. C. Putative Diels−Alder-Catalyzed Cyclization during the Biosynthesis of Lovastatin. *J. Org. Chem.* **1996***, 61*, 2613-2623.

50. Auclair, K.; Sutherland, A.; Kennedy, J.; Witter, D. J.; Van, d. H.; Hutchinson, C. R.; Vederas, J. C. Lovastatin Nonaketide Synthase Catalyzes an Intramolecular Diels−Alder Reaction of a Substrate Analogue. *J. Am. Chem. Soc.* **2000***, 122*, 11519-11520.

51. Barriuso, J.; Nguyen, D. T.; Li, J. W.; Roberts, J. N.; MacNevin, G.; Chaytor, J. L.; Marcus, S. L.; Vederas, J. C.; Ro, D. Double Oxidation of the Cyclic Nonaketide Dihydromonacolin L to Monacolin J by a Single Cytochrome P450 Monooxygenase, LovA. *J. Am. Chem. Soc.* **2011***, 133*, 8078-8081.

52. Vederas, J. C. Explorations of fungal biosynthesis of reduced polyketides - a personal viewpoint. *Nat. Prod. Rep.* **2014***, 31*, 1253-1259.

53. Mootz, H. D.; Schorgendorfer, K.; Marahiel, M. A. Functional characterization of 4 '-phosphopantetheinyl transferase genes of bacterial and fungal origin by complementation of Saccharomyces cerevisiae lys5. *FEMS Microbiol. Lett.* **2002***, 213*, 51-57.

54. Yue, S.; Duncan, J. S.; Yamamoto, Y.; Hutchinson, C. R. Macrolide Biosynthesis - Tylactone Formation Involves the Processive Addition of 3 Carbon Units. *J. Am. Chem. Soc.* **1987***, 109*, 1253-1255.

55. Cane, D. E.; Yang, C. C. Macrolide Biosynthesis .4. Intact Incorporation of a Chain-Elongation Intermediate into Erythromycin. *J. Am. Chem. Soc.* **1987***, 109*, 1255-1257.

56. Yoshizawa, Y.; Li, Z.; Reese, P. B.; Vederas, J. C. Intact Incorporation of Acetate-Derived Diketides and Tetraketides during Biosynthesis of Dehydrocurvularin, a Macrolide Phytotoxin from Alternaria-Cinerariae. *J. Am. Chem. Soc.* **1990***, 112*, 3212-3213.

57. Blanchette, M. A.; Choy, W.; Davis, J. T.; Essenfeld, A. P.; Masamune, S.; Roush, W. R.; Sakai, T. Horner-Wadsworth-Emmons Reaction - use of Lithium-Chloride and an Amine for Base Sensitive Compounds. *Tetrahedron Lett.* **1984***, 25*, 2183-2186.

58. Yin, N.; Wang, G.; Qian, M.; Negishi, E. Stereoselective synthesis of the side chains of mycolactones A and B featuring stepwise double substitutions of 1,1-dibromo-1-alkenes. *Angew. Chem. Int. Ed. Engl.* **2006***, 45*, 2916-2920.

59. Claus, R. E.; Schreiber, S. L. Ozonolytic cleavage of cyclohexene to terminally differentiated products: methyl 6-oxohexanoate, 6,6-dimethoxyhexanal, and methyl 6,6-dimethoxyhexanoate. *Organic Syntheses* **1986***, 64*, 150-156.

60. Dess, D. B.; Martin, J. C. Readily Accessible 12-I-5 Oxidant for the Conversion of Primary and Secondary Alcohols to Aldehydes and Ketones. *J. Org. Chem.* **1983***, 48*, 4155-4156.

61. Wadsworth, W. S. Synthetic Applications of Phosphoryl-Stabilized Anions. In *Organic Reactions*John Wiley & Sons, Inc.: 2012.

62. Schlosser, M.; Christmann, K. F. Trans-Selective Olefin Syntheses. *Angew. Chem. Int. Ed. Engl.* **1966***, 5*, 126.

63. Bal, B. S.; Childers, W. E.; Pinnick, H. W. Oxidation of α,β-un saturated aldehydes. *Tetrahedron* **1981***, 37*, 2091-2096.

64. Sorensen, J. The biosynthesis of lovastatin: Examining the assembly and elaboration steps, University of Alberta, 2003.

65. Schreiber, S. L.; Claus, R. E.; Reagan, J. Ozonolytic Cleavage of Cycloalkenes to Terminally Differentiated Products. *Tetrahedron Lett.* **1982***, 23*, 3867-3870.

66. Diels, O.; Alder, K. Synthesis in the hydro-aromatic tier. *Justus Liebigs Ann. Chem.* **1928***, 460*, 98-122.

67. Kelly, W. L. Intramolecular cyclizations of polyketide biosynthesis: mining for a "Diels-Alderase"? *Org. Biomol. Chem.* **2008**, *6*, 4483-4493.

68. Oikawa, H. Diels-Alderases. *Comprehensive Natural Products II: Chemistry and Biology, Vol 8: Enzymes and Enzyme Mechanisms* **2010**, 277-314.

69. Kim, H. J.; Ruszczycky, M. W.; Liu, H. Current developments and challenges in the search for a naturally selected Diels-Alderase. *Curr. Opin. Chem. Biol.* **2012**, *16*, 124-131.

70. Klas, K.; Tsukamoto, S.; Sherman, D. H.; Williams, R. M. Natural Diels-Alderases: Elusive and Irresistable. *J. Org. Chem.* **2015**, *80*, 11672-11685.

71. Zheng, Q.; Tian, Z.; Liu, W. Recent advances in understanding the enzymatic reactions of [4+2] cycloaddition and spiroketalization. *Curr. Opin. Chem. Biol.* **2016**, *31*, 95-102.

72. Minami, A.; Oikawa, H. Recent advances of Diels-Alderases involved in natural product biosynthesis. *J. Antibiot.* **2016**, *69*, 500-506.

73. Cottet, K.; Kolympadi, M.; Markovic, D.; Lallemand, M. Natural Products Biosynthesis Involving a Putative Diels-Alder Reaction. *Curr. Org. Chem.* **2016**, *20*, 2421-2442.

74. Hashimoto, T.; Kuzuyama, T. Mechanistic insights into Diels-Alder reactions in natural product biosynthesis. *Curr. Opin. Chem. Biol.* **2016**, *35*, 117-123.

75. Katayama, K.; Kobayashi, T.; Oikawa, H.; Honma, M.; Ichihara, A. Enzymatic activity and partial purification of solanapyrone synthase: first enzyme catalyzing Diels-Alder reaction. *Biochim. Biophys. Acta-Protein Struct. Molec. Enzym.* **1998**, *1384*, 387-395.

76. Oikawa, H.; Kobayashi, T.; Katayama, K.; Suzuki, Y.; Ichihara, A. Total synthesis of (-)-solanapyrone A via enzymatic Diels-Alder reaction of prosolanapyrone. *J. Org. Chem.* **1998**, *63*, 8748-8756.

77. Ugai, T.; Minami, A.; Fujii, R.; Tanaka, M.; Oguri, H.; Gomi, K.; Oikawa, H. Heterologous expression of highly reducing polyketide synthase involved in betaenone biosynthesis. *Chem. Commun.* **2015**, *51*, 1878-1881.

78. Tian, Z.; Sun, P.; Yan, Y.; Wu, Z.; Zheng, Q.; Zhou, S.; Zhang, H.; Yu, F.; Jia, X.; Chen, D.; Mandi, A.; Kurtan, T.; Liu, W. An enzymatic [4+2] cyclization cascade creates the pentacyclic core of pyrroindomycins. *Nat. Chem. Biol.* **2015**, *11*, U91.

79. Pang, B.; Zhong, G.; Tang, Z.; Liu, W. Enzymatic [4+2] Cycloadditions in the Biosynthesis of Spirotetramates and Spirotetronates. *Methods Enzymol.* **2016**, *575*, 39-63.

80. Kato, N.; Nogawa, T.; Hirota, H.; Jang, J.; Takahashi, S.; Ahn, J. S.; Osada, H. A new enzyme involved in the control of the stereochemistry in the decalin formation during equisetin biosynthesis. *Biochem. Biophys. Res. Commun.* **2015**, *460*, 210-215.

81. Li, L.; Yu, P.; Tang, M.; Zou, Y.; Gao, S.; Hung, Y.; Zhao, M.; Watanabe, K.; Houk, K. N.; Tang, Y. Biochemical Characterization of a Eukaryotic Decalin-Forming Diels-Alderase. *J. Am. Chem. Soc.* **2016***, 138*, 15837-15840.

82. Ose, T.; Watanabe, K.; Mie, T.; Honma, M.; Watanabe, H.; Yao, M.; Oikawa, H.; Tanaka, I. Insight into a natural Diels-Alder reaction from the structure of macrophomate synthase. *Nature* **2003***, 422*, 185-189.

83. Kim, R.; Illarionov, B.; Joshi, M.; Cushman, M.; Lee, C. Y.; Eisenreich, W.; Fischer, M.; Bacher, A. Mechanistic Insights on Riboflavin Synthase Inspired by Selective Binding of the 6,7-Dimethyl-8-ribityllumazine Exomethylene Anion. *J. Am. Chem. Soc.* **2010***, 132*, 2983-2990.

84. Kim, H. J.; Ruszczycky, M. W.; Choi, S.; Liu, Y.; Liu, H. Enzyme-catalysed [4+2] cycloaddition is a key step in the biosynthesis of spinosyn A. *Nature* **2011***, 473*, 109-112.

85. Medvedev, M. G.; Zeifman, A. A.; Novikov, F. N.; Bushmarinov, I. S.; Stroganov, O. V.; Titov, I. Y.; Chilov, G. G.; Svitanko, I. V. Quantifying Possible Routes for SpnF-Catalyzed Formal Diels–Alder Cycloaddition. *J. Am. Chem. Soc.* **2017**.

86. Byrne, M. J.; Lees, N. R.; Han, L.; van der Kamp, Marc W; Mulholland, A. J.; Stach, J. E. M.; Willis, C. L.; Race, P. R. The Catalytic Mechanism of a Natural Diels-Alderase Revealed in Molecular Detail. *J. Am. Chem. Soc.* **2016***, 138*, 6095-6098.

87. Wever, W. J.; Bogart, J. W.; Baccile, J. A.; Chan, A. N.; Schroeder, F. C.; Bowers, A. A. Chemoenzymatic Synthesis of Thiazolyl Peptide Natural Products Featuring an Enzyme-Catalyzed Formal [4+2] Cycloaddition. *J. Am. Chem. Soc.* **2015***, 137*, 3494-3497.

88. Hudson, G. A.; Zhang, Z.; Tietz, J. I.; Mitchell, D. A.; van der Donk, Wilfred A In Vitro Biosynthesis of the Core Scaffold of the Thiopeptide Thiomuracin. *J. Am. Chem. Soc.* **2015***, 137*, 16012-16015.

89. Kakule, T. B.; Lin, Z.; Schmidt, E. W. Combinatorialization of Fungal Polyketide Synthase-Peptide Synthetase Hybrid Proteins. *J. Am. Chem. Soc.* **2014***, 136*, 17882-17890.

90. Berkhan, G.; Hahn, F. A Dehydratase Domain in Ambruticin Biosynthesis Displays Additional Activity as a Pyran-Forming Cyclase. *Angew. Chem. Int. Ed. Engl.* **2014***, 53*, 14240-14244.

91. Sato, K.; Mizuno, S.; Hirayama, M. A Total Synthesis of Phytol. *J. Org. Chem.* **1967***, 32*, 177.

92. den Hartog, T.; van Dijken, D. J.; Minnaard, A. J.; Feringa, B. L. An enantioselective catalytic approach to syn deoxypropionate units combining asymmetric Cu-catalyzed 1,6-and 1,4-conjugate addition. *Tetrahedron-Asymmetry* **2010***, 21*, 1574-1584.

93. Mutka, S. C.; Bondi, S. M.; Carney, J. R.; Da Silva, N. A.; Kealey, J. T. Metabolic pathway engineering for complex polyketide biosynthesis in Saccharomyces cerevisiae. *FEMS Yeast Res.* **2006***, 6*, 40-47.

94. Kealey, J. T.; Liu, L.; Santi, D. V.; Betlach, M. C.; Barr, P. J. Production of a polyketide natural product in nonpolyketide-producing prokaryotic and eukaryotic hosts. *Proc. Natl. Acad. Sci. U. S. A.* **1998**, *95*, 505-509.

95. Claridge, T.; Perez-Victoria, I. Enhanced C-13 resolution in semi-selective HMBC: a band-selective, constant-time HMBC for complex organic structure elucidation by NMR. *Org. Biomol. Chem.* **2003**, *1*, 3632-3634.

96. Auclair, K. Biosynthetic Studies on the Polyketide Lovastatin: Enzyme -Catalyzed Diels -Alder Reactions, University of Alberta, 1999.

97. Keatinge-Clay, A. T. The structures of type I polyketide synthases. *Nat. Prod. Rep.* **2012**, *29*, 1050-1073.

98. Haslinger, K.; Peschke, M.; Brieke, C.; Maximowitsch, E.; Cryle, M. J. X-domain of peptide synthetases recruits oxygenases crucial for glycopeptide biosynthesis. *Nature* **2015**, *521*, 105-109.

99. Crosby, J.; Crump, M. P. The structural role of the carrier protein - active controller or passive carrier. *Nat. Prod. Rep.* **2012**, *29*, 1111-1137.

100. Prescott, D. J.; Vagelos, P. R. Acyl Carrier Protein. *Adv. Enzymol. Relat. Areas Mol. Biol.* **1972**, *36*, 269.

101. Beld, J.; Sonnenschein, E. C.; Vickery, C. R.; Noel, J. P.; Burkart, M. D. The phosphopantetheinyl transferases: catalysis of a post-translational modification crucial for life. *Nat. Prod. Rep.* **2014**, *31*, 61-108.

102. Holak, T. A.; Kearsley, S. K.; Kim, Y.; Prestegard, J. H. 3-Dimensional Structure of Acyl Carrier Protein Determined by Nmr Pseudoenergy and Distance Geometry Calculations. **1988**, *27*, 6135-6142.

103. Cantu, D. C.; Forrester, M. J.; Charov, K.; Reilly, P. J. Acyl carrier protein structural classification and normal mode analysis. *Protein Sci.* **2012**, *21*, 655-666.

104. Maier, T.; Leibundgut, M.; Ban, N. The crystal structure of a mammalian fatty acid synthase. *Science* **2008**, *321*, 1315-1322.

105. Masoudi, A.; Raetz, C. R. H.; Zhou, P.; Pemble, C. W. Chasing acyl carrier protein through a catalytic cycle of lipid A production. *Nature* **2014**, *505*, 422.

106. Chi Nguyen; Haushalter, R. W.; Lee, D. J.; Markwick, P. R. L.; Bruegger, J.; Caldara-Festin, G.; Finzel, K.; Jackson, D. R.; Ishikawa, F.; O'Dowd, B.; McCammon, J. A.; Opella, S. J.; Tsai, S.; Burkart, M. D. Trapping the dynamic acyl carrier protein in fatty acid biosynthesis. *Nature* **2014**, *505*, 427-431.

107. Alekseyev, V. Y.; Liu, C. W.; Cane, D. E.; Puglisi, J. D.; Khosla, C. Solution structure and proposed domain-domain recognition interface of an acyl carrier protein domain from a modular polyketide synthase. *Protein Sci.* **2007**, *16*, 2093-2107.

108. Ploskon, E.; Arthur, C. J.; Evans, S. E.; Williams, C.; Crosby, J.; Simpson, T. J.; Crump, M. P. A mammalian type I fatty acid synthase acyl carrier protein domain does not sequester acyl chains. *J. Biol. Chem.* **2008***, 283*, 518-528.

109. Wattana-amorn, P.; Williams, C.; Ploskon, E.; Cox, R. J.; Simpson, T. J.; Crosby, J.; Crump, M. P. Solution structure of an acyl carrier protein domain from a fungal type I polyketide synthase. *Biochemistry* **2010***, 49*, 2186-2193.

110. Lim, J.; Kong, R.; Murugan, E.; Ho, C. L.; Liang, Z.; Yang, D. Solution Structures of the Acyl Carrier Protein Domain from the Highly Reducing Type I Iterative Polyketide Synthase CalE8. *PLoS ONE* **2011***, 6*, e20549.

111. Kyte, J.; Doolittle, R. F. A Simple Method for Displaying the Hydropathic Character of a Protein. *J. Mol. Biol.* **1982***, 157*, 105-132.

112. Wishart, D. S.; Boyko, R. F.; Willard, L.; Richards, F. M.; Sykes, B. D. Seqsee - a Comprehensive Program Suite for Protein-Sequence Analysis. *Comput. Appl. Biosci.* **1994***, 10*, 121-132.

113. Yang, Z.; Zhang, L.; Zhang, Y.; Zhang, T.; Feng, Y.; Lu, X.; Lan, W.; Wang, J.; Wu, H.; Cao, C.; Wang, X. Highly Efficient Production of Soluble Proteins from Insoluble Inclusion Bodies by a Two-Step-Denaturing and Refolding Method. *PLoS One* **2011***, 6*, e22981.

114. Pfeifer, B. A.; Admiraal, S. J.; Gramajo, H.; Cane, D. E.; Khosla, C. Biosynthesis of complex polyketides in a metabolically engineered strain of E-coli. *Science* **2001***, 291*, 1790-1792.